

# Charge-exchange excitations of nuclei

N. I. Pyatov

Joint Institute for Nuclear Research, Dubna

S. A. Fayans

I. V. Kurchatov Institute of Atomic Energy, Moscow

Fiz. Elem. Chastits At. Yadra 14, 953-1019 (July-August 1983)

The modern microscopic approaches used to describe the properties of nuclear charge-exchange excitations in the low-energy part of the spectrum, including the region of giant resonances, are reviewed. The results of calculations based on the theory of finite Fermi systems with exact allowance for the single-particle continuum are compared in detail with experimental data with the aim of extracting information about the effective nucleon-nucleon interaction and the local quasiparticle charge  $e_q[\sigma\tau]$  with respect to the spin-isospin field. The part played by this charge in quenching the strength of spin-flip transitions is discussed. Strength functions characterizing the distribution of the strengths of transitions of different multipolarities over the excitation spectrum are given for a number of nuclei.

PACS numbers: 25.40.Ep, 25.40.Fq, 24.30.Cz

## INTRODUCTION

Charge-exchange processes are processes accompanied by a change in the charge of the nucleus [or the third projection of the isotopic spin  $T_z = (N - Z)/2$ ] without a change in the mass number  $A$ . The excitations of the daughter nuclei corresponding to these processes are also called *charge-exchange* or *isobaric* excitations. The processes that have so far been most fully studied are those in which the nuclear charge changes by unity ( $\Delta T_z = \pm 1$ ). Typical examples are  $\beta$  decay, the  $(p, n)$  and  $(n, p)$  reactions, reactions of the type ( $^3\text{He}, t$ ), ( $^6\text{Li}, ^6\text{He}$ ), and ( $^7\text{Li}, ^7\text{Be}$ ) with light ions, pion ( $\pi^+$ ,  $\pi^-$ ) charge-exchange reactions, etc. From these processes, extensive experimental information has been obtained about charge-exchange excitations of nuclei (see, for example, Refs. 1-4). In particular, many data have been obtained on low-lying noncollective excitations (from  $\beta$  decay). There have also been intensive studies of analogs of the ground and low-lying excited states of the parent nuclei. These investigations are made mainly with beams of hadrons or light ions with relatively low energies. Until recently, only one collective state—the isobar analog of the ground state—had been well studied. The use in charge-exchange reactions of protons and light ions with energies  $\geq 100$  MeV and the improvement in the methods of measuring cross sections at small scattering angles have led in recent years to the discovery of other collective isobar states of nuclei, in particular, the Gamow-Teller resonance with angular momentum and parity  $J^\pi = 1^+$ .

The roots of theoretical investigations of isobar states go back to the time of the creation of the theory of  $\beta$  decay and the introduction of the isotopic-spin formalism. The possibility of isobar collective states was implicit in schemes such as isotopic SU(2) and supermultiplet (spin-isospin) SU(4) symmetry (see, for example, Ref. 5). Careful study of the experimental data on the probabilities of allowed Gamow-Teller transitions between low-lying nuclear states and comparison of them with calculations in the shell model led to the independent conclusion that there could exist a Gamow-Teller resonance (near the isobar analog state) in

which the bulk ( $\approx 90\%$ ) of the strength of the Gamow-Teller transitions is concentrated.<sup>6</sup> Simple microscopic calculations of charge-exchange  $0^+$  and  $1^+$  excitations and their corresponding  $\beta$ -decay strength functions were made, for example, in Refs. 7 and 8 and also in the reviews of Refs. 9 and 10.

The discovery in  $(p, n)$  experiments of the Gamow-Teller resonance and other collective isobar resonances greatly stimulated the development of theoretical investigations of charge-exchange excitations, especially in the framework of modern microscopic approaches. For the discovery of new collective degrees of freedom associated with isobar resonances opens up unique possibilities for obtaining information about nuclear structure, effective interactions, and the part played by different nuclear-excitation mechanisms in the low-energy part of the spectrum (below or around the Fermi energy  $\varepsilon_F$ ). In particular, for this part of the spectrum probing questions were for the first time posed about the effects associated with meson exchange, multipair correlations, the excitation of baryon resonances, including the  $\Delta$  resonance, and so forth.

The main task we set ourselves here is to review the modern microscopic approaches to the description of charge-exchange excitations in nuclei and compare their predictions with the existing experimental data. We have felt it necessary to include in the review a section on the theoretical foundations of the method of calculating the response of a nucleus to a low-frequency external field. This uses the concept of quasiparticles. Thus, we make a small digression into the theory of finite Fermi systems.<sup>11</sup> In it, in contrast to the standard shell approach (and in contrast to the Hartree-Fock method), there appear automatically important quantities such as the local quasiparticle charge  $e_q[V_0]$ , which is different from unity for fields  $V_0 \sim \sigma\tau$ . It is associated with the quenching of the strength of the corresponding transitions in the low-energy part of the spectrum. In addition, the charge  $e_q[\sigma\tau]$ , which occurs in all axial-vector vertices, renormalizes the one-pion exchange amplitude, which may lead to important consequences for the problem of the softening of the pion

mode and precritical effects, the so-called precursors of pion condensation.

The main attention in the review is devoted to the Gamow-Teller and dipole excitation modes, much less to the isobar analog excitations. A considerable number of reviews have already been devoted to the latter (see, for example, Ref. 12).

## 1. SOME ASPECTS OF THE THEORY OF FINITE FERMION SYSTEMS

We here briefly present the theoretical approach to the low-frequency response of a many-body Fermi system, the key to which is the existence in such systems of a quasiparticle excitation branch. This approach is based on the ideas of Landau's theory of a Fermi liquid. As applied to finite systems, it was developed by Migdal and has become known as the *theory of finite Fermi systems*. In this approach, the charge-exchange channel is in no way distinguished, and the entire treatment will be given in general form without explicit introduction of isotopic (and spin) indices.

### Polarization operator and strength function

The physical processes that take place in the considered system subject to an external perturbation are completely determined by the polarization operator  $P$ , which can be represented in the form

$$P = -\frac{V_0}{\pi} \mathcal{T}_0 \left( \begin{array}{c} 2 \\ 1 \end{array} \right) \frac{G}{G} \left( \begin{array}{c} 3 \\ 4 \end{array} \right) \frac{V_0}{G} = (\mathcal{T}_0[V_0]G\mathcal{T}[V_0])^{-1}. \quad (1)$$

Here, we have introduced a symbolic notation for  $P$ , in which the round brackets denote integration over all the intermediate coordinates  $\{x_i\}$  in 4-space. Written out in more detail,

$$P = \int dx_1 \dots dx_4 \left[ \int dx_5 \mathcal{T}_0(x_1, x_5, x_2) V_0(x_5) \right] \times G(x_2, x_3) \left[ \int dx_6 \mathcal{T}(x_3, x_6, x_4) V_0(x_6) \right] G(x_4, x_1). \quad (2)$$

Of course, we also understand summation over the intermediate spin and isotopic indices. Here,  $\mathcal{T}_0[V_0]$  is the irreducible vertex for the external field  $V_0$  ("irreducible" means that  $\mathcal{T}_0$  does not contain two nucleon lines in a vertical section). For some fields  $V_0$ , the vertex  $\mathcal{T}_0$  can be found from the conservation laws and gauge invariance (see below). In the simplest case,  $\mathcal{T}_0[V_0] = V_0^Q(x)\delta(x-y)$  is a local vertex with

$$V_0^Q(x) = V_0(x) Q \exp(i\omega t); \quad (3)$$

$Q$  is some operator (for example,  $1, \tau_\alpha, \sigma_\alpha, \sigma_\alpha \tau_\beta$ , etc.). Further,  $\mathcal{T}[V_0]$  is the total ("dressed") vertex, in which all interaction processes are taken into account;  $G$  are the exact single-particle Green's functions. After taking the Fourier transform with respect to the time for the polarization operator, we can write down an expansion with respect to the exact quantum states  $|s\rangle$  of the system analogous to the Källén-Lehmann expansion for the photon propagator in quantum field theory:

$$P(\omega) = - \sum_s \left\{ \frac{|s|V_0^Q|0\rangle|^2}{\omega_s - \omega + i\delta} + \frac{|s|V_0^{Q+}|0\rangle|^2}{\omega_s + \omega - i\delta} \right\}. \quad (4)$$

It can be seen from this that the distribution of the

strength of the transitions in the system under the influence of the perturbation  $V_0^Q$  can be expressed in terms of the imaginary part of the polarization operator:

$$S(\omega) = -\frac{1}{\pi} \text{Im } P(\omega) = \sum_s |s|V_0^Q|0\rangle|^2 \delta(\omega - \omega_s). \quad (5)$$

We shall call  $S(\omega)$  the *strength function*. The direct calculation of the polarization operator  $P(\omega)$  and the strength function  $S(\omega)$  in general form for a many-body system, especially with a strong interaction, is a difficult task. However, for a Fermi system at low excitation energies  $\omega \ll \epsilon_F$  and small momentum transfers  $q \ll p_F$ , this problem can be solved on the basis of a phenomenological theory—the theory of finite Fermi systems. In this theory, one calculates the contribution to the polarization operator (4) from quasiparticle excitations (or, more precisely, from the particle-hole branch), this contribution being predominant at small  $\omega$  and  $q$ . We recall how this is done.

The point of departure is the separation of the quasiparticle term  $aG^a$  in the single-particle Green's function:  $G = aG^a + G^R$ , where  $G^R$  is the so-called *regular part*;  $aG^a$  has poles,  $\sim a/[\epsilon - \epsilon_\lambda + i\delta(\epsilon_\lambda)]$ , and energies  $\epsilon_\lambda$ , these determining the spectrum of the single-particle excitations [ $a = (\partial G^{-1}/\partial \epsilon)^{-1}$  is the renormalization, or spectroscopic, factor, the weight of the single-quasiparticle state in the exact Green's function on the Fermi surface, near which the quasiparticle damping is small:  $\delta(\epsilon_\lambda \approx \epsilon_F) \approx 0$ ]. The existence of such poles leads to an essential singularity in  $P(\omega)$  at small  $\omega$ . Indeed, we rewrite (2), making a Fourier transformation with respect to the time variables:

$$P(\omega) = \int \frac{d\epsilon}{2\pi i} \mathcal{T}_0 G\left(\epsilon + \frac{\omega}{2}\right) \mathcal{T}\left(\epsilon + \frac{\omega}{2}, \epsilon - \frac{\omega}{2}\right) G\left(\epsilon - \frac{\omega}{2}\right). \quad (6)$$

Here, we have written out explicitly only the energy variables ( $\mathcal{T}_0$  may also contain a dependence on  $\epsilon$  and  $\omega$ ). It is now clear that as  $\omega \rightarrow 0$  and  $\epsilon \approx \epsilon_F$  the quasiparticle poles in the product  $GG$  approach each other, and this gives the essential singularity in the integrand in  $P(\omega)$ . It must be correctly separated.

### Renormalization and local charge

This is achieved by means of a renormalization procedure, the essence of which is the following. We first write down the exact equations for the vertex  $\mathcal{T}$  and the total two-particle amplitude  $\Gamma$ ; they can be represented especially clearly in diagram language:

$$\begin{aligned} \text{---} \mathcal{T} \text{---} &= \text{---} \mathcal{T}_0 \text{---} + \text{---} \mathcal{T}_0 \text{---} \frac{G}{G} \text{---} \mathcal{T}_0 \text{---} + \text{---} \mathcal{T}_0 \text{---} \frac{G}{G} \text{---} \mathcal{T}_0 \text{---} \\ \text{---} \Gamma \text{---} &= \text{---} \mathcal{U} \text{---} + \text{---} \mathcal{U} \text{---} \frac{G}{G} \text{---} \Gamma \text{---} \end{aligned} \quad (7a)$$

Here, we have introduced the irreducible block  $\mathcal{U}$ , which by definition does not contain two lines in a vertical section and does not have a singularity as  $\omega \rightarrow 0$ . In a compact symbolic expression, these equations become

$$\mathcal{T} = \mathcal{T}_0 + \mathcal{U}G\mathcal{T}G \equiv \mathcal{T}_0 + \mathcal{T}_0G\Gamma G; \quad \Gamma = \mathcal{U} + \mathcal{U}G\Gamma G. \quad (7b)$$

To separate the essential singularity, we split the product  $GG$  into "singular" and "nonsingular" parts:



$$GG = a^2 G^q G^q + (G^q G^R + G^R G^q + G^R G^R) \equiv a^2 A + B, \quad (8)$$

where  $B$  is the regular part of  $GG$ —it does not have quasiparticle poles that pile up. We introduce the auxiliary quantities  $\Gamma^\omega$  and  $\mathcal{T}^\omega$ , which satisfy the equations

$$\Gamma^\omega = \mathcal{U} + \mathcal{U} B \Gamma^\omega; \quad \mathcal{T}^\omega = \mathcal{T}_0 + \mathcal{U} B \mathcal{T}^\omega. \quad (9)$$

The initial equations (7b) can be renormalized by multiplying them from the left by the operator  $\Gamma^\omega B + 1$  and using (9); we obtain

$$\Gamma = \Gamma^\omega + a^2 \Gamma^\omega A \Gamma; \quad \mathcal{T} = \mathcal{T}^\omega + a^2 \Gamma^\omega A \mathcal{T}. \quad (10)$$

The same operation applied to the second equation in (9) gives

$$\mathcal{T}^\omega = (1 + \Gamma^\omega B) \mathcal{T}_0 \equiv e_q \mathcal{T}_0 / a, \quad (11)$$

where we have introduced the operator  $e_q = a(1 + \Gamma^\omega B)$ , which is called the *local charge of the quasiparticles*. Using (9) and (10), we find for the polarization operator

$$P(\omega) = (\mathcal{T}^\omega a^2 A \mathcal{T}) + (\mathcal{T}_0 B \mathcal{T}^\omega). \quad (12)$$

For the moment, we shall assume that  $\mathcal{T}_0$  is a local vertex and is identical to (3). Then  $a \mathcal{T}^\omega = e_q V_0$ , and, defining the effective field by the relation  $V = a \mathcal{T}$ , we obtain for the polarization operator

$$P(\omega) = (e_q V_0 A V) + \left( V_0 B \frac{1}{a} e_q V_0 \right). \quad (13)$$

As follows from (10), the effective field  $V$  satisfies the equation

$$V = e_q V_0 + \mathcal{T} A V, \quad (14)$$

where we have introduced the effective interaction  $\mathcal{T} = a^2 \Gamma^\omega$  (in the particle-hole channel). The second term in the polarization operator (12)–(13) is due to the contribution of many-particle processes in which more than one particle-hole pair is excited in the intermediate state. We shall therefore call this a *multipair* term.

What have we achieved by these identical transformations? Above all, we can now formulate a universal prescription for calculating the first term in the polarization operator (12) at the price of the introduction of a certain parametrization for  $e_q$  and  $\mathcal{T}$ , this being the same for systems with a large number of particles. Indeed,  $\mathcal{T}^\omega$  and  $\Gamma^\omega$  ( $e_q$  and  $\mathcal{T}$ ) can be assumed to be smooth functions of their arguments with a characteristic scale of variation  $\Delta \varepsilon \sim \varepsilon_F$  with respect to the energies. They do not have singularities as  $\omega \rightarrow 0$  [the pole terms that enter  $B$  in accordance with (8) from the solitary Green's functions are also integrated in  $P(\omega)$ ].

The strongest dependence on  $\varepsilon$  and  $\omega$  for  $\varepsilon \approx \varepsilon_F$  and  $\omega \rightarrow 0$  is contained in the product  $A = G^q(\varepsilon + \omega/2) G^q(\varepsilon - \omega/2)$ . Therefore, when integrating over  $\varepsilon$  in (13) and (14) we can assume that  $e_q$  and  $\mathcal{T}$  (and, accordingly,  $V$ ) are taken at  $\varepsilon \approx \varepsilon_F$ ,<sup>1)</sup> and by  $A$  we can now understand the in-

<sup>1)</sup>In an infinite system, the spectrum of single-quasiparticle excitations is continuous and the contribution from the accumulating poles to  $G^q G^q$  is "pressed" to the Fermi surface, so that in the integration over  $\varepsilon$  this contribution can be assumed proportional to  $\delta(\varepsilon - \varepsilon_F)$ . In finite systems, this contribution is "smeared" over an interval of width  $\Delta \varepsilon \approx \varepsilon_F A^{-1/3}$  near  $\varepsilon_F$  because of the discrete nature of the quasiparticle levels. In this case, the residue  $a$  in (10)–(13) is the mean value of the matrix elements  $\langle \partial \varepsilon^{-1} \partial \varepsilon \rangle_{\lambda \lambda'}$  over the quasiparticle states  $|\lambda\rangle$  in that energy interval. It should be noted that  $a$  does not occur explicitly in the quasiparticle part of the polarization operator (13) or in (14).

tegral

$$\int_{-\infty}^{+\infty} G^q(\varepsilon + \omega/2) G^q(\varepsilon - \omega/2) d\varepsilon / 2\pi i,$$

which we shall call the *particle-hole propagator*; after this there actually remains in (14) and in the first term in (13) an integration over only spatial variables. It can be seen that in the momentum space too  $e_q$  and  $\mathcal{T}$  are also determined by integrals over the regions  $\Delta p \sim p_F$ . These quantities are local and universal functions of the coordinates. Therefore, they can be parametrized comparatively easily by introducing a small number of constants found experimentally (or, in principle, calculated from the vacuum nucleon-nucleon interaction in, for example, the Brueckner approach). In a self-consistent theory, this is sufficient, since for a given amplitude  $\mathcal{T}$  one can completely construct the average field and calculate the propagator  $A$ , which occurs in Eq. (14) for the effective field and in the polarization operator (13). Thus, for the calculation of the low-frequency response the real physical Fermi system (the nucleus) can be replaced by a system of interacting quasiparticles in a self-consistent field (essentially, this is the justification for the shell model with a residual interaction). Such an approach is the basis of the theory of finite Fermi systems.

We have dwelt on these more or less well-known matters to draw the attention of the reader to the second term in (13) and to the local charge  $e_q$ . The following questions arise naturally: 1) What is the contribution of this second term to the total response of the nucleus; 2) how does it influence the distribution of the transition probabilities over the excitation spectrum; 3) and what is the part played by the local charge  $e_q$ ? Comparison with experiments shows that for fields of electric type inducing transitions of normal parity  $0^+, 1^-, 2^+, \dots$  the first term in (13) with  $e_q \approx 1$  gives an almost complete description of both the distribution of the transitions and their integrated strength over the excitation spectrum, and the second term does not appear to make any appreciable contribution up to the Fermi energy, this applying not only to the neutral but also to the charged channel (we may mention, for example, the analog  $0^+$  excitations).

With regard to fields of magnetic type (axial-vector vertices containing the operator  $\sigma_\alpha \tau_\beta$ ), experimental difficulties have had the consequence that until recently there were no systematic data on excitations of anomalous parity (of the type  $0^-, 1^+, 2^-, \dots$ ) in a wide range of energies. Only low-energy transitions (including  $\beta$  decays) had been sufficiently well studied; here, the quasiparticle picture works well and on its basis one can give a reasonable description of the positions of the states and the transition probabilities (for an appropriate choice of the operator  $e_q$ , which, in general, is not equal to the identity). The situation changed dramatically in recent years following the discovery and detailed investigation of charge-exchange spin-flip ( $\Delta S = 1$ ) giant resonances, in the first place Gamow-Teller resonances. There are strong indications that the total strength of the corresponding transitions in a wide range of excitation energies in heavy nuclei is about

half of the model-independent  $3(N-Z)$  sum rule for Gamow-Teller transitions, and approximately the same strength shortfall is observed for excitations of other multiplicities if comparison is made with ordinary shell calculations. As will be shown in the present paper, calculations based on the theory of finite Fermi systems lead to the conclusion that the first term in (13) correctly reproduces the region of localization of spin-flip charge-exchange excitations and gives absolute transition probabilities in agreement with the experiments for  $e_q[\sigma_T] \approx 0.8$ . Note that the local charge occurs in the polarization operator quadratically, so that this value of  $e_q$  corresponds to a quenching of the transition strength by about 40%.

It should be pointed out that a deviation of  $e_q$  from unity is no novelty in nuclear physics. Indeed, an analysis made almost 20 years ago simultaneously with the introduction of local charges into the theory of finite Fermi systems and dealing with low-energy  $M1$  and  $\beta$  transitions, and also with the magnetic moments of odd nearly magic nuclei, led to the conclusion that this charge probably lies in the range  $0.8 \leq e_q \leq 0.9$  (see the book of Ref. 11 and its appendices). The recent experiments clearly showed, first, that the quenching of the transitions due to  $e_q[\sigma_T]$  is completely universal, covering the region of the giant spin-flip resonances; second, they indicate that the local charge  $e_q[\sigma_T]$  corresponds to the lower limit of the previously found admissible range.

Whence comes such a pronounced difference between the quasiparticle responses of the nucleus to vector and axial-vector fields? The answer is that the former have rigorous conservation laws; the latter do not. Let us consider this in more detail.

### Gauge transformations and local charge

We shall use the fact that for some fields there is a simple connection between the vertices  $\mathcal{T}$  and the Green's functions  $G$  in the polarization operator (1). Suppose that the system is described by the Lagrangian (summation over all particles is understood)

$$\mathcal{L} = -\frac{1}{2m}(\nabla_\alpha \psi^\dagger)(\nabla_\alpha \psi) - \frac{1}{2i}\left(\psi^\dagger \frac{\partial \psi}{\partial t} - \frac{\partial \psi^\dagger}{\partial t} \psi\right) + \mathcal{L}_{\text{int}},$$

where the first two terms are the free Lagrangian and  $\mathcal{L}_{\text{int}}$  is the interaction Lagrangian. We transform the  $\psi$  operators as follows:

$$\psi(x) \rightarrow \exp[i f(x) Q] \psi(x) \approx \psi(x) + i f(x) Q \psi(x). \quad (15)$$

Using the equations of motion  $\delta \mathcal{L} / \delta \psi - \partial_\nu (\delta \mathcal{L} / \delta \partial_\nu \psi) = 0$ , we can write the change in the Lagrangian under this transformation in the form<sup>13</sup>

$$\delta \mathcal{L} = -\partial_\nu (j_\nu^Q f) = -j_\nu^Q \frac{\partial f}{\partial x_\nu} - \left(\frac{\partial j_\nu^Q}{\partial x_\nu}\right) f. \quad (16)$$

Here, we introduce the 4-dimensional "Q current"

$$j_\nu^Q = -i \frac{\delta \mathcal{L}}{\delta \partial_\nu \psi} Q \psi; \quad (17)$$

since  $\mathcal{L}_{\text{int}}$  does not depend explicitly on the time, its fourth component is

$$j_0^Q = \frac{1}{2}(\psi^\dagger Q \psi + \text{h.c.}). \quad (18)$$

If the Q current is conserved, i.e., its 4-divergence

satisfies  $\partial j_\nu^Q / \partial x_\nu = 0$ ,<sup>2)</sup> then in (16) there remains only the first term, and in this case the transformation of the  $\psi$  operators can be interpreted as the application of an external gauge field  $\partial f / \partial x_\nu$ , which interacts with the Q current of the system. If this current is not conserved, then we have an addition to the Lagrangian containing its 4-divergence.

The transformation (15) leads to the change  $\delta G = \delta(-i \langle T \psi(x) \psi^\dagger(y) \rangle) = i f(x) Q G(x, y) - i G(x, y) Q^\dagger f^\dagger(y)$  in the single-particle Green's function, from which, using the relation  $\delta G^{-1} = -G^{-1} \delta G G^{-1}$ , we obtain for the change in the reciprocal Green's function

$$\delta G^{-1}(x, y) = -\delta \Sigma(x, y) = -i [G^{-1}(x, y) Q f(y) - f^\dagger(x) Q^\dagger G^{-1}(x, y)]. \quad (19)$$

By definition, the change in the mass operator  $\delta \Sigma$  must be equal to the vertex part  $\mathcal{T}[\delta \mathcal{L}] = -\mathcal{T}[\delta \mathcal{L}]$ , so that  $\delta G^{-1} = \mathcal{T}[\delta \mathcal{L}]$ . The last relation is a generalized Ward identity. Going over to the Fourier representation with respect to the time, we have [for  $f(x) Q = \varphi(\mathbf{x}) Q \exp(i \omega t)$ , i.e., for fields of the type (3)]

$$\begin{aligned} & \omega \int \mathcal{T}(\mathbf{x}, \mathbf{y}, \mathbf{z}; \varepsilon, \omega; [j_0^Q]) \varphi(\mathbf{z}) d\mathbf{z} \\ & - i \int \mathcal{T}(\mathbf{x}, \mathbf{y}, \mathbf{z}; \varepsilon, \omega; [j_\alpha^Q]) \frac{\partial \varphi}{\partial x_\alpha} d\mathbf{z} \\ & - i \int \mathcal{T}(\mathbf{x}, \mathbf{y}, \mathbf{z}; \varepsilon, \omega; [\mathcal{D}^Q]) \varphi(\mathbf{z}) d\mathbf{z} \\ & = G^{-1}(\mathbf{x}, \mathbf{y}; \varepsilon + \frac{\omega}{2}) Q \varphi(\mathbf{y}) - \varphi^*(\mathbf{x}) Q^\dagger G^{-1}(\mathbf{x}, \mathbf{y}; \varepsilon - \frac{\omega}{2}). \end{aligned} \quad (20)$$

Note that we have here vertices for the time and space components of the Q current, and also the vertex for its divergence. We now consider the case when the transformation of the  $\psi$  operators leaves the functional  $\int \mathcal{L} d\mathbf{x}$  unchanged, i.e., the case of a conserved Q current. Then all the terms with a divergence in the expressions written down above are equal to zero. Further, if we assume that  $\varphi(\mathbf{x}) = \text{const}$  (this corresponds to application of a spatially constant field, i.e., to zero momentum transfer  $q$ ), we obtain from (20) in the  $\omega \rightarrow 0$  limit<sup>3)</sup>

$$\mathcal{T}[j_0^Q] = \frac{\partial G^{-1}}{\partial \varepsilon} Q. \quad (21)$$

Thus, from the Ward identity we have obtained an exact expression for  $q=0$  and  $\omega \rightarrow 0$  for the vertex of the operator  $j_\nu^Q$  given by the expression (18). Substituting (21) in the polarization operator (6) and using the relations

<sup>2)</sup> Conservation of the Q current means constancy in time of the integral  $\int j_0^Q d\mathbf{x}$ . For systems with a strong interaction, there follows from this the law of conservation of the number of particles (baryons) for  $Q=1$ , the law of conservation of the electric charge for  $Q=(1+\tau_z)/2$ , the law of conservation of the third projection  $T_z=(N-Z)/2$  for  $Q=\tau_z$ , and the law of conservation of the total isospin for  $Q=\tau$ . Together with the hypothesis of an isotriplet nature of the vector current (CVC), this leads, as we shall see, to the local quasiparticle charges being equal to unity as  $\omega, q \rightarrow 0$  for isoscalar ( $Q=1$ ) and isovector ( $Q=\tau_\alpha$ ) vertices.

<sup>3)</sup> Here, we do not consider the case of spontaneous symmetry breaking, i.e., we assume that the operator Q corresponding to the conserved current commutes with the Hamiltonian and with the mass operator  $\Sigma$ . In the case of spontaneous symmetry breaking there appears in the total vertex a singularity, the separation of which leads to the consistency conditions.<sup>14</sup> This in no way affects the following discussion.



$$\partial G^{-1}/\partial \varepsilon = -G^{-1} (\partial G/\partial \varepsilon) G^{-1};$$

$$\int dx G^{-1}(x, z; \varepsilon) G(z; y; \varepsilon) = \delta(x - y),$$

we find that  $P(\omega \rightarrow 0) = 0$  [since  $G(\varepsilon = -\infty) = G(\varepsilon = +\infty) = 0$ ]. This is no surprise, since a field constant in space and time does not induce physical transitions in the system. The performed gauge transformation with  $Q=1$  (or with  $Q=\tau_\alpha$ ) corresponds to a shift of the phases of the wave functions (or their rotation in isotropic space) by the same angle. We now show that

$$e_q[1] = 1; \quad e_q[\tau_\alpha] = 1. \quad (22)$$

It is particularly easy to do this for an infinite system; then  $A$  in (10) and (12)–(14) is proportional to  $q \cdot v / (\omega - q \cdot v)$ , where  $v$  is the quasiparticle velocity on the Fermi surface. In the limit when  $\omega \rightarrow 0$  and  $q \rightarrow 0$ , this expression is equal to 0 or  $-1$ , depending on the order in which the limit is taken: If we first set  $\omega = 0$  and then go to the limit  $q \rightarrow 0$ , we obtain  $-1$ ; if we do the reverse, 0. This is a manifestation of the essential singularity that we discussed above. In the considered case, the second alternative is realized, and from (10) we have  $\mathcal{T} = \mathcal{T}^\omega$ . In accordance with (21), the vertex  $\mathcal{T}$  on the Fermi surface contains as a factor and reciprocal residue  $a$  of the single-particle Green's function, and, recalling the definition (11), we obtain  $a\mathcal{T}^\omega = \mathcal{T}_0$ , which leads to the local charges (22).

For finite systems, the result will be the same. Indeed, if  $P(\omega \rightarrow 0) = 0$ , then both terms in (13) vanish: The system of quasiparticles possesses the properties of the real physical system and is not polarized in a constant external field. Introducing for it an effective Lagrangian and applying the same gauge transformations, we can show that the quasiparticle part of the polarization operator vanishes when  $q=0$  and  $\omega \rightarrow 0$  for operators  $Q$  that correspond to conservation laws. In such a field, there is no change in the density matrix of the quasiparticles:  $\delta\rho = AV = 0$ . This means that the propagator  $A$  is "orthogonal" to the effective field  $V$ , i.e., to the vertex  $\mathcal{T}$ , and from (10) we have  $\mathcal{T} = \mathcal{T}^\omega$ , which again leads to (22).

From the vanishing of the second term in (13) when  $\omega=0$  and from the fact that the regular part  $B$  does not have singularities at small  $\omega$  and  $q$  it follows that in all physical processes for which conservation laws exist it must behave in the limit  $\omega \rightarrow 0$  as  $\omega^\alpha$ , where  $\alpha > 0$  (in  $\text{Im}P$ , independently of  $q$ ). In fact, this multipair term vanishes at least as  $\omega^2$  or  $q^2$ , since it contains the characteristic parameters  $(\omega/\varepsilon_F)^2$  and  $(q/\varepsilon_F)^2$ .<sup>4)</sup>

We emphasize once more that this conclusion is valid only for vertices corresponding to a conserved cur-

rent.<sup>5)</sup> At the same time, the quasiparticle part of  $P(\omega)$  is not small of the same order, and in real physical processes it will be predominant (we recall the essential singularity in it and also the fact that the excitation energy can be made arbitrarily small, but not the momentum transfer). It is worth slightly changing the configuration of the external field  $V_0^q(x)$ , i.e., to regard it no longer as constant in time and space, when the quasiparticle excitation branch begins to respond "to the total force."

We now turn to the spin vertices. If the total spin of the system is an integral of the motion (there is no spin-orbit interaction or it plays a small part, as can be assumed for infinite nuclear matter), then by analogy with the foregoing we shall have  $e_q[\sigma_\alpha] = 1$ . With regard to the vertex  $\sim \sigma_\alpha \tau_\beta$ , for it no *a priori* conclusions can be drawn, and the corresponding local charge must be taken from experiments. The simplest parametrization is achieved by introducing a single constant  $\xi_s$  (see Ref. 11):

$$e_q[\sigma_\alpha \tau_\beta] = 1 - 2\xi_s. \quad (23)$$

Together with  $e_q[\sigma_\alpha] = 1$  this means that for an external field  $\sigma_\alpha$  acting, for example, on only the neutrons there is not only the local charge of the neutrons  $e_q^n[\sigma_\alpha^n] = 1 - \xi_s$  but also a local charge of the protons  $e_q^p[\sigma_\alpha^n] = \xi_s$ .

Since the " $\sigma\tau$  current" is not conserved and it is very difficult to calculate its divergence in the nucleus, it is not possible from the generalized Ward identity (20) to find the vertex  $\mathcal{T}[\sigma_\alpha \tau_\beta]$  for  $q=0$  and  $\omega \rightarrow 0$ , and one can only obtain the connection between the static vertex from the divergence  $\mathcal{T}[\mathcal{D}^{\sigma\tau}]$  and the commutator  $[G^{-1}, \sigma_\alpha \tau_\beta]$ . Further, if we write down an equation for  $\mathcal{T}[\mathcal{D}^{\sigma\tau}]$  analogous to (9) and use this connection, we can show<sup>13</sup> that the parameter  $\xi_s$  can be expressed in terms of an arbitrary local vertex  $\mathcal{T}^\omega[\mathcal{D}^{\sigma\tau}]$  with respect to the frequency  $\omega$  as  $\omega \rightarrow 0$ . In Ref. 13 qualitative arguments are advanced for smallness of this derivative and, accordingly, of  $\xi_s$ . Comparison with the experiments shows that  $\xi_s \approx 0.05$ – $0.1$ .<sup>11</sup>

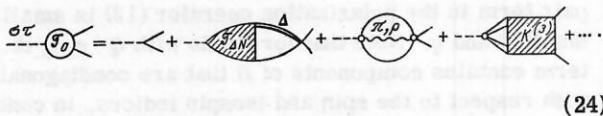
It is important to emphasize that, in contrast to the case of a conserved current, it is impossible to conclude rigorously for a field with  $Q \sim \sigma_\alpha \tau_\beta$  that the multipair term in the polarization operator (12) is small at small  $\omega$  and  $q$ . Note that for fields with  $Q \sim \sigma_\alpha \tau_\beta$  this term contains components of  $B$  that are nondiagonal with respect to the spin and isospin indices, in contrast to a field with  $Q \sim 1$ , when only diagonal  $B$  terms remain. This can also lead to a difference in the behavior of the multipair response, especially at small  $\omega$ . All one can hope is that the singularities in the regular part  $B$  (and in  $e_q$ ) lie far from the Fermi surface and that the multipair contribution in the region in which the quasiparticle response is mainly concentrated is

<sup>4)</sup>In accordance with their definition, the local charges  $e_q$  are associated with the "far" parts of  $B$  and  $\Gamma^\omega$ , and for non-vanishing  $\omega$  and  $q$  they can contain corrections of the same order of smallness. In this sense, one can speak of a quasiparticle form factor that differs from the vacuum nucleon form factor, for which the characteristic parameter is  $(q/\Lambda)^2$  with  $\Lambda \approx 1$  GeV.

<sup>5)</sup>The breaking of the isotopic invariance in the nucleus by the Coulomb interaction does not change the situation and, in particular, does not affect  $e_q$ . The divergence of the current for the operators  $\tau_\mp$ —the smooth Coulomb average field—is well known, and its contribution to the various processes, including charge-exchange reactions, can be taken into account fully.

small. At the same time, we have seen that the quasi-particle-quasihole excitations are suppressed, the quenching factor being the square  $e_q^2[\sigma\tau] = (1 - 2\zeta_s)^2$  of the local charge. It is not impossible that the remaining fraction of the strength of the  $\sigma\tau$  transitions missing in accordance with the model-independent  $3(N-Z)$  sum rule (or the essential part of this fraction) is "mixed" over multipair excitations in a broad interval, possibly in a region above the Gamow-Teller resonance up to energies  $\omega \sim \epsilon_F$ . We note in this connection that the absence of conservation laws fosters mixing effects: it is sufficient to compare the width of the analog  $0^+$  resonance ( $\Gamma \approx 200$  keV) and the width of the Gamow-Teller resonance ( $\Gamma \approx 4$  MeV) situated at approximately the same energy for the isobaric  $^{208}\text{Pb} \rightarrow ^{208}\text{Bi}$ .

A field containing the operator  $\sigma_\alpha \tau_\beta$  is unique in one respect: It can excite not only degrees of freedom of the nucleus regarded as a system of neutrons and protons but also internal degrees of freedom of a nucleon itself, transforming it into a  $\Delta$  isobar. For this, large energies are required (about 300 MeV). In connection with the "shortage" of strength of the Gamow-Teller transitions, there has recently been much discussion of the possibility that the process we are discussing could be responsible for, on the one hand, virtual  $\Delta$ -isobar-nucleon-hole excitations quenching the strength of the Gamow-Teller transitions at low excitation energies and in the region of the GT resonance and, on the other, the real process of  $\Delta$ -isobar production taking over the withdrawn strength. It is very difficult to test the second assumption experimentally, since in processes involving the real production of the  $\Delta$  isobar on a nucleus it is necessary to select events with small momentum transfer in order to recognize the probability distribution of the Gamow-Teller transitions at  $q = 0$ . At the same time, the first assumption can be regarded as true in the sense that virtual  $\Delta N$  excitations make one of the possible contributions to the renormalization of the  $\sigma\tau$  vertex. In diagram language, allowance for such processes reduces, in particular, to one having to use as the vertex  $\mathcal{T}_0$  in the polarization operator (1) not simply the local field  $V(x)\sigma_\alpha \tau_\beta$  but a generalized vertex of the form



(24)

Here,  $\mathcal{T}_{\Delta N}$  is the irreducible (in the particle-hole channel)  $N \rightarrow \Delta$  vertex. The graph with irreducible (in the same channel) three-particle interaction amplitude  $\mathcal{K}^{(3)}$  is given to show that the operator of the nonconserved axial-vector current can contain many-particle components. The dots at the end indicate that there may also be a contribution of other mechanisms associated, in particular, with the excitation of higher baryon resonances and mesons. It is very difficult to calculate all processes of such type; at low energies  $\omega$  they are strongly virtual and give, as one could expect, a universal contribution, this appearing in the theory of finite Fermi systems as a single phenomenological quantity—the local charge  $e_q[\sigma\tau]$ .

## 2. EFFECTIVE NUCLEON-NUCLEON INTERACTION

Thus, in the theory of finite Fermi systems<sup>11</sup> the behavior of the nucleus in the external field  $V_0$  can be described by means of an effective field  $V$  satisfying Eq. (14). In more detail, this equation has the form

$$V(\mathbf{r}; \omega) = e_q V_0(\mathbf{r}) + \int \mathcal{F}(\mathbf{r}, \mathbf{r}_1) A(\mathbf{r}_1, \mathbf{r}_2; \omega) V(\mathbf{r}_2; \omega) d\mathbf{r}_1 d\mathbf{r}_2, \quad (25)$$

where  $\mathcal{F}$  is the irreducible (in the particle-hole channel) quasiparticle interaction amplitude, which we shall simply call the *effective interaction*;  $A$  is the particle-hole propagator;  $e_q$  is the effective charge of a nucleon quasiparticle relative to the field  $V_0$ ; and  $\omega$  is the excitation energy of the nucleus. For simplicity, we omit as before the isotopic and spin indices. The form of Eq. (25) presupposes that  $\mathcal{F}$  does not contain nonlocal terms in the transverse scattering channel (velocity forces); in addition, retardation effects are not included explicitly in (25). Because of this last circumstance, (25) looks like the equation of the random-phase approximation (RPA); differences are that in the standard RPA with a Hartree-Fock basis the amplitude  $\mathcal{F}$  in (25) is replaced by the (antisymmetrized) two-body interaction potential and, in addition, in the RPA there is no concept of a local charge, i.e., for all fields  $e_q = 1$  [the corrections to the RPA from diagrams of the type (24) can be taken into account separately].

To describe the properties of the charge-exchange nuclear excitations, it is necessary to know the isospin-dependent components of the amplitude  $\mathcal{F}$ . In the theory of finite Fermi systems, this reduces to the parametrization of the amplitude  $\mathcal{F} = 2\mathcal{F}'$ , which occurs in the equation for the corresponding effective field. The simplest parametrization, which was proposed by Landau in the theory of Fermi liquids and was taken into nuclear physics by Migdal in the sixties,<sup>11</sup> consists of introducing just two constants  $f'$  and  $g'$ , which characterize the zeroth harmonics in the expansion of the amplitude  $\mathcal{F}'$  in a series in Legendre polynomials in the angle between the momenta of colliding quasiparticles on the Fermi surface, which in the coordinate representation reduces to the expression

$$\mathcal{F}' = C_0 (f' + g' \sigma_1 \sigma_2) \tau_1 \tau_2 \delta(\mathbf{r}_1 - \mathbf{r}_2). \quad (26)$$

Here,  $C_0 = (dn/d\epsilon)^{-1} = \pi^2/p_F m$  is a normalization factor, the reciprocal of the density of single-particle levels at the Fermi surface.<sup>6)</sup> In many studies in the early period of the application of the theory of finite Fermi systems to nuclei (see, for example, the appendices to Ref. 11), such a parametrization was used quite effectively to describe phenomena in which small momentum transfers play the leading part. The investigations made in recent years have shown that when applied to finite nuclei the parametrization (26) is too simplified.

<sup>6)</sup> Here we shall stick to the value  $C_0 = 300 \text{ MeV} \cdot \text{F}^3$ , which corresponds to the density  $\rho_0 = 0.0859 \text{ F}^{-3}$  of nucleons of one species in symmetric ( $N=Z$ ) nuclear matter, to Fermi momentum  $p_F = 1.365 \text{ F}^{-1}$ , and to Fermi energy  $\epsilon_F = 38.66 \text{ MeV}$ ; at the same time, the parameter  $r_0$ , which determines the asymptotic behavior of the nuclear radius at large mass numbers  $A (R = r_0 A^{1/3})$ , is equal to  $r_0 = 1.116 \text{ F}$ . The effective mass  $m^*$  is assumed equal to the mass  $m$  of a free nucleon.



Let us consider what modifications must be introduced in the amplitude (26) from a modern point of view.

#### Spin-independent components of the effective interaction

In the first place, the introduction into the theory of the consistency conditions<sup>14</sup> shows that the isospin amplitude, which is proportional to  $f'$ , depends on the nucleon density  $\rho$ , and, therefore, the corresponding constant may vary from some value  $f'_{in}$  within the nucleus to a value  $f'_{ex}$  outside it. In a simple example we shall see that such a transition from an internal to a vacuum value does indeed occur, but, in contrast to the isoscalar amplitude  $f$ , it is not very abrupt; at the least, it takes place without a change of sign. In certain situations, this made possible a restriction to the introduction of a single constant  $f'_{in}$ , which is related to the parameter  $\beta$  that occurs in the symmetry energy  $E_{sym} = \beta(N-Z)^2/A$  in the semiempirical mass formula by the relation<sup>11</sup>  $\beta = \epsilon_F(1 + 2f'_{in})/3$ , which is one of the consistency conditions in infinite nuclear matter. For a finite nucleus, if nonlocality of the effective interaction  $\mathcal{F}$  in the scattering channel is ignored (velocity harmonics) and the interaction is assumed to be nonretarded, the condition of self-consistency between the single- and two-particle characteristics will have the simple form<sup>14,15</sup>

$$\partial U^i / \partial \mathbf{r} = \sum_k \int \mathcal{F}^{ik}(\mathbf{r}, \mathbf{r}'; [\rho]) (\partial \rho^k / \partial \mathbf{r}') \partial \mathbf{r}', \quad (27)$$

where the indices  $i, k$  ( $=n, p$ ) refer to a definite nucleon species. For a given form of the amplitudes  $\mathcal{F}^{ik}$ , this equation makes it possible to find self-consistent potentials  $U^i$ , which are local in the indicated approximations, and the nucleon densities  $\rho^i$ . The condition (27) and the appearance of a density dependence of  $\mathcal{F}$  are a consequence of the spontaneous breaking of a symmetry—translational invariance in the given case—in a finite nucleus. The origin of the dependence  $\mathcal{F}([\rho])$  can be seen particularly clearly from the consistency conditions of higher order, for example, from the condition that relates the sum of the derivatives with respect to all spatial coordinates of the two-particle amplitude  $\mathcal{F}$  to the sum of the gradients of the density matrix by an integral equation whose kernel is the irreducible amplitude  $\mathcal{K}^{(3)}$  of the three-particle interaction<sup>15</sup>:

$$\left( \frac{\partial}{\partial \mathbf{r}_1} + \dots + \frac{\partial}{\partial \mathbf{r}_4} \right) \mathcal{F}(\mathbf{r}_1, \dots, \mathbf{r}_4) = \int \mathcal{K}^{(3)}(\mathbf{r}_1, \dots, \mathbf{r}_6) \left( \frac{\partial}{\partial \mathbf{r}_5} + \frac{\partial}{\partial \mathbf{r}_6} \right) \rho(\mathbf{r}_5, \mathbf{r}_6) d\mathbf{r}_5 d\mathbf{r}_6.$$

If this amplitude is also assumed to be local, then from this integral equation it follows directly that the two-particle amplitude  $\mathcal{F}$  contains not only terms that depend only on the coordinate differences (translationally invariant!) but also terms linear in the density. Taking into account the Pauli principle, which prevents three identical particles being at one spatial point, we can write down in this simple model

$$\left. \begin{aligned} \mathcal{F}^{pp}(\mathbf{r}_1, \mathbf{r}_2; [\rho]) &= C_0 \left[ v_1(\mathbf{r}_1 - \mathbf{r}_2) + \frac{b}{\rho_0} \rho^n \left( \frac{\mathbf{r}_1 + \mathbf{r}_2}{2} \right) \delta(\mathbf{r}_1 - \mathbf{r}_2) \right] + \mathcal{F}^{Comt}; \\ \mathcal{F}^{nn}(\mathbf{r}_1, \mathbf{r}_2; [\rho]) &= C_0 \left[ v_1(\mathbf{r}_1 - \mathbf{r}_2) + \frac{b}{\rho_0} \rho^p \left( \frac{\mathbf{r}_1 + \mathbf{r}_2}{2} \right) \delta(\mathbf{r}_1 - \mathbf{r}_2) \right]; \\ \mathcal{F}^{np}(\mathbf{r}_1, \mathbf{r}_2; [\rho]) &= C_0 \left[ v_2(\mathbf{r}_1 - \mathbf{r}_2) + \frac{b}{\rho_0} \rho^+ \left( \frac{\mathbf{r}_1 + \mathbf{r}_2}{2} \right) \delta(\mathbf{r}_1 - \mathbf{r}_2) \right], \end{aligned} \right\} \quad (28)$$

where  $b$  is the dimensionless constant of the local "three-particle" forces, and  $\rho^+ = \rho^n + \rho^p$ . Note that in nuclei with  $N \neq Z$ , even in the absence of a Coulomb potential ( $\mathcal{F}_{Coul} = 0$ ), the amplitudes  $\mathcal{F}^{nn}$  and  $\mathcal{F}^{pp}$  in (28) are not equal, since  $\rho^n \neq \rho^p$ . Thus, the interaction (28) effectively includes a dependence on the isospin of the ground state. At the same time, the relation  $\mathcal{F}^- = \mathcal{F}^{nn} - \mathcal{F}^{pp} = \mathcal{F}^{pp} - \mathcal{F}^{nn}$ , which is valid for (26), no longer holds. Which amplitude  $\mathcal{F}^-$  must in this case occur in the equation for the charge-exchange effective field? One further self-consistency condition, associated with the spontaneous breaking of isotopic symmetry, helps us to answer this question<sup>14,15</sup>:

$$U^-(\mathbf{r}) = \int \mathcal{F}^-(\mathbf{r}, \mathbf{r}'; [\rho]) \rho^-(\mathbf{r}') d\mathbf{r}'. \quad (29)$$

Here  $U^-(\mathbf{r}) = U^n(\mathbf{r}) - U^p(\mathbf{r})$ ,  $\rho^-(\mathbf{r}) = \rho^n(\mathbf{r}) - \rho^p(\mathbf{r})$ . This condition reflects the fact that in nuclei with  $N \neq Z$  all states must, if the isotopic spin is conserved, be degenerate with respect to the isospin projections, this including the ground state and analog state. The relation (29) is valid when the Coulomb interaction is switched off, but in the model considered here it also remains true, as follows from (27) and (28), when  $\mathcal{F}_{Coul}$  is taken into account, except that the proton potential  $U^p$  in the difference  $U^n - U^p$  in (29) is not complete—it must not contain the direct contribution  $\mathcal{F}_{Coul}$ , although there are included in it (and also in  $U^n$ ) contributions in higher orders that arise as a result of the self-consistency. Indeed, when  $\mathcal{F}_{Coul}$  is included the densities  $\rho^p$  and  $\rho^n$  and the amplitudes  $\mathcal{F}^{ik}[\rho]$  themselves change, and the solutions of the system of nonlinear equations (27) change accordingly. In our simple model, we can readily construct from these equations with the amplitudes (28) the potentials  $U^n$  and  $U^p$  in analytic form and obtain the relation (29), in which it is necessary to set

$$\mathcal{F}^-(\mathbf{r}, \mathbf{r}'; [\rho]) = C_0 \left[ v_1(\mathbf{r} - \mathbf{r}') - v_2(\mathbf{r} - \mathbf{r}') - \frac{b}{2\rho_0} \rho^+ \left( \frac{\mathbf{r} + \mathbf{r}'}{2} \right) \delta(\mathbf{r} - \mathbf{r}') \right]. \quad (30)$$

It is this amplitude that must occur in the equation for the charge-exchange effective field, replacing the component proportional to  $f'$  in (26). The fulfillment of the condition (29) in the solution of the equation for the effective field (or in RPA calculations) in the case of Fermi transitions guarantees the absence of spurious isospin-mixing effects; at the same time, the single-particle basis must be complete. We decompose the translationally invariant terms proportional to  $(v_1 - v_2)$  in (30) into local and nonlocal parts, so that finally the interaction  $\mathcal{F}^-$  takes the form

$$\mathcal{F}^-(\mathbf{r}, \mathbf{r}'; [\rho]) = 2C_0 \left[ a'_0 \delta(\mathbf{r} - \mathbf{r}') + a'_r v'(\mathbf{r} - \mathbf{r}') - \frac{b}{4\rho_0} \rho^+ \left( \frac{\mathbf{r} + \mathbf{r}'}{2} \right) \delta(\mathbf{r} - \mathbf{r}') \right], \quad (31)$$

where  $a'_0$ ,  $a'_r$ , and  $b$  are dimensionless constants;  $v'$  is a function that has a finite range and is normalized by the condition  $\int v'(\mathbf{r}) d\mathbf{r} = 1$ ; for it we shall use the Yukawa form

$$v'(\mathbf{r} - \mathbf{r}') = \frac{1}{4\pi(r'_0)^3 |\mathbf{r} - \mathbf{r}'|} \exp \left( -\frac{|\mathbf{r} - \mathbf{r}'|}{r'_0} \right)$$

with "nonlocality range"  $r'_0$ . The introduced parameters are related to the ordinary constants  $f'_{in} = 2f'_{in}$  and  $f'_{ex}$

$= 2f'_{\text{ex}}$  of the theory of finite Fermi systems by

$$f_{\text{in}} = 2(a'_0 + a'_1) - b; \quad f_{\text{ex}} = 2(a'_0 + a'_1). \quad (32)$$

We estimate the possible values of the force constants. In the considered model, this can be done particularly easily. It can be shown that with the interaction (28) one can construct<sup>15</sup> the equation of state of infinite nuclear matter, and from the equilibrium condition—the vanishing of the pressure at normal density—one can obtain the relation<sup>7)</sup>

$$b = (f_{\text{in}}^* - f_{\text{ex}}^*)/3 = -3\mu_{\infty}/\epsilon_F^0 + 3/5, \quad (33)$$

where  $\mu_{\infty}$  is the chemical potential;  $f_{\text{in}}^*$  and  $f_{\text{ex}}^*$  are isoscalar constants that can also be expressed in terms of  $\mu_{\infty}$  and  $\epsilon_F^0$ :

$$f_{\text{in}}^* = -3\mu_{\infty}/\epsilon_F^0 - 3/5; \quad f_{\text{ex}}^* = 6\mu_{\infty}/\epsilon_F^0 - 12/5. \quad (34)$$

For  $\mu_{\infty} = -16$  MeV, we obtain from this  $b \approx 2$ ,  $f_{\text{in}}^* \approx 0.6$ , and  $f_{\text{ex}}^* \approx -5$ . From the expression for the symmetry energy  $\beta_{\infty}$  mentioned above and from Eqs. (32)–(34) we have

$$f_{\text{in}} = 3\beta_{\infty}/\epsilon_F^0 - 1; \quad f_{\text{ex}} = f_{\text{in}} + b = 3(\beta_{\infty}/\epsilon_F^0 - \mu_{\infty}/\epsilon_F^0) - 2/5. \quad (35)$$

For  $\beta_{\infty} \approx 30$  MeV, we obtain  $f_{\text{in}}^* \approx 1.3$  and  $f_{\text{ex}}^* \approx 3.3$ . It can be seen from these estimates that the effective interaction must change appreciably on the surface of the nucleus, the isoscalar amplitude  $\mathcal{F}$  having a particularly strong change on the transition from the internal to the external region. The analysis of Ref. 15 shows that such behavior is necessary for stability of the nuclear ground state. How much does the density dependence in the isovector channel  $\mathcal{F}^-$  influence observable quantities, in particular the positions of the analog resonance and other charge-exchange excitations of normal parity? One of the aims of the present paper is to answer this question.

To conclude this section, we make a small historical digression. The need for the introduction of a density dependence (in the isoscalar channel) of the effective interaction was demonstrated for the first time<sup>16</sup> in 1965–1966 in the analysis of the experimental data on isotopic shifts and quadrupole moments, and for its simulation a simple interpolation law of variation from  $\mathcal{F}_{\text{in}}^*$  to  $\mathcal{F}_{\text{ex}}^*$  corresponding to a linear dependence on  $\rho$  was proposed. Soon after this, such a law was obtained in Ref. 17 at an elementary qualitative level by considering the simplest energy functional ensuring a mini-

<sup>7)</sup>The energy density  $\epsilon = E/V$ , where  $E$  is the total energy and  $V$  is the volume of the system, is given for isosymmetric ( $\rho^n = \rho^{\bar{n}} = \rho$ ) nuclear matter in the considered model by the expression  $\epsilon = 2\rho\epsilon_F^0\varphi(x)$  with the function  $\varphi(x) = 3x^{2/3}/5 + f_{\text{ex}}^*x/3 + bx^2/3$  of the dimensionless variable  $x = \rho/\rho_0$ . Here,  $\epsilon_F^0$  is the Fermi energy in the equilibrium state, i.e., for  $x=1$ , and  $f_{\text{ex}}^* = \int [v_1(r) + v_2(r)]dr$  is the sum of the volume integrals of the first terms in the amplitude  $\mathcal{F}^m$  and  $\mathcal{F}^{n\bar{n}}$  in (28), which corresponds to zero momentum transfer. In terms of the function  $\varphi(x)$  and its derivatives we can find the following quantities: the chemical potential  $\mu = \partial\epsilon/\partial\rho = \epsilon_F^0(\varphi + x\partial\varphi/\partial x)$ , the pressure  $P = -\partial\epsilon/\partial V = 2\rho\mu - \epsilon = 2\rho_0\epsilon_F^0x^2\partial\varphi/\partial x$ , i.e., the equation of state at zero temperature, the compressibility  $K = 9\rho_0^2\partial\rho/\partial\rho = 9\epsilon_F^0x(2\partial\varphi/\partial x + x\partial^2\varphi/\partial x^2)$ , and, thus, the adiabatic velocity of sound in units of the velocity of light:  $c_s/c = (\partial P/\partial\epsilon)^{1/2} = (K/9(mc^2 + \mu))^{1/2}$ . At the same time, the internal isoscalar constant  $f_{\text{in}}^*$  is determined by the relation  $f_{\text{in}}^* = f_{\text{ex}}^* + 3b$ .

mum of the binding energy at the equilibrium nuclear density. After the formulation at the beginning of the seventies of the self-consistency conditions,<sup>14,15</sup> it became clear that the origin of the dependence of  $\mathcal{F}$  on  $\rho$  is fundamental in nature, following from the general laws that hold in systems with spontaneous breaking of translational invariance and is a "price" that must be paid to compensate the lost "displacement" symmetry and correctly separate the gapless (Goldstone) excitations corresponding to displacement of the system as a whole (isoscalar "ghost" dipole for the nucleus; for details of this, see Ref. 15). In the simple model we see that the isovector amplitude  $\mathcal{F}^-$  also begins to depend on  $\rho$ . We add that the calculation of the Fermi-liquid parameters using the vacuum nucleon–nucleon potentials through the reaction matrix by Brückner's method made in Ref. 18 confirms the growth of the constant  $f'$  with decreasing density, the scale of its variation agreeing qualitatively with the estimates given here.

The dependence  $\mathcal{F}[\rho]$  is determined by the properties of the three-particle amplitude  $\mathcal{K}^{(3)}$  in the nucleus, about which little is known. The explicit form of  $\mathcal{F}[\rho]$  can be obtained only under very special assumptions about the amplitude  $\mathcal{K}^{(3)}$ , as was done above. Note that in the Hartree–Fock method with effective Skyrme-type forces<sup>19</sup> the introduction of a density dependence in the effective interaction is associated with the consideration of, not the three-particle amplitude, but the original contact three-particle potential with its averaging over the coordinates of one particle. Such a prescription could be justified to some extent if in reality there existed large "bare" three-particle forces. However, in the nucleus this is not so.<sup>20</sup> Therefore, the transition in the Hartree–Fock method from the original potentials to effective forces must be regarded as a very artificial device. In the construction of the RPA equation with a corresponding Hartree–Fock basis the relations  $\mathcal{F}^{ik} = \delta U^i/\delta\rho^k$  are used, i.e., some of the fundamental relations of the theory of Fermi liquids. As a result, such an approach would link up to the approach based on the ideas of the theory of finite Fermi systems. Essentially, the former is a consequence of the latter, i.e., the Hartree–Fock method follows from the theory of finite Fermi systems if retardation effects in the effective interaction are ignored.<sup>15</sup> In particular, there is a common element of phenomenology: the main parameters of the forces in both approaches can be fixed using the properties of nuclear matter (the binding energies, compressibilities, equilibrium density, symmetry energy, etc.). But we see that the points of departure of these approaches are quite different.

We come to one further point. It is well known that to describe nuclear properties such as the rms radii and the binding energy the Hartree–Fock method uses two-body potentials of finite range (or the first terms of the expansion with respect to this range containing gradient operators), and because of the antisymmetrization conditions this leads to the appearance of rather large velocity forces and an appreciable deviation of the effective mass  $m^*$  from the vacuum value  $m$ . There also



arise unrealistic spin-dependent components, which frequently lead to spin collapse, and to ward off this it is necessary to use special measures (see, for example, Ref. 21 and the references there). Phenomenological analysis of the consistency conditions [of the type (27) and (29)] does not help here at all, since for nuclei with vanishing spin these components hardly occur at all. The spectra of the single-particle levels with such forces are too "rarefied," and their density near the Fermi surface is lower than the observed density. The experiments also show that on the Fermi surface  $m^* \approx m$ . There are attempts to explain the "compression" of the levels to bring them into agreement with experiment by the influence of low-lying collective states<sup>22</sup> and to justify the use of "rarefied" Hartree-Fock spectra to calculate some selected properties of nuclei<sup>23</sup> in the framework of a "dynamical theory".<sup>24</sup> However, the self-consistent calculations of Ref. 25 show that the level shifts due to the coupling to surface vibrations are small and are certainly quite inadequate to bring the scheme of single-particle levels obtained, say, using the popular variant III of the Skyrme forces into agreement with the experiments. Allowance for an energy dependence in the potential of the average field and in the effective interaction at the quantitative rather than the qualitative level is not possible within the framework of the standard RPA and requires the development of a new self-consistent approach. First steps in this direction have already been taken.<sup>26</sup>

In the calculations whose results will be given here we prefer not to come into conflict with the fundamental principles of the theory,<sup>11</sup> according to which the particle-hole propagator in Eq. (25) must correspond to a self-consistent potential that, by definition, ensures the experimental single-particle spectrum. As effective forces, we shall use the amplitude (31) matched to the isovector potential and the density by (29).

### Spin-dependent effective forces

As we have already pointed out, the parametrization of the amplitude  $\mathcal{F}$  by the simple expression (26) is intended for the description of phenomena corresponding to small momentum transfers  $q \ll p_F$ . However, in nuclei there are few such phenomena. Large momenta are essential, in particular, in the description of low-lying states of both electric<sup>15, 27</sup> and magnetic<sup>28-31</sup> type. In the first case, this is due to the finite-size effects, which lead to the appearance of a sharp surface peak in the form factors and transition densities; the correct description of these effects requires self-consistency and the introduction of a density dependence of the interaction, and this leads to the presence of high-momentum components in  $\mathcal{F}$ . In the second case, to describe anomalous-parity excitations it is important to take into account the pionic degrees of freedom and possible "softening" of the pionic mode, which requires the separation in the equations of the theory of the one-pion exchange amplitude  $G_\pi(k)$  in the annihilation channel.<sup>32</sup> The distinguished role of  $G_\pi(k)$  is determined by the fact that one-pion exchange generates the longest-range attractive component of the nuclear forces with characteristic momenta  $k \sim m_\pi \sim p_F/2$ , whereas the ex-

change of other mesons corresponds to momenta of the order of the reciprocal of the core radius  $r_c$ , i.e.,  $k \sim 2p_F$ , and gives short-range repulsion, which is generally simulated in the spin-isospin channel by the Landau-Migdal constant  $g'$ . In particular, the  $\rho$ -meson exchange amplitude has the same characteristic scale of variation ( $k \sim m_\rho \sim 2p_F$ ). The contributions to the interaction that vary smoothly over the interval  $0 \leq k \leq 2p_F$  are local, and they can be included in the single effective constant  $g'$ . In principle,  $g'$  may depend on the density, so that the internal value of  $g'$  may differ from the vacuum value; however, as calculations<sup>18</sup> by the Brückner method show, the jump in  $g'$  on the surface of the nucleus is small. At least, no phenomena have yet been detected from which the necessity of introducing interpolation for  $g'$  follows. Thus, we represent the spin-isospin interaction (in the momentum space) in the form

$$\left. \begin{aligned} G' &= (G^- + G_\pi)/2; \quad G^- = 2C_0 g' \sigma_1 \sigma_2; \\ G_\pi &= 2C_0 g_\pi (e_q^\pi)^2 (\sigma_1 k) (\sigma_2 k) / [m_\pi^2 + k^2 + P(k^2)]. \end{aligned} \right\} \quad (36)$$

Such a form of the interaction has been widely used to analyze the part played by the pionic degrees of freedom in nuclei and to investigate the effects of the proximity to the point of the  $\pi$ -condensate instability (see the review of Ref. 31). Here,  $g_\pi = 4\pi (f_\pi^2/m_\pi^2)/C_0$ , where  $f_\pi$  is the pion-nucleon coupling constant (as  $k^2 \rightarrow 0$ ). Using the known values  $f_\pi^2 = 0.081$  and  $m_\pi = 135$  MeV and the normalization parameter  $C_0 = 300$  MeV  $\cdot$  F<sup>3</sup>, we obtain  $g_\pi = -1.45$ . The momentum dependence of the local charge  $e_q^\pi$  with respect to the field  $(\sigma \cdot k)\tau_\alpha$  has the same characteristic scale ( $\approx 2p_F$ ) as the constant  $g'$ , and therefore we shall assume

$$e_q^\pi(k^2) \approx e_q^\pi(0) = 1 - 2\zeta_s, \quad (37)$$

where  $\zeta_s$  is a constant that in accordance with (23) determines the deviation from unity of the local quasiparticle charge  $e_q[\sigma\tau]$  for the field  $V_0 \sim \sigma_\alpha \tau_\beta$ . We have discussed this in detail in Sec. 1. With the same reason as permits the substitution (37), we shall in the one-pion exchange amplitude in (36) ignore the momentum dependence of the form factor of the pion-nucleon vertex, simply setting it equal to unity. In the denominator of the second term in the square brackets in (36),  $P(k^2)$  is the irreducible polarization operator of a pion in the nuclear medium; it does not include transitions of particle-hole type, the main contribution to which is associated with the virtual production of the  $\Delta$  isobar.<sup>29, 30</sup> For our purposes, it is sufficient to use the standard phenomenological expression (see, for example, Refs. 30-32).

$$P(k^2) = -0.9 (1 - \alpha) k^2 / (1 + 0.23k^2/m_\pi^2), \quad (38)$$

where the factor  $1 - \alpha$  takes into account the possible difference between the  $\pi N\Delta$  vertex and the vacuum vertex. In Ref. 30, the estimate  $-0.2 \leq \alpha \leq 0.3$  is obtained. Here, we take the value  $\alpha = 0$ . Note that from the very beginning we have not included in the pion propagator a dependence on the nuclear excitation energy  $\omega$ , since we here consider the case of low frequencies  $\omega < \varepsilon_F < m_\pi$ .

The one-pion exchange amplitude in (36) corresponds

to a nonlocal tensor interaction. In  $G'$  there may be tensor components with much shorter nonlocality range, resulting, for example, from exchange of the same  $\rho$  meson.<sup>33</sup> Such components are not included in (36), since they play an important part only in the description of nuclear properties at large momentum transfers, which are not considered here. However, the neglect of these components, and also the contributions from meson exchange in the transverse scattering channel (including the velocity harmonics) and the possible dependence of  $g'$  on the density (and thus on  $A$  and  $N-Z$ ) has the consequence that  $g'$  in (36) is not a strictly universal constant—it may differ somewhat for different states and different nuclei. Of course, the scale of these differences cannot be large, since otherwise the entire argument used in the choice of the parametrization (36) falls to the ground. One of the aims of the review—besides the investigation of the part played by one-meson exchange in the charged channel—is the determination of the constant  $g'$  and possible fluctuations of it by comparison with experimental data on charge-exchange excitations using the comparatively simple interaction (36). In conclusion, we mention Ref. 34, in which various contributions to the interaction are considered in more detail.

### 3. SUM RULES FOR CHARGE-EXCHANGE EXCITATIONS

The sum rules are intended to describe integrated characteristics of the spectrum of nuclear excitations in a given external field  $V_0$ . For the charge-exchange channel, one generally considers the moments of the strength function (5):

$$m_k^{(\pm)} = \int d\omega \omega^k S^{(\pm)}(\omega) = \sum_s \omega_s^k |\langle s | V_0^\pm | 0 \rangle|^2, \quad (39a)$$

where  $k=0, \pm 1, \pm 2, \dots$ , the signs  $(\pm)$  refer to the fields containing the operators  $\tau_\pm$ , and the integration (summation) is over all states of the corresponding branch. Knowing the first few moments  $m_k$ , we can determine the mean excitation energy of the nucleus in the field  $V_0$  and estimate its dispersion. In the cases when the dispersion is small and the transition strength is concentrated in a narrow region of energies (one collective state is predominant), the sum rules make it possible to find the energy of this state and establish how it varies from nucleus to nucleus without recourse to complicated microscopic calculations.

Unfortunately, model-free sum rules can be obtained in closed form only in some of the simplest situations in which general laws (such as particle-number conservation) operate and only the completeness properties of the eigenstates of the system are used. In the majority of cases, it is not possible to calculate  $m_k$  without recourse to models. In particular, an approach that has recently become popular for these purposes is based on the Hartree-Fock method with effective forces in conjunction with the RPA (see, for example, Ref. 35). Our task here is to develop a technique for calculating sum rules in the framework of the theory of finite Fermi systems. We are actually talking about the calculation of the moments  $m_k$  of the strength function for parti-

cle-hole excitations that is associated with the imaginary part of the first term in the polarization operator (13):

$$m_k^{(\pm)} = \int d\omega \omega^k \left[ -\frac{1}{\pi} \text{Im} (e_q V_0^{(\pm)} A V^{(\pm)}) \right]. \quad (39b)$$

Of course, we consider moments  $m_k$  that converge at energies  $\omega < \varepsilon_F$ , which corresponds to the region of applicability of the theory of finite Fermi systems. We show here that the moments  $m_k$  can be expressed for  $k \geq 0$  in the form of certain mean values of effective interactions over the quasiparticle distributions in the nuclear ground state. An important part is here played by the consistency conditions, which not only enable us to simplify the expressions for the moments but also to give them a perspicuous physical meaning.

#### Technique for calculating sum rules

The effective field  $V$  in (39b) satisfied Eq. (14) or (25). However, the imaginary part of the polarization operator actually contains the residues  $g^s$  of the field  $V$  at the poles  $\omega = \omega_s$  corresponding to eigenstates of the system. These residues satisfy a homogeneous equation that can be obtained from (14) by omitting the bare term  $e_q V_0$ ; for our purposes, it is convenient to express it in the  $\lambda$  representation:

$$g_{\lambda\lambda'}^s = \sum_{\lambda_1\lambda_2} \mathcal{F}_{\lambda\lambda';\lambda_1\lambda_2} \frac{n_{\lambda_1} - n_{\lambda_2}}{e_{\lambda_1} - e_{\lambda_2} - \omega_s} g_{\lambda_1\lambda_2}^s. \quad (40)$$

The residues  $g^s$  are normalized by the condition<sup>11</sup>

$$(g^s \frac{dA}{d\omega} g^s)_{\omega=\omega_s} \equiv \sum_{\lambda\lambda'} g_{\lambda\lambda'}^s \frac{n_{\lambda} - n_{\lambda'}}{(e_{\lambda} - e_{\lambda'} - \omega_s)^2} g_{\lambda\lambda'}^s = \Lambda_s, \quad (41)$$

where  $\Lambda_s$  takes the value  $+1$  or  $-1$ , depending on the branch to which the given excitation corresponds (the  $+$  sign for fields  $V_0 \sim \tau_+$ , the  $-$  sign for  $V_0 \sim \tau_-$ ). We determine this quantity by means of the relation

$$\Lambda_s = -\omega_s / |\omega_s|$$

and call it the *signature of the excitation*. The part played by  $\Lambda_s$  will become clear in what follows. Apart from the residue  $g^s$ , which is sometimes called the transition potential, it is convenient to introduce the transition density  $\rho^s \sim A g^s$ , which in the  $\lambda$  representation is given by the expression

$$\rho_{\lambda\lambda'}^s = \frac{n_{\lambda} - n_{\lambda'}}{e_{\lambda} - e_{\lambda'} - \omega_s} g_{\lambda\lambda'}^s. \quad (42)$$

By means of  $\rho^s$  we can find the matrix element of the transition from the ground state  $|0\rangle$  to the excited state  $|s\rangle$  in the field  $V_0$ :

$$M_{0s} = \sum_{\lambda\lambda'} (e_q V_0)_{\lambda\lambda'} \rho_{\lambda\lambda'}^s.$$

It can be seen from (40) and (42) that the transition density matrix satisfies the equation

$$(e_{\lambda} - e_{\lambda'} - \omega_s) \rho_{\lambda\lambda'}^s = (n_{\lambda} - n_{\lambda'}) \sum_{\lambda_1\lambda_2} \mathcal{F}_{\lambda\lambda';\lambda_1\lambda_2} \rho_{\lambda_1\lambda_2}^s. \quad (43)$$

It is on the properties of this equation that the general method of calculating the sum rules in the theory of finite Fermi systems is based. First, using Eqs. (41) and (42), we obtain for the coefficients of the density matrix from (43) the orthogonality and completeness conditions

$$\left. \begin{aligned} \sum_{\lambda\lambda'} \rho_{\lambda\lambda'}^s (n_{\lambda} - n_{\lambda'}) \rho_{\lambda\lambda'}^s &= \Lambda_s \delta_{ss'}; \\ \sum_s \rho_{\lambda_1\lambda_2}^s \Lambda_s \rho_{\lambda_3\lambda_4}^s &\equiv \delta_{\lambda_1\lambda_3} \delta_{\lambda_2\lambda_4} (n_{\lambda_1} - n_{\lambda_2}) \equiv (\mathcal{N}_0)_{12}^{34} \end{aligned} \right\} \quad (44)$$



By analogy with the last relation, we introduce the matrix quantity

$$(\mathcal{R}_k)_{12}^{34} = \sum_s \omega_s \rho_{12}^s \Lambda_s \rho_{34}^s, \quad (45)$$

and, using the definitions of  $\Lambda_s$  and  $M_{0s}$ , we obtain

$$\begin{aligned} m_k^{(-)} - (-1)^k m_k^{(+)} &= - \sum_s \omega_s \Lambda_s |M_{0s}|^2 \\ &= - \sum_{1234} (e_q V_0)_{12} (\mathcal{R}_k)_{12}^{34} (e_q V_0)_{34}. \end{aligned} \quad (46)$$

Multiplying both sides of Eq. (43) by  $\omega_s^k \rho_{34}^s \Lambda_s$  and taking the sum over the index  $s$ , we obtain the recursion relation

$$(\mathcal{R}_{k+1})_{12}^{34} = \sum_{56} \mathcal{F}_{12}^{56} (\mathcal{R}_k)_{56}^{34}, \quad (47)$$

where

$$\mathcal{F}_{12}^{56} = (e_1 - e_2) \delta_{15} \delta_{26} - (n_1 - n_2) \cdot \mathcal{F}_{12,56}$$

and the initial value of  $\mathcal{R}_k$  at  $k=0$  is given in (44). The relations (44)–(47) solve the problem of calculating the moments. It can be seen from (46) that the presence of the signature  $\Lambda_s$  makes it possible to calculate explicitly from (43) only the sum of the odd moments or only the difference of the even moments between the two excitation branches. Note that for the neutral channel, when there exist “symmetric” solutions of Eq. (43) with frequencies  $\pm \omega_s$ , the strength function  $S(\omega)$  is an odd function of  $\omega$  and from (43) it is possible to calculate only the odd moments. In the charged channel, because of the Coulomb interaction (and for nuclei with  $N \neq Z$ ), the symmetry of the excitations is lost and the difference between the even moments for the branches with different signature  $\Lambda_s$  becomes nonzero. We shall consider some examples.

#### Sum rules for squares of matrix elements

It is not difficult to calculate the difference between the zeroth (without energy weight) moments  $m_0^{(-)} - m_0^{(+)}$  for single-particle operators of the form

$$V_0^{(\pm)} = v_0 \tau_{\pm} = f(r) T_{JLS}^M(u, \sigma) \tau_{\pm},$$

where  $f(r)$  is a function of only the radial coordinate;  $T_{JLS}^M = [\sigma^s \otimes Y_L]^J M$  are operators that change the nucleon charge state. From (44) and (46), using the completeness of the quasiparticle basis, we obtain

$$\begin{aligned} m_0^{(-)} - m_0^{(+)} &= \sum_{np} (e_q v_0)_{np} (n_n - n_p) (e_q v_0)_{pn}^\dagger \\ &= \sum_n n_n \langle n | (e_q v_0)^\dagger (e_q v_0) | n \rangle \\ &\quad - \sum_p n_p \langle p | (e_q v_0) (e_q v_0)^\dagger | p \rangle. \end{aligned} \quad (48)$$

Summing over the projections of  $M$ , which is equivalent to introducing sum rules for the squares of the reduced matrix elements, we obtain

$$[m_0^{(-)} - m_0^{(+)}]^{(q)} = \frac{2J+1}{4\pi} \{N \langle (e_q f)^2 \rangle_n - Z \langle (e_q f)^2 \rangle_p\}, \quad (49)$$

where  $\langle \dots \rangle_{n,p}$  denotes the mean value over the density distribution of the neutron (proton) quasiparticles, and the index  $(q)$  on the left-hand side is introduced to emphasize that the corresponding quantity reflects the contribution of the quasiparticle excitations to the sum rule (or rather, the quasihole excitations). To calculate (49), it is necessary to know the local charges  $e_q$  for the fields  $V_0$  and the quasiparticle densities  $\rho^r$ . The

former are constants of the theory, and the latter can be found by means of the self-consistency conditions (27) for a given effective interaction  $\mathcal{F}$  characterized by a definite set of parameters. In this sense, the actual value of (49) depends on the model that is used.

For Fermi transitions, when  $J=L=S=0$  and  $f(r) = \sqrt{4\pi}$ , we obtain from (49) ( $V_0^\pm = \tau_\pm$  and  $e_q = 1$ )

$$[m_0^{(-)} - m_0^{(+)}]_F^{(q)} = N - Z, \quad (50a)$$

and for Gamow–Teller transitions when  $J=S=1$ ,  $L=0$ , and  $f(r) = \sqrt{4\pi}$ , we obtain ( $V_0^\pm = \sigma \tau_\pm$ , and we assume  $e_q = 1 - 2\xi_s = \text{const}$ )

$$[m_0^{(-)} - m_0^{(+)}]_{GT}^{(q)} = 3(N - Z) e_q^2. \quad (51a)$$

It should be noted that the first of these sum rules is completely model-independent. Indeed, it can be obtained using solely the completeness of the exact eigenstates of the system:

$$\begin{aligned} [m_0^{(-)} - m_0^{(+)}]_F &= \sum_s |\langle s | \sum_{i=1}^A \tau_i^\pm | 0 \rangle|^2 \\ &\quad - \sum_s |\langle s | \sum_{i=1}^A \tau_i^\pm | 0 \rangle|^2 \\ &= \langle 0 | \sum_{i=1}^A (\tau_i^\pm \tau_i^\pm - \tau_i^\mp \tau_i^\mp) | 0 \rangle \\ &= \langle 0 | \sum_{i=1}^A \tau_i^\pm | 0 \rangle = N - Z. \end{aligned} \quad (50b)$$

If such operations are performed for the Gamow–Teller single-particle operator  $\sum_i \sigma_i \tau_i^\pm$ , then for each projection  $\mu$  the result is the same, and after summation over  $\mu$  we also have the strictly model-independent result

$$[m_0^{(-)} - m_0^{(+)}]_{GT} = 3(N - Z). \quad (51b)$$

The agreement between the expressions (50a) and (50b) is a consequence of the conservation law for the vector current (and the theorem on the equality of the number of quasiparticles and the number of particles). At the same time, the difference between (51a) and (51b) is due to the absence of corresponding conservation laws for the axial-vector vertices. This difference shows that the strength of transitions of Gamow–Teller type can somehow be redistributed between the particle–hole and other degrees of freedom (multipair excitations, and also degrees of freedom associated with the production of mesons,  $\Delta$  isobars, and so forth).

#### Energy-weighted sum rules

In the theory of finite Fermi systems, the sum of the first moments of the strength functions  $S^*$  is given by (46) for  $k=1$ . With allowance for (44) and (47), we have in an obvious notation

$$\begin{aligned} [m_1^{(-)} + m_1^{(+)}]^{(q)} &= \sum_{np} \langle p | e_q v_0 | n \rangle (e_n - e_p) \langle n | e_q v_0 | p \rangle \\ &\quad + \sum_{np, n'p'} \langle p | e_q v_0 | n \rangle (n_n - n_p) \\ &\quad \times \mathcal{F}_{np, n'p'} (n_{n'} - n_{p'}) \langle n' | e_q v_0 | p' \rangle. \end{aligned} \quad (52)$$

We consider first the case of Gamow–Teller transitions ( $v_0 = \sigma_\mu$ ). Apart from the main components of the effective interaction discussed in Sec. 2, an important contribution to  $m_k$  is made by the spin–orbit forces, for which we adopt the standard form<sup>11</sup>

$$\mathcal{F}_{sl}^{ik} = C_0 r_0^2 \kappa^{ik} [\nabla_1 \delta(\mathbf{r}_1 - \mathbf{r}_2) (\mathbf{p}_1 - \mathbf{p}_2)] \cdot (\boldsymbol{\sigma}_1 + \boldsymbol{\sigma}_2).$$

Here,  $\kappa^{ik}$  are dimensionless constants, and the factor  $r_0$  ( $\approx 1$  F) is introduced for convenience. In the self-consistent approach, these forces generate the single-particle potential

$$\begin{aligned} U_{sl(l)}^i &= C_0 r_0^2 \sum_k \kappa^{ik} \frac{1}{r} \frac{d\rho^k}{dr} \boldsymbol{\sigma} l \\ &- C_0 r_0^2 \sum_k \kappa^{ik} \frac{1}{r^2} \frac{d}{dr} (\rho_{sl}^k r) \\ &= U_{sl}^i(r) \boldsymbol{\sigma} l + U_{sl(c)}^i, \end{aligned} \quad (53)$$

where

$$\begin{aligned} \rho_{sl}^k(r) &= \sum_\lambda n_\lambda^k \Phi_\lambda^{*k} \boldsymbol{\sigma} l \Phi_\lambda^k \\ &= \frac{1}{4\pi} \sum_\lambda n_\lambda^k \langle \boldsymbol{\sigma} l \rangle_\lambda (R_l^k(r))^2; \end{aligned} \quad (54)$$

$\langle \boldsymbol{\sigma} l \rangle_\lambda = j(j+1) - l(l+1) - 3/4$ . It can be seen that in the complete potential  $U_{sl(l)}^i$ , there is the ordinary term  $U_{sl\sigma}^i$  and the central component  $U_{sl(c)}^i$ . Taking into account  $\rho$ -meson exchange to complete the picture, we obtain after simple algebraic calculations and summation over  $\mu$  the equation<sup>36</sup>

$$\begin{aligned} [m_1^{(-)} + m_1^{(+)}]_{\text{eff}}^{(q)} &= e_q^2 \left\{ 3(U_{\text{Coul}} \rho^-) - 3(U^- \rho^-) \right. \\ &\quad \left. + 3(\rho^- G^- \rho^-) - 4\langle U_{sl} \rangle \right. \\ &\quad \left. + \int [\rho^-(k)]^2 [G_\pi^-(k^2) + 2G_\rho^-(k^2)] \frac{d^3k}{(2\pi)^3} \right\}, \end{aligned} \quad (55)$$

where in accordance with (36) the one-pion exchange contribution in the direct channel is given by the amplitude  $G_\pi^-(k^2) = 2C_0 g_\pi^2 (e_q^2)^2 k^2 / [m_\pi^2 + k^2 + P_\Delta(k^2)]$ , and the  $\rho$ -meson exchange contribution in the same channel is given by the amplitude  $G_\rho^-(k^2) = 2C_0 g_\rho^2 (e_q^2)^2 k^2 / (m_\rho^2 + k^2)$ . The coefficient 2 of  $G_\rho^-$  in (55) is due to the fact that the  $\rho NN$  vertex is transverse ( $\sim [\boldsymbol{\sigma} \times \mathbf{k}]$ ), in contrast to the case of the  $\pi NN$  vertex, for which it is longitudinal ( $\sim \boldsymbol{\sigma} \cdot \mathbf{k}$ ). The constant  $g_\rho$  is introduced by analogy with  $g_\pi$  in (36):  $g_\rho = 4\pi(f_\rho^2/m_\rho^2)/C_0 = 2.62$  (for  $m_\rho = 773$  MeV and  $f_\rho^2 = 4.86$ , i.e., for a so-called strong  $\rho$  meson). For estimates, we shall in what follows assume  $e_q^2 = e_q^2 = e_q^2 [\sigma\tau]$ . The other quantities in (55) are  $\rho^-(k) = 4\pi \int \rho^-(r) j_0(kr) r^2 dr$ , the Fourier transform of the isovector density  $\rho^- = \rho^n - \rho^p$ ;  $U^- = U_0^n - U_0^p$ , the difference between the central nuclear self-consistent potentials (here, the contribution from  $U_{sl(c)}^i$  is not included);  $U_{\text{Coul}}$ , the Coulomb self-consistent potential; and  $\langle U_{sl} \rangle$ , the mean over the ground state of the spin-orbit potential  $U_{sl\sigma}^i$ :  $\langle U_{sl} \rangle = (U_{sl}^n \rho_{sl}^n) + (U_{sl}^p \rho_{sl}^p)$ . In the relations we have written down, the round brackets denote, as usual, integration over the spatial coordinates; for example,  $(U^- \rho^-) = 4\pi \int U^-(r) \rho^-(r) r^2 dr$ . Note that the spin-orbit contribution  $-4\langle U_{sl} \rangle$  in (55) is accumulated as follows: the ordinary component  $U_{sl\sigma}^i$  in the first term in (52) gives  $(U_{sl}^n \rho_{sl}^n) - 4\langle U_{sl} \rangle$ , the central component gives  $-3(U_{sl}^n \rho_{sl}^n)$ , and in the second term of (52)  $+2(U_{sl}^n \rho_{sl}^n)$  arises from the amplitude  $\mathcal{F}_{sl}^i = \mathcal{F}_{sl}^{nn} - \mathcal{F}_{sl}^{np}$ , here,  $\rho_{sl}^i = \rho_{sl}^n$ ;  $U_{sl}^i = U_{sl}^n - U_{sl}^p$ .

The contribution of the spin-orbit interactions to (55) can be estimated from experimental data on the splitting of spin-orbit doublets in neighboring odd nuclei, the estimate containing only levels situated on different sides of the Fermi surface. If there is a completely

filled level with energy  $\epsilon_{j=l+1/2}$ , and the level with energy  $\epsilon_{j=l-1/2}$  is free, then

$$-4\langle U_{sl} \rangle \approx \frac{8l(l+1)}{2l+1} (\epsilon_{j=l-1/2} - \epsilon_{j=l+1/2}). \quad (56)$$

If there are several such doublets, the sum over them must be taken.

For Fermi transitions ( $\nu_0 = 1$  and  $e_q = 1$ ) we obtain from (52)

$$[m_1^{(-)} + m_1^{(+)}]_{\text{eff}}^{(q)} = (U_{\text{Coul}} \rho^-) - (U^- \rho^-) + (\rho^- \mathcal{F}^- \rho^-). \quad (57)$$

In a self-consistent approach, the last two terms must cancel each other in accordance with the condition (29). Note that in the case of complete self-consistency there is also no contribution of the spin-orbit forces in (57): From the amplitude  $\mathcal{F}_{sl}^i$  in the second term in (52) there arises  $+2(U_{sl}^n \rho_{sl}^n)$ , whereas from the first term  $-2(U_{sl}^n \rho_{sl}^n)$  is obtained, and the contributions of the "ordinary" ( $U_{sl\sigma}^i$ ) and the central ( $U_{sl(c)}^i$ ) potentials are the same.

We introduce the mean energies  $\bar{\omega} = [m_1^{(-)} + m_1^{(+)}]_{\text{eff}}^{(q)} / [m_0^{(-)} - m_0^{(+)}]_{\text{eff}}^{(q)}$  of the excitations for the corresponding fields and consider the difference between the energies of the centroids of the Gamow-Teller and Fermi transitions. Using (50a) and (57), (51a) and (55), we obtain

$$\begin{aligned} \bar{\omega}_{GT} - \bar{\omega}_F &= \frac{1}{N-Z} \left\{ (\rho^- [G^- - \mathcal{F}^-] \rho^-) \right. \\ &\quad \left. - \frac{4}{3} \langle U_{sl} \rangle + \frac{1}{3} \int \frac{d^3k}{(2\pi)^3} [\rho^-(k)]^2 [G_\pi^-(k^2) + 2G_\rho^-(k^2)] \right\} \\ &= \bar{\omega}_{gf} + \bar{\omega}_{sl} + (\bar{\omega}_\pi + \bar{\omega}_\rho). \end{aligned} \quad (58)$$

We consider the individual terms in (58). Taking into account the condition (29) and the relation  $C_0 \rho_0 = 2e_F/3$ , we can rewrite the contribution from the difference of the amplitudes  $G^- - \mathcal{F}^-$  in the form

$$\bar{\omega}_{gf} = \frac{2}{3} e_F \frac{N-Z}{A} \gamma (g^- - f_{\text{eff}}), \quad (59)$$

where we have introduced the parameters  $\gamma = (\rho^- \rho^-) A / \rho_0 (N-Z)^2$  and  $f_{\text{eff}} = (\rho^- U^-) / C_0 (\rho^- \rho^-)$ . For estimates, we represent  $\rho^-$  in the form of the Fermi density  $\rho^-(r) = 2(N-Z)\rho_0 f(r)/A$ , where  $f(r) = [1 + \exp(-R/a)]^{-1}$  (the normalization is  $\rho_0 \int f(r) d^3r = A/2$ ). Then with allowance for terms  $\sim A^{-1/3}$ ,

$$\gamma \approx 2 \left( 1 - 3 \frac{a}{R} \right); \quad f_{\text{eff}} \approx f_{\text{in}} + b \frac{3}{2} \frac{a}{R}. \quad (60)$$

In the last estimate we have assumed that  $\mathcal{F}^-$  contains only terms  $\sim \delta(\mathbf{r} - \mathbf{r}')$ ; the presence in  $\mathcal{F}^-$  of components with nonlocality range  $\sim r_0$  leads to corrections  $\sim r_0/R$ .

We estimate the spin-orbit contribution to (58) as follows. For the lowest level of the doublet with  $j = l \pm 1/2$ , we have  $\rho_{sl}^i(r) = l(l+1)R_\lambda^2(r)/2\pi$  in accordance with (54). For estimates, we ignore the isovector spin-orbit potential  $[\sim \kappa^i(N-Z)/A]$  and take  $U_{sl}^i = C_0 r_0^2 \kappa^i + 1/r \partial \rho / \partial r \boldsymbol{\sigma} l$ . Then, assuming that  $l \sim A^{1/3} \gg 1$ , and approximating  $\rho$  and  $R_\lambda^2$  by the Fermi function  $f(r)$ , we obtain (we use  $\int dr r f df/dr \approx -R/2$ )

$$\bar{\omega}_{sl} = -\frac{4}{3} \frac{\langle U_{sl} \rangle}{N-Z} \approx \frac{8}{3} e_F \frac{\kappa^i \nu(A, Z)}{N-Z} \approx 43 \frac{\nu(A, Z)}{N-Z} \text{ MeV}, \quad (61)$$

where  $\nu(A, Z)$  is the effective occupation factor; in the simplest case, it is the number of doublets for which the lower level is completely occupied and the upper is free ( $\nu = 1$  for  $^{48}\text{Ca}$  and  $^{90}\text{Zr}$  and  $\nu = 2$  for  $^{208}\text{Pb}$ ). But if the upper level is partly filled and there are  $k$  particles in it, the additional factor  $(1 - k/2l)$  is introduced. If,



in addition,  $l$  for such doublets in a concrete nucleus differs appreciably from  $A^{1/3}$ , the correction coefficient  $l(l+1)A^{2/3}$  must be introduced. In (61), the value  $\kappa^* = 0.42$  is used. The expression (61) agrees excellently with the estimate (56); for some nuclei, this can be readily verified by using, for example, the experimental differences  $\varepsilon_{5/2}^n - \varepsilon_{7/2}^n = 9.0$  for  $^{48}\text{Ca}$ ,  $\varepsilon_{5/2}^n - \varepsilon_{7/2}^n = 7.50$  for  $^{90}\text{Zr}$ , and  $\varepsilon_{11/2}^n - \varepsilon_{13/2}^n = 5.87$  and  $\varepsilon_{9/2}^p - \varepsilon_{11/2}^p = 5.55$  MeV for  $^{208}\text{Pb}$ .

We now estimate the meson contribution to the difference  $\bar{\omega}_{GT} - \bar{\omega}_F$ . First of all, we have

$$\begin{aligned} & \int \frac{d^3k}{(2\pi)^3} \frac{k^2}{m_\rho^2 + k^2} [\rho^-(k)]^2 \\ & \approx \frac{1}{m_\rho^2} \int \frac{d^3k}{(2\pi)^3} d^3r d^3r' \bar{\rho}(\mathbf{r}) \bar{\rho}(\mathbf{r}') \\ & \times \left[ \frac{\partial}{\partial \mathbf{r}} \frac{\partial}{\partial \mathbf{r}'} e^{i\mathbf{k}(\mathbf{r}-\mathbf{r}')} \right] = \frac{1}{m_\rho^2} \left( \frac{\partial \rho^-}{\partial \mathbf{r}} \frac{\partial \rho^-}{\partial \mathbf{r}} \right). \end{aligned} \quad (62)$$

In the denominator of the  $\rho$ -meson propagator we have here ignored  $k^2$  compared with  $m_\rho^2$ , since small momenta  $k < p_F$  are mainly represented in  $\bar{\rho}(k)$  (we recall that  $m_\rho = 3.92 \text{ F}^{-1}$ , and  $p_F \approx 1.3-1.4 \text{ F}^{-1}$ ). Approximating  $\bar{\rho}$  by a Fermi function and calculating the integral in (62) by the method of steepest descent, we obtain the asymptotic estimate

$$\begin{aligned} \bar{\omega}_\rho & \approx \frac{8}{9} \varepsilon_F g_\rho (1 - 2\xi_s)^2 \frac{1}{(m_\rho r_0)(m_\rho a)} \frac{N-Z}{A^{1/3}} \\ & \approx 4.8 \frac{N-Z}{A} \frac{1}{A^{1/3}} \text{ MeV}. \end{aligned} \quad (63)$$

If similar operations are performed for the one-pion exchange contribution, we obtain

$$\bar{\omega}_\pi = \bar{\omega}_\rho \left( \frac{m_\rho}{m_\pi} \right)^2 \frac{g_\pi}{g_\rho} \approx -4.4 \frac{N-Z}{A} \frac{1}{A^{1/3}} \text{ MeV}. \quad (64)$$

As is shown by exact calculations using the expression (58) and, for example, the densities  $\bar{\rho}(\mathbf{r})$  in the Woods-Saxon potential, the estimate (64) is too large by almost a factor 2. As a result, the total contribution of  $\bar{\omega}_\pi + \bar{\omega}_\rho$  to  $\bar{\omega}_{GT}$  for nuclei heavier than  $^{40}\text{Ca}$  is small and negative, not exceeding in modulus  $\approx 1$  MeV.

If we associate  $\bar{\omega}_{GT}$  with the position of the Gamow-Teller resonance, and  $\bar{\omega}_F$  with the position of the isobar analog state, then on the basis of the above treatment we can propose the following expression for describing the energy scheme of these charge-exchange resonances:

$$E_{GTR} - E_{IAS} = \frac{4}{3} \varepsilon_F \left[ \left( \alpha_1 + \frac{\alpha_2}{A^{1/3}} \right) \frac{N-Z}{A} + 2\kappa^* \frac{v(A, Z)}{N-Z} \right]. \quad (65)$$

Here,  $\alpha_1 = g^- - f_{in}^-$ , and  $\alpha_2$  is a parameter by means of which allowance is made for the total contribution from meson exchange, from the nonlocality effects of the effective interaction, and the finite size of the nucleus. Comparison with experimental data shows that this expression does indeed work well for  $\alpha_1 = g^- - f_{in}^- \approx -(0.10-0.15)$  and  $\alpha_2 \approx -(0.0-0.12)$ . Note that (65) differs appreciably from the approximations proposed in Ref. 35. Using the expression (35), we obtain for the Landau-Migdal parameter  $g' \approx 0.6$ . This result is rather paradoxical, since it means that nuclei are very close to the point of the  $\pi$ -condensation instability<sup>30,31</sup> and for such  $g'$  there must be strong precritical effects in them, but these are not observed (there are at present no clear indications of even weak effects associated with possible proximity to the threshold of  $\pi$

condensation). Indeed, as is shown by direct calculations of the strength functions and comparison of them with experiments, the real value of this parameter is much greater:  $g' \approx 1.1$ . The paradox arose because on the transition from (58) to (65) the difference  $\bar{\omega}_{GT} - \bar{\omega}_F$  of the centroid energies was replaced by the difference  $E_{GTR} - E_{IAS}$  of the resonance energies, these being taken from the experiments. Such a replacement is unjustified, since in fact the centroid of the Gamow-Teller transitions lies appreciably above the maximum in the strength function corresponding to the Gamow-Teller resonance, and the same applies, though to a lesser extent, to the transitions of Fermi type, namely, even for  $g^- = f_{in}^-$  the effects of the isotopic (Coulomb) mixing and the spin-orbit splitting are very different for different types of transition. We note, for example, that in  $^{208}\text{Pb}$  for  $g' = 1.1$  the calculated position of the Gamow-Teller resonance relative to the ground state of  $^{208}\text{Pb}$  is found to be at 19.2 MeV, in agreement with experiment, while the centroid energy  $\bar{\omega}_{GT}$  is equal to 23.7 MeV, i.e., is 4.5 MeV greater! At the same time, the isobar analog state is approximately 1 MeV below  $\bar{\omega}_F$ . We note the importance of correct allowance for the single-particle continuum in these calculations.

The conclusion is this: The expression (65) is to be regarded only as a simple dependence permitting convenient approximation of the empirical data.

## 4. CALCULATIONS AND DISCUSSION OF RESULTS

### Choice of the single-particle potential

Here, we give results of calculations for three typical nuclei with closed shells,  $^{48}\text{Ca}$ ,  $^{90}\text{Zr}$ , and  $^{208}\text{Pb}$ , in which there are no features associated with pairing correlations in the particle-particle channel.

Remaining within the framework of the traditional scheme for the theory of finite Fermi systems, we used a common shell potential and single-particle spectrum to describe the low-lying and resonance states. For the charge-exchange excitations, we made the matching described below of the isovector quantities  $\mathcal{F}^-$ ,  $U^-$ , and  $\rho^-$ . Matching for the corresponding isoscalar quantities was not made, since the isoscalar interactions do not enter directly into the considered problem but appear in an averaged manner through the propagator  $A$ . However, the isoscalar potential  $(U^n + U^p)/2$  was chosen to give (together with  $U^-$ ) a single-particle spectrum close to the experimental one. Only if this requirement is satisfied can one, as numerous calculations show (see, for example, Refs. 15 and 37), correctly describe the properties of low-lying collective states. All calculations were made in the coordinate representation. A description of the program for the calculation of the propagator  $A$ , which makes it possible to take into account exactly the single-particle continuum and allows the introduction of artificial damping of the quasiparticles, is contained in Ref. 38.

In the calculations that we shall discuss, a shell potential of Woods-Saxon type was used:

$$\begin{aligned} U^k & = -V_0^k f_h(r) - V_{ls}^k (r_0^k)^2 \frac{1}{r} \frac{\partial f_h}{\partial r} (ls); \\ f_h(r) & = \left( 1 + \exp \frac{r-R_h}{a_h} \right)^{-1}; \quad R_h = r_0^k A^{1/3}, \end{aligned} \quad (66)$$

where  $V_0^k, V_{1s}^k, r_0^k, a_k$  are parameters. The Coulomb potential has the standard form corresponding to a uniformly charged sphere of radius  $R_c = r_{0c} A^{1/3}$ , where  $r_{0c}$  is determined from the experimental rms charge radius  $\langle r_c^2 \rangle^{1/2}$  by the equation  $R_c = \sqrt{5/3} \langle r_c^2 \rangle^{1/2}$ . The parameters of the potential were fitted using the experimental single-particle spectra given in Ref. 39. Besides this, we required the calculated values of  $\langle r_c^2 \rangle^{1/2}$ , and also the differences  $\Delta r_{np}$  of the rms radii of the neutrons and protons to agree with the experimental data. The parameters of the potential (66) obtained on the basis of these requirements are given in Table I together with the values of  $\langle r_{np}^2 \rangle^{1/2}$ . It can be seen that there is good agreement of the calculated  $\langle r_c^2 \rangle^{1/2}$  and  $\Delta r_{np}$  with the experimental values, although the data on  $\Delta r_{np}$  of different studies are as yet ambiguous. As a rule, the energies of the single-particle levels near the Fermi surface differ from the experimental energies by not more than 0.5 MeV.

### Matching of $\mathcal{F}^-$ and $U^-$

For spherical symmetry, the consistency condition (29) relates the monopole component  $\mathcal{F}_0^-$  to the isovector potential

$$U^-(r) = \int \mathcal{F}_0^-(r, r') \rho^-(r') r'^2 dr'. \quad (67)$$

Since the potential  $U^-$  is given, for the chosen form (31) of the amplitude  $\mathcal{F}^-$  the exact fulfillment of the condition (67) is hard to achieve in practice. There remains the freedom of variation of the parameters  $a_0', a_r',$  and  $b$  to make the "self-consistent" potential  $U_{sc}^-$  [the right-hand side of Eq. (67)] agree best with the given shell potential when the shell density  $\rho^-$  is used. Calculating the potential symmetry energy, we obtain from (67) a relation that establishes a linear connection between the parameters  $a_0', a_r',$  and  $b$  ( $N \neq Z$ ):

$$\begin{aligned} \mathcal{E}_s &= 2\pi \int U^-(r) \rho^-(r) r^2 dr \\ &= 2\pi \int \rho^-(r) \mathcal{F}_0^-(r, r') \rho^-(r') r^2 r'^2 dr dr' = \beta_s (N-Z)^2/A. \end{aligned} \quad (68)$$

This relation is an integral analog of the consistency condition. The values of  $\beta_s$  for the single-particle potentials used here are given in Table I. The connection between the parameters of  $\mathcal{F}^-$  established in (68) is different for each nucleus. However, the calculations made for  $^{48}\text{Ca}$ ,  $^{90}\text{Zr}$ , and  $^{208}\text{Pb}$  with the chosen potentials give an entirely universal relationship with the

TABLE I. Parameters of single-particle potentials and characteristics of the ground states of the nuclei.

| Nucleus           | Particle | $V_0$ , MeV | $r_0$ , F | $a$ , F | $V_{1s}$ , MeV | $r_{0c}$ , F | $\langle r_c^2 \rangle^{1/2}$ , F | $\langle r_{np}^2 \rangle^{1/2}$ , F |                              |                  |                                                                   | $\beta_s$ , MeV |
|-------------------|----------|-------------|-----------|---------|----------------|--------------|-----------------------------------|--------------------------------------|------------------------------|------------------|-------------------------------------------------------------------|-----------------|
|                   |          |             |           |         |                |              |                                   | calcu-<br>lation                     | experi-<br>ment<br>(Ref. 40) | calcu-<br>lation | experi-<br>ment<br>(Ref. 41)                                      |                 |
| $^{48}\text{Ca}$  | Neutrons | 49.9        | 1.21      | 0.65    | 25.4           | —            | 3.56                              | —                                    | —                            | 0.17             | $\begin{pmatrix} 0.19 \\ 0.20 \\ 0.10 \end{pmatrix}$              | 23.9            |
|                   | Protons  | 56.0        | 1.29      | 0.61    | 19.7           | 1.23         | 3.39                              | 3.48                                 | 3.476                        | —                | —                                                                 |                 |
| $^{90}\text{Zr}$  | Neutrons | 48.5        | 1.26      | 0.64    | 20.9           | —            | 4.33                              | —                                    | —                            | 0.14             | $\begin{pmatrix} 0.11 \\ 0.09 \\ 0.13 \end{pmatrix}$              | 25.5            |
|                   | Protons  | 55.2        | 1.275     | 0.64    | 20.8           | 1.228        | 4.19                              | 4.266                                | 4.266                        | —                | —                                                                 |                 |
| $^{208}\text{Pb}$ | Neutrons | 47.0        | 1.22      | 0.65    | 21.1           | —            | 5.56                              | —                                    | —                            | 0.10             | $\begin{pmatrix} 0 \\ 0.14 \\ 0.08 \\ 0.18 \\ 0.21 \end{pmatrix}$ | 29.5            |
|                   | Protons  | 60.2        | 1.26      | 0.65    | 27.5           | 1.20         | 5.46                              | 5.516                                | 5.502                        | —                | —                                                                 |                 |

following arithmetic-mean numerical coefficients (with nonlocality range  $r_0' = 0.8$  F in the Yukawa potential):

$$a_0' + 0.86a_r' - 0.35b - 0.92 = 0. \quad (69)$$

If we take  $r_0' = 0.4$  F, then the coefficient 0.86 of  $a_r'$  is replaced by 0.97. The spread of the numerical coefficients for different nuclei is not more than 5–10% for variation of  $a_r'$  and  $b$  in the intervals  $0 \leq a_r' \leq 2$  and  $0 \leq b \leq 4$ . The relation (69) can be rewritten in terms of the parameters  $f_{in}^-$  and  $f_{ex}^-$ :

$$\begin{aligned} f_{in}^- &= 1.84 + 0.28a_r' - 0.3b; \quad f_{ex}^- = 1.84 \\ &+ 0.28a_r' + 0.7b. \end{aligned} \quad (70)$$

For  $r_0' = 0.4$  F, the coefficient 0.28 that appears here is replaced by 0.06, and the dependence of the constants  $f_{in}^-$  and  $f_{ex}^-$  on  $a_r'$  becomes very weak. From (70) for  $b = 2$  and  $a_r' = 0$  it follows that  $f_{in}^- = 1.24$  and  $f_{ex}^- = 3.24$ ; these values agree excellently with the estimates (35).

Additional restrictions on the parameters of the amplitude  $\mathcal{F}^-$  can arise from the calculation of the energies of  $J^\pi = 0^+$  isobar analog states. Our calculations show that the energies of these states change rather little (by less than 200 keV) when  $a_r'$  is varied from 0 to 2. There is a somewhat greater sensitivity to variation of the parameter  $b$  from 0 to 4 (up to 1, 0.7, and 2 MeV for  $^{48}\text{Ca}$ ,  $^{90}\text{Zr}$ , and  $^{208}\text{Pb}$ , respectively). In particular, for  $b = 2$  we obtain the following energies of isobar analog states: 8 MeV for  $^{48}\text{Ca}$ , 12.5 MeV for  $^{90}\text{Zr}$ , and 17.8 MeV for  $^{208}\text{Pb}$ ; the corresponding experimental energies of the states are 7.2, 12, and 18.8 MeV.<sup>3</sup> An interpolation of  $\mathcal{F}^-$  corresponding to  $b \approx 2.2$  ( $a_r' = 0$ ) was introduced in Ref. 23, and for  $^{208}\text{Pb}$  the same energy of the isobar analog state was obtained as here; it is important to note that the experimental single-particle spectrum was also used. In Ref. 42, we noted that in  $^{208}\text{Pb}$  it is possible to achieve agreement between the calculations and experiment for the values  $a_r' = 0.8$  and  $b \approx 4$ , at which the best correspondence is achieved between the given shell potential  $U^-$  and  $U_{sc}^-$  calculated using the right-hand side of (67). However, the interpolation in  $\mathcal{F}^-$  then seems too strong:  $f_{ex}^-/f_{in}^- \approx 5$ . We add that variation of the relationship between the local ( $\sim a_0'$ ) and nonlocal ( $\sim a_r'$ ) terms in  $\mathcal{F}^-$  strongly influences the form of  $U_{sc}^-$ , though it has rather little influence on the position of the isobar analog states.

It should be noted that because of the incomplete matching there are errors in the calculations of the isobar analog energies and the effects of the isospin mixing. Estimates on the basis of sum rules show that these errors may lead to a shift of the isobar analog state in  $^{208}\text{Pb}$  by 0.5–1.0 MeV, i.e., by an amount characteristic of the variations associated with the variation of the parameters of the amplitude  $\mathcal{F}^-$ . In addition, it is clear from physical considerations that in a completely self-consistent approach the isobar analog position is determined basically by the Coulomb potential averaged over the ground state, and, if this is kept fixed in some way, the isobar analog energy should not depend strongly on the parameters of the effective interaction. For these reasons, exact fitting of the calculations to the experimental isobar analog energies does not make much sense, since it does not give



stringent bounds on the parameters of  $\mathcal{F}^-$ . In the following sections, we discuss the sensitivity of the positions of the charge-exchange resonances ( $S=0$ ) to variations of the parameters in (69) [or (70)]. In particular, we shall see that their energies depend rather strongly on the parameter  $b$ , which determines the degree of interpolation in  $\mathcal{F}^-$ .

## 5. LOW-ENERGY BOUND STATES

Calculations of noncollective bound states of odd-odd nuclei can be used to test the correctness of the choice of the single-particle potentials and the parametrization of the effective interactions. Naturally, not all levels of an odd-odd nucleus can be described in terms of particle-hole excitations in the charged channel. Among them are levels whose structure is better described in terms of the excitation of a valence neutron and valence proton above the even-even core  $A-2$  (in the neutral channel). Moreover, in the same odd-odd nucleus there exist both  $(p, n^{-1})$  excitations above the core with isospin  $T_0$  of the parent nucleus and  $(n, p^{-1})$  states above the core with isospin  $T_0-2$ . All these states can be distinguished by selective excitation of them in different reactions, for example, in  $(p, n)$  and  $(n, p)$  reactions on different targets. Here, calculations are made only for excitations of the type  $(p, n^{-1})$  for a number of low-energy multiplets in  $^{48}\text{Sc}$  and  $^{208}\text{Bi}$ . The parameters of the interaction  $\mathcal{F}^-$  were specified in accordance with the condition (68), the value  $b=0$  being chosen in  $^{48}\text{Sc}$  and  $b=4$  in  $^{208}\text{Bi}$  (for which the theoretical isobar analog energy agrees with the experimental energy). The interaction  $G^-$  was parametrized to describe the observed energy of the Gamow-Teller resonance in  $^{208}\text{Bi}$  (see below). The one-pion exchange amplitude (36) was also taken into account.

The results of the calculations are given in Table II, which contains the unperturbed particle-hole configurations, the energy differences  $\varepsilon_p - \varepsilon_n$  corresponding to them, and the calculated and experimental<sup>43,44</sup> energies  $\omega$ . Note that in different studies the energies are given either relative to the ground states of the daughter nuclei, or relative to the isobar analog energies, or, finally, relative to the ground states of the parent nuclei. It appears to us convenient to use the last method, for which the excitation energies are equal to the  $-Q$  values of the  $(p, n)$  charge-exchange reactions (the Coulomb energy shifts are generally measured in this way).

Among the considered levels, we can distinguish the anomalous-parity levels ( $1^+, 2^-, 3^+, \dots$ ), whose shift relative to  $\varepsilon_p - \varepsilon_n$  is due to the interactions  $G^-$  and  $G_r^-$ , the importance of the second increasing with increasing  $J$ . For example, in  $^{48}\text{Sc}$  the energy of the  $7^+$  level for  $g_r=0$  is 2.15 MeV, i.e., the interaction  $G_r^-$  shifts the level by about 0.65 MeV, whereas the shift of the  $1^+$  level associated with it is 0.35 MeV. As can be seen from Table II, the theory describes rather well the energies of the anomalous-parity levels, and it is only for the  $1^+$  and  $2^-$  states that the calculated shifts are significantly smaller than the observed values. This could be due to the over-simple form of the employed spin-isospin interactions.

TABLE II. Some levels of multiplets of coupled states in  $^{48}\text{Sc}$  and  $^{208}\text{Bi}$ .

| Configuration. ( <i>p</i> , <i>n</i> <sup>-1</sup> )                    | $\varepsilon_p - \varepsilon_n$ ,<br>MeV | <i>J</i> $\pi$       | $\omega$ , MeV |            |
|-------------------------------------------------------------------------|------------------------------------------|----------------------|----------------|------------|
|                                                                         |                                          |                      | theory         | experiment |
| <sup>48</sup> Ca $\rightarrow$ <sup>48</sup> Sc                         |                                          |                      |                |            |
| (1 <i>f</i> <sub>7/2</sub> , 1 <i>f</i> <sub>7/2</sub> <sup>-1</sup> )  | 0.32                                     | 6 <sup>+</sup>       | 0.55           | 0.500      |
|                                                                         |                                          | 5 <sup>+</sup>       | 0.78           | 0.631      |
|                                                                         |                                          | 4 <sup>+</sup>       | 0.75           | 0.752      |
|                                                                         |                                          | 3 <sup>+</sup>       | 0.85           | 1.122      |
|                                                                         |                                          | 7 <sup>+</sup>       | 1.50           | 1.596      |
|                                                                         |                                          | 2 <sup>+</sup>       | 1.22           | 1.643      |
|                                                                         |                                          | 1 <sup>+</sup>       | 2.30           | 3.02       |
|                                                                         |                                          | 0 <sup>+</sup> (IAS) | 7.20           | 7.17       |
| <sup>208</sup> Pb $\rightarrow$ <sup>208</sup> Bi                       |                                          |                      |                |            |
| (1 <i>h</i> <sub>9/2</sub> , 3 <i>p</i> <sub>1/2</sub> <sup>-1</sup> )  | 3.56                                     | 5 <sup>+</sup>       | 3.63           | 3.650      |
|                                                                         |                                          | 4 <sup>+</sup>       | 3.66           | 3.713      |
| (1 <i>h</i> <sub>9/2</sub> , 2 <i>f</i> <sub>5/2</sub> <sup>-1</sup> )  | 4.12                                     | 2 <sup>+</sup>       | 4.43           | 4.576      |
|                                                                         |                                          | 3 <sup>+</sup>       | 4.20           | 4.284      |
|                                                                         |                                          | 4 <sup>+</sup>       | 4.22           | 4.253      |
|                                                                         |                                          | 5 <sup>+</sup>       | 4.18           | 4.279      |
| (1 <i>h</i> <sub>9/2</sub> , 3 <i>p</i> <sub>3/2</sub> <sup>-1</sup> )  | 4.45                                     | 3 <sup>+</sup>       | 4.53           | 4.720      |
|                                                                         |                                          | 4 <sup>+</sup>       | 4.54           | 4.610      |
|                                                                         |                                          | 5 <sup>+</sup>       | 4.47           | 4.537      |
| (2 <i>f</i> <sub>7/2</sub> , 3 <i>p</i> <sub>1/2</sub> <sup>-1</sup> )  | 4.48                                     | 3 <sup>+</sup>       | 4.59           | 4.589      |
|                                                                         |                                          | 4 <sup>+</sup>       | 4.63           | 4.688      |
| (1 <i>h</i> <sub>9/2</sub> , 4 <i>i</i> <sub>13/2</sub> <sup>-1</sup> ) | 5.20                                     | 2 <sup>-</sup>       | 6.05           | 6.551      |
|                                                                         |                                          | 3 <sup>-</sup>       | 5.52           | 5.575      |
|                                                                         |                                          | 4 <sup>-</sup>       | 5.42           | 5.494      |
| (1 <i>h</i> <sub>9/2</sub> , 2 <i>f</i> <sub>7/2</sub> <sup>-1</sup> )  | 5.93                                     | 1 <sup>+</sup>       | 6.09           | 6.542      |
|                                                                         |                                          | 2 <sup>+</sup>       | 6.13           | 6.158      |
|                                                                         |                                          | 3 <sup>+</sup>       | 5.96           | 6.115      |
|                                                                         |                                          | 4 <sup>+</sup>       | 6.05           | 6.041      |
|                                                                         |                                          | 5 <sup>+</sup>       | 5.95           | 6.041      |
| (2 <i>f</i> <sub>5/2</sub> , 3 <i>p</i> <sub>1/2</sub> <sup>-1</sup> )  | 6.38                                     | 2 <sup>+</sup>       | 6.51           | 6.595      |

The shifts of the normal-parity levels ( $1^-, 2^+, 3^-, 4^+, \dots$ ) relative to  $\varepsilon_p - \varepsilon_n$  are due to the simultaneous contributions of the interactions  $\mathcal{F}^-$  and  $G_r^-$  ( $G^-$  does not contribute), although their importance depends on the particular  $(p, n^{-1})$  configuration. If a particle-hole transition takes place with spin flip, the interaction  $G^-$  is dominant; otherwise, the interaction  $\mathcal{F}^-$  (for example, in  $^{48}\text{Sc}$ ). The calculations showed that the shifts of the low-lying levels vary within about 100 keV when the parameters  $a_r'$  and  $b$  in  $\mathcal{F}^-$  are varied. Basically, the calculated energies of the normal-parity levels are in good agreement with the experimental data.

## 6. GAMOW-TELLER EXCITATIONS

Strength functions and matrix elements of Gamow-Teller transitions

Excitations of this type with  $J^\pi = 1^+ (L=0, S=1)$  can be studied by means of external symmetry fields  $\sigma\tau_\mp$ . Like the isobar analog states, these excitations are among the most studied, mainly in  $(p, n)$  reactions. In particular, for the nuclei considered here many new data are contained in Refs. 45-51. Of greatest interest are the matrix elements of the Gamow-Teller transitions and the distributions of the transition strength over the excitation spectrum. This information now enables us to augment significantly and make more accurate our knowledge about spin-isospin interactions in nuclei.

In calculations of Gamow-Teller excitations, the effective interactions  $G^-$  and  $G_+^-$  contribute to the energy. Therefore, calculations of the Gamow-Teller resonance make possible the most direct estimate of the constant  $g'$  in the amplitude  $G^-$ . Such an estimate was made in Ref. 42 using the experimental energy (19.2 MeV) of the Gamow-Teller resonance in  $^{208}\text{Bi}$ ; it gave

$$\left. \begin{aligned} g' &= 0.95, & \text{if } g_\pi &= 0; \\ g' &= 1.1, & \text{if } g_\pi &= -1.45 (\xi_s = 0.1). \end{aligned} \right\} \quad (71)$$

Thus, the one-pion exchange contribution to the energy of the Gamow-Teller resonance can be imitated by a comparatively small renormalization of  $g'$ , though the influence of  $G_+^-$  on the properties of the modes with pion quantum numbers does not of course merely reduce to this (see below). The parameters in (71) are used in all the calculations discussed below.

The strength functions of the spin-multipole excitations were calculated for the external fields

$$V_0 \tau_\mp = [(2L+1)!!/q^L] j_L(qr) T_{LS}^M(n, \sigma) \tau_\pm. \quad (72)$$

For  $L=0$  and as  $q \rightarrow 0$  the external field becomes identical (up to a factor  $1/\sqrt{4\pi}$ ) with the standard Gamow-Teller operator of  $\beta$  decay. Above the nucleon-emission threshold, the excitations acquire the width  $\Gamma_{\text{esc}}$  due to single-nucleon decay to the continuum (escape width), and they appear in the strength functions as resonances. Near the threshold, the  $\Gamma_{\text{esc}}$  values are rather small. With increasing excitation energy, the  $\Gamma_{\text{esc}}$  values increase, and high in the continuum the resonances begin to overlap. For resonances lying above the Coulomb and centrifugal barriers,  $\Gamma_{\text{esc}}$  may reach several mega-electron-volts.

To achieve a unified representation of the discrete and resonance excitations and to reduce the volume of numerical calculations in the particle-hole propagator, an artificial quasiparticle damping<sup>38</sup> was introduced; it has the consequence that all states (including the discrete ones) acquire a width  $\Gamma_D$  in addition to  $\Gamma_{\text{esc}}$ . In our calculations, we used a damping corresponding to  $\Gamma_D = 1$  MeV. Such damping does not change the sum rules but makes it possible to calculate the strength functions with energy step  $\Delta\omega = 0.5$  MeV. It appears to us that  $\Gamma_D = 1$  MeV is an optimal value, since then the fine structure in  $S(\omega)$  does not vanish and there is hardly any distortion of the distribution of the transition strength over the excitation spectrum. The "smearing" sometimes practiced with a width of about 4 MeV, which is close to the observed width of the giant resonances, may lead to a distortion of these distributions, in particular to superfluous transfer of transition strength to the low-energy excitations. Figures 1-3 show the strength functions of Gamow-Teller transitions with  $\Delta T_z = -1$ , calculated for  $q=0$  and  $\Gamma_D = 1$  MeV. We shall discuss some of the characteristic features of these strength functions.

In the strength function of the particle-hole transitions ( $g' = g_\pi = 0$ ) in  $^{48}\text{Ca}$  (see Fig. 1, dotted curve) there are two dominant peaks associated with transition of a neutron from the state  $1f_{7/2}$  to the proton levels of the spin-orbit partners  $1f_{7/2}$  and  $1f_{5/2}$ . There is a similar situation in  $^{90}\text{Zr}$  ( $\xi$

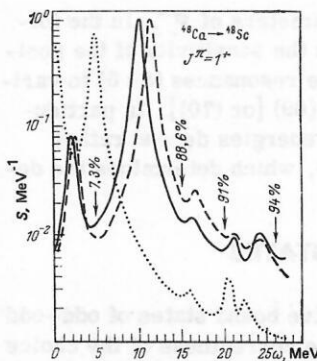


FIG. 1. Strength functions of Gamow-Teller transitions ( $L=0$ ) for the isobars  $^{48}\text{Ca} \rightarrow ^{48}\text{Sc}$ . The dotted curve corresponds to particle-hole transitions ( $g' = g_\pi = 0$ ); the broken curve is a calculation for  $g' = 1.1$  and  $g_\pi = 0$ ; the continuous curve, a calculation for  $g' = 1.1$  and  $g_\pi = -1.45 (\xi_s = 0.1)$ . The numbers in the figure show the percentages of the  $3(N-Z)$  sum rule exhausted in the section of the spectrum from 0 to the indicated energy.

ment of the  $1f$  states by  $1g_{9/2}$  and  $1g_{7/2}$ . The energies and matrix elements of the Gamow-Teller transitions for these configurations are given in Table III. It can be seen that the sum of the squares of the matrix elements of the particle-hole transitions in both nuclei is exactly equal to  $3(N-Z)$ . The contribution of the particle-hole transitions in the sections of the continuum to the strength function is very small and indicates weakness of the Gamow-Teller transitions with  $\Delta T_z = +1$ , i.e.,  $^{48}\text{Ca} \rightarrow ^{48}\text{K}$  and  $^{90}\text{Zr} \rightarrow ^{90}\text{Y}$ . Because of their smallness, we do not give here the corresponding strength functions.

The strength function of the particle-hole transitions in  $^{208}\text{Pb}$  (Fig. 3) has a more complicated shape. Here, the lowest peak at  $\omega \approx 5$  MeV is due to the transition  $n2f_{5/2} \rightarrow p2f_{7/2}$ . Then, near  $\omega \approx 7$  MeV there is grouped an entire conglomeration of states associated with allowed transitions of the type  $1i_{13/2} \rightarrow 1i_{13/2}$ ,  $1h_{9/2} \rightarrow 1h_{9/2}$ ,  $2f_{7/2} \rightarrow 2f_{7/2}$ , etc. On their background one cannot discern the weak transition  $n2f_{7/2} \rightarrow p1h_{9/2}$  corresponding to the  $1^+$  state at 6.55 MeV given in Table II. Finally, at energy  $\omega \approx 12.5$  MeV there are grouped transitions between the  $(np)$  levels of the spin-orbit partners:  $1h_{11/2} \rightarrow 1h_{9/2}$ ,  $1i_{13/2} \rightarrow 1i_{11/2}$ , etc. The details of these transitions, which are predominant in the structure of the Gamow-Teller resonance, are given in Table III. At excitation energies above 20 MeV there are many transitions forbidden with respect to the

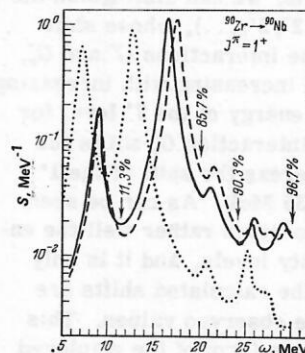


FIG. 2. The same as in Fig. 1, for  $^{90}\text{Zr} \rightarrow ^{90}\text{Nb}$ .



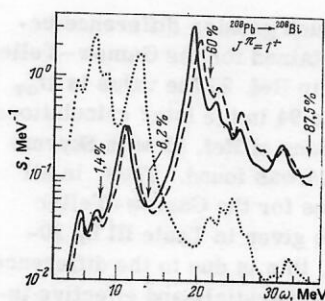


FIG. 3. The same as in Fig. 1, for  $^{208}\text{Pb} \rightarrow ^{208}\text{Bi}$ .

quantum numbers  $N$  and  $L$ . The spin-isospin repulsion  $G^-$  shifts the strength of the particle-hole transitions upward in energy and forms a clearly expressed resonance, in which most of the transition strength is concentrated (see the dashed curves in Figs. 1–3). Allowance for  $G^-$  (attraction) partly compensates the effect of the amplitude  $G$  at small momentum transfers (continuous curves in Figs. 1–3). At the same time, the low-lying  $1^+$  states are shifted rather weakly downward. The shifts of the maxima of the Gamow-Teller resonance are appreciably larger: 1.2 MeV in  $^{48}\text{Sc}$ ,  $\approx 1$  MeV in  $^{90}\text{Nb}$ , and  $\approx 0.8$  MeV in  $^{208}\text{Bi}$ . It can be seen that there is a systematic decrease in the shift, this being approximately proportional to  $A^{-1/3}$ . Physically, this influence of  $G^-$  can be understood, since the excitation of the Gamow-Teller resonance is associated with rather small  $q$  (below, we shall show that for  $q \approx 1 \text{ F}^{-1}$  the Gamow-Teller resonance can hardly be observed compared with the other  $1^+$  excitations). In the limit of an infinite system, because of the momentum conservation law  $G^-$  would not influence the properties of the excitations at all, in which values  $q \approx 0$  play the main role. In finite nuclei, the momentum nonconservation effects have the scale  $R^{-1}$ , and this explains the decrease in the shift of the Gamow-Teller resonance with increasing  $A$  in accordance with the law  $A^{-1/3}$  when  $G^-$  is taken into account. The characteristics of the low-lying and resonance states calculated for  $g' = 1.1$  and  $g_r = -1.45$  ( $\xi_s = 0.1$ ), and also the matrix elements of the Gamow-Teller transitions,<sup>8)</sup> are given in Table III. We shall discuss these results.

We have already noted that the constants  $g' = 1.1$  and  $g_r = -1.45$  were found by fitting the results to the experimental energy of the Gamow-Teller resonance in  $^{208}\text{Bi}$ . For these parameters, there is also fairly good agreement with the experiments for the calculated energies of the Gamow-Teller resonances in  $^{48}\text{Sc}$  and  $^{90}\text{Nb}$ . The theory also excellently describes the energy of the lowest  $1^+$  excitation in  $^{90}\text{Nb}$ . However, in  $^{48}\text{Sc}$  the theoretical energy is too low, as it is for the  $1^+$  state at 6.55 MeV in  $^{208}\text{Bi}$ . As for the  $2^-$  level in  $^{208}\text{Bi}$ , agreement with experiment cannot be achieved even by an appreciable increase in the parameter  $g'$ . To a certain extent, the difference between the theory and experiment is due to the uncertainty in the "experimen-

TABLE III. Results of calculations for  $J^\pi = 1^+ (L=0, S=1)$  excitations and experimental data<sup>43, 45-51</sup> [calculations in the theory of finite Fermi systems (TFFS) with the parameters  $g' = 1.1$  and  $g_r = -1.45$  ( $\xi_s = 0.1$ ); GTR: Gamow-Teller resonance].

| Isobars                                       | "Bare" configuration or TFFS calculation | $\omega$ , MeV  | $M_{GT}^2$ , theory    |      | Experiment     |                 |
|-----------------------------------------------|------------------------------------------|-----------------|------------------------|------|----------------|-----------------|
|                                               |                                          |                 | $eq[\sigma\tau] = 1.0$ | 0.8  | $\omega$ , MeV | $M_{GT}^2$      |
| $^{48}\text{Ca} \rightarrow ^{48}\text{Sc}$   | $(1f_{7/2}, 1f_{7/2}^{-1})$              | 0.32            | 10.3                   | 6.6  | —              | —               |
|                                               | TFFS                                     | 2.3             | 2.1                    | 1.3  | 3.0            | $1.83 \pm 0.3$  |
|                                               | $(1f_{5/2}, 1f_{7/2}^{-1})$              | 5.9             | 13.7                   | 8.8  | —              | —               |
|                                               | TFFS (GTR)                               | 10.8            | 19.5                   | 12.5 | $\sim 11$      | $11.2 \pm 1.2$  |
|                                               | TFFS                                     | 15–20           | 0.8                    | 0.5  | $\sim 17.3$    | $0.64 \pm 0.07$ |
|                                               | TFFS                                     | 0–27            | 23                     | 14.7 | —              | $13.7 \pm 1.8$  |
| $^{90}\text{Zr} \rightarrow ^{90}\text{Nb}$   | $(1g_{9/2}, 1g_{9/2}^{-1})$              | 7.2             | 12.3                   | 7.9  | —              | —               |
|                                               | TFFS                                     | 9.0             | 3.5                    | 2.2  | 9.0            | 1.8             |
|                                               | $(1g_{7/2}, 1g_{9/2}^{-1})$              | 12.7            | 17.7                   | 11.3 | —              | —               |
|                                               | TFFS (GTR)                               | 16.4            | 23.0                   | 14.7 | $\sim 15.6$    | $\sim 13$       |
|                                               | TFFS                                     | 20–24           | 1.4                    | 0.9  | $\sim 20.3$    | —               |
|                                               | TFFS                                     | 0–30            | 29                     | 18.6 | —              | $18.3 \pm 3$    |
| $^{208}\text{Pb} \rightarrow ^{208}\text{Bi}$ | TFFS                                     | 5.4             | 0.32                   | 0.2  | —              | —               |
|                                               | TFFS                                     | 6.1             | 0.04                   | 0.03 | 6.55           | —               |
|                                               | TFFS                                     | $\sim 11(9-13)$ | 8.0                    | 5.1  | —              | —               |
|                                               | $(1h_{9/2}, 1h_{11/2}^{-1})$             | 11.7            | 21.8                   | 14.0 | —              | —               |
|                                               | $(1i_{11/2}, 1i_{13/2}^{-1})$            | 12.9            | 25.2                   | 16.1 | —              | —               |
|                                               | TFFS (GTR)                               | 19.2            | 73.8                   | 47.2 | 19.2           | $\sim 55$       |
|                                               | TFFS                                     | 0–34            | 116                    | 74   | —              | $67 \pm 13$     |
|                                               | TFFS                                     | —               | —                      | —    | —              | —               |

tal" single-particle levels, in particular, the energies of the spin-orbit splitting. However, it appears more probable that for the low-lying  $2^-$  and  $1^+$  levels the discrepancies are due to the simplicity of the local spin-isospin forces that we employed rather than uncertainties in the choice of the single-particle basis.

Let us consider in somewhat more detail the situation with the  $1^+$  excitations in  $^{208}\text{Bi}$ . Here, the theoretically predicted lowest level at 5.4 MeV associated with the configuration  $(p2f_{7/2}, n2f_{5/2}^{-1})$  has not yet been observed experimentally. The state which follows it at 6.1 MeV (not distinguished in the strength function in Fig. 3 because of the smallness of  $M_{GT}^2$ ) is characterized by the presence of large components in the form factor at  $q \approx 1 \text{ F}^{-1}$ . Therefore, the total interaction  $G^- + G_r^-$  in this case is greatly weakened and makes a small contribution to the energy ( $\approx 0.16$  MeV; see Table II). Obviously, to obtain the correct energy of this state it is necessary in some way to strengthen the  $q$  dependence of the spin-isospin forces.

The maximum at  $\approx 11$  MeV is interesting; it gathers the transition strength of a number of closely spaced narrow resonances, which merge on the introduction of  $\Gamma_D = 1$  MeV. The Gamow-Teller transition strength concentrated in this "mini"-resonance appreciably exceeds the  $M_{GT}^2$  for the lowest  $1^+$  excitations (see Table III).

We compare our results with calculations in other studies. In Ref. 52, calculations were made for  $1^+$  excitations with realistic single-particle spectra and local spin-isospin interactions (without allowance for one-meson exchange). In  $^{48}\text{Sc}$  and  $^{90}\text{Nb}$ , the calculated energies of the lowest  $1^+$  levels are appreciably less than the experimental energies. It is concluded that nonlocal interactions must be taken into account. The difference

$$M_{GT}^2 = 4\pi \int_{\Delta\omega} S(\omega) d\omega \approx 2\pi^2 \Gamma S(\omega_R),$$

<sup>8)</sup>where  $\omega_R$  is the energy of the centroid of the resonance, and  $\Gamma$  is the width of the resonance when it is approximated by a Lorentz curve.

between our results in  $^{90}\text{Nb}$  and those obtained in Ref. 52 is most probably due to the difference between the single-particle level schemes.

In Ref. 53, a Hartree-Fock potential with Skyrme forces was used. Since the single-particle spectrum which is then obtained is far from realistic, the calculated energies of the lowest  $1^+$  excitations and the Gamow-Teller resonance were found to be appreciably higher than the known experimental energies and those predicted in the quoted theoretical studies. Phenomenological allowance for  $\Delta$ -isobar-nucleon-hole interactions only slightly corrects the situation.

Finally, in Ref. 54 Suzuki *et al.* calculated  $1^+$  excitations and a  $7^+$  level in  $^{48}\text{Sc}$  using empirical single-particle levels (Woods-Saxon potential). They took into account  $\pi$ - and  $\rho$ -meson exchange, and also a local interaction, whose parameter  $\delta g'$  was chosen by fitting the calculations to the experimental energies of the  $1^+$  levels. They succeeded in describing simultaneously the energies of the lowest  $1^+$  level and the Gamow-Teller resonance. However, the employed effective interactions are characterized by a strong  $q$  dependence. A similar computational scheme applied to  $^{208}\text{Pb}$  leads, however, to a too low energy of the Gamow-Teller resonance. Here, in accordance with the so-called dynamical theory, a Hartree-Fock potential with Skyrme forces ( $m^*/m = 0.76$ ) was used, but this certainly cannot be used to describe low-lying bound levels.

We now discuss the values of  $M_{\text{GT}}^2$  obtained in different studies. As can be seen from Figs. 1-3, only about 7-11% of the total transition strength is contained in the excitations below the Gamow-Teller resonance. The introduction of an effective charge  $e_q[\sigma\tau] < 1$  reduces the absolute values of the matrix elements, but does not change the distribution of the transition strength over the spectrum (see also Table III). Appreciably larger matrix elements for the low-lying  $1^+$  excitations are obtained in Ref. 52 ( $\approx 20\%$  of the total transition strength). The  $M_{\text{GT}}^2$  values for the low-lying states obtained in Ref. 53 exceed the values in Table III by 2-3 times. A value closer to ours,  $M_{\text{GT}}^2 = 2.4$ , is obtained in Ref. 54 for the lowest  $1^+$  excitation in  $^{48}\text{Sc}$ . This difference between the theoretical results is due to the fact that the transition probabilities for the low-lying (noncollective) states are very sensitive to the details of the single-particle schemes and the employed effective interactions. In addition, in our view the  $M_{\text{GT}}^2$  excess obtained in Refs. 52 and 53 is strongly related to the insufficient completeness of the single-particle basis. A much more complete basis was used in Ref. 54.

According to all the theoretical calculations, the main strength of the Gamow-Teller transitions is concentrated in the Gamow-Teller resonance, although here too there are some differences in the absolute values of  $M_{\text{GT}}^2$ . For  $^{48}\text{Sc}$ , our calculated value of  $M_{\text{GT}}^2$  agrees well with the value obtained in Ref. 54 ( $M_{\text{GT}}^2 \approx 21$ ). A smaller value (18.2) was found in Ref. 53, this being due to the too large transition matrix element predicted for the low-lying  $1^+$  state. In  $^{90}\text{Nb}$ , our calculations of  $M_{\text{GT}}^2$  for the Gamow-Teller resonance are close to the value

$M_{\text{GT}}^2 = 22.2$  in Ref. 53. A much greater difference between the  $M_{\text{GT}}^2$  values is obtained for the Gamow-Teller resonance in  $^{208}\text{Bi}$ . Thus, in Ref. 23 the value is  $M_{\text{GT}}^2 \approx 108$ , this being reduced to 94 in the later calculations of Ref. 55. In the calculations of Ref. 53 with Skyrme forces, the value  $M_{\text{GT}}^2 = 89.4$  was found. Thus, in all these papers the  $M_{\text{GT}}^2$  values for the Gamow-Teller resonance exceed the value given in Table III by 20-40%. To a certain degree, this is due to the difference between the single-particle potentials and effective interactions used in the calculations. But, as can be seen from Fig. 3, the strength function of the Gamow-Teller transitions for  $^{208}\text{Pb}$  decreases rather slowly in the high-energy part of the spectrum, exhibiting some structure. In the region of the continuum above the Gamow-Teller resonance there is about one third of the complete transition strength. Such a result is obtained only when the single-particle continuum is taken into account exactly. The calculations in all the other studies were either made with a small single-particle basis or the continuum was taken into account too crudely.

In  $^{48}\text{Ca}$  and  $^{90}\text{Zr}$  a much smaller fraction of the total strength of the Gamow-Teller transitions is distributed in the continuum than in  $^{208}\text{Pb}$  (see Figs. 1 and 2), and therefore our values of  $M_{\text{GT}}^2$  for the Gamow-Teller resonance in these nuclei is close to the values obtained in the other studies. Thus, we conclude that it is important to take into account correctly the single-particle continuum, especially in heavy nuclei. This is necessary for a correct estimate of the effective charge  $e_q[\sigma\tau]$  (see below).

As can be seen from Figs. 1-3, a certain structure is observed in the strength functions of the transitions above the Gamow-Teller resonance, i.e., resonance states with fairly large values of  $\Gamma_{\text{esc}}$  are observed. In  $^{48}\text{Ca}$  and  $^{90}\text{Zr}$  they are more clearly expressed and are well separated from the Gamow-Teller resonance. The integrated characteristics of the "mini"-resonances in these nuclei are given in Table III. It can be seen that they contain approximately 3-5% of the total transition strength. The existence of the  $1^+$  resonances in  $^{48}\text{Sc}$  and  $^{90}\text{Nb}$  above the Gamow-Teller resonance was confirmed in  $(p, n)$  experiments,<sup>45, 46, 51</sup> the theoretically predicted regions of localization of the resonances agreeing well with the experimental data. The interest in these excitations is due to the attempt to interpret them as isobar analogs of the  $M1$  resonances in the parent nuclei, which is in agreement with energy arguments<sup>45, 46</sup> and shell calculations for  $^{48}\text{Ca}$  in a scheme that presupposes isospin conservation.<sup>56</sup> A similar interpretation of the third  $1^+$  excitation in  $^{48}\text{Sc}$  can be found in Ref. 57. This means that in their structural characteristics the Gamow-Teller resonance and the analog of the  $M1$  resonance are similar (i.e., they are formed by the same allowed particle-hole transitions), but they differ in isospin. Therefore, the ratios of the intensities of the Gamow-Teller transitions for them are determined by the ratios of the squares of the corresponding isospin Clebsch-Gordan coefficients. However, it should not be forgotten that in nuclei isospin is not conserved and that the resonances under discussion are in the continuum. As a result, there is a strong in-



crease in the influence of particle-hole transitions to the continuum (including  $l$ -forbidden transitions), which change the radial quantum numbers of a higher-lying resonance compared with the Gamow-Teller resonance. Below, we shall demonstrate this in the transition densities of the excitations.

Before we compare the calculated  $M_{GT}^2$  with the experimental data, we discuss the transition densities of the  $1^+$  excitations.

### Transition densities

For well-isolated resonances with centroid energy  $\omega_R$ , as for discrete states, one can introduce the concept of a transition density, which is characterized by the quantum numbers  $J^\pi$  of the excitation. By its form one can distinguish transition densities for anomalous-parity states ( $0^-, 1^+, 2^-, \dots; S=1$ ),

$$\rho_{tr}^{JM}(r, \sigma) = \sum_{L=J \pm 1} \rho_{tr}^{LJ}(r) T_{JL}^M(n, \sigma), \quad (73)$$

and normal-parity states ( $J=L; 0^+, 1^-, 2^+, \dots$ ),

$$\rho_{tr}^{JM}(r, \sigma) = \sum_{S=0,1} (\rho_{tr}^{LJ}(r))_S T_{JL}^M(n, \sigma), \quad (74)$$

where

$$\rho_{tr}^{LJ}(r) = C \operatorname{Im} \sum_{L', S'} \int A_{LS, L'S'}^J(r, r'; \omega) \times V^{LSJ}(r', \omega) r'^2 dr' |_{\omega=\omega_R}. \quad (75)$$

Here,  $V^{LSJ}(r, \omega)$  are the radial components of the effective fields that arise in the nucleus when the external fields  $V_0$  are applied. Thus, except for the case  $J=0$ , all states are characterized by two radial components of the transition density, these differing in  $L$  or  $S$ . The normalization constant  $C$  is determined by the matrix element of the transition in the external field:

$$M_{0 \rightarrow J}^2 = (2J+1) \left| \sum_L \int \rho_{tr}^{LJ}(r) V_0^L(r) r^2 dr \right|^2 \quad (76)$$

for the anomalous-parity states ( $S=1$ ) and

$$M_{0 \rightarrow J}^2 = (2J+1) \left| \sum_S \int (\rho_{tr}^{LJ}(r))_S V_0^{LSJ}(r) r^2 dr \right|^2 \quad (L=J) \quad (77)$$

for the normal-parity states. In the continuum (or for the discrete states when the width  $\Gamma_D$  is introduced) the value of  $M_{0 \rightarrow J}^2$  for an isolated resonance can be obtained by integrating the strength function for the corresponding  $V_0$  over the neighborhood  $\omega_R \pm \Delta\omega/2$  of the centroid of the resonance:

$$M_{0 \rightarrow J}^2 = \int_{\Delta\omega} S(\omega) d\omega. \quad (78)$$

In particular, if the resonance is approximated by a Lorentz shape with parameters  $\omega_R$  and  $\Gamma$ , then

$$M_{0 \rightarrow J}^2 \approx (\pi/2) \Gamma S(\omega_R). \quad (79)$$

In this case, we obtain for  $C$  the expression

$$C = [(2J+1) \Gamma / 2\pi S(\omega_R)]^{1/2}. \quad (80)$$

For a resonance with a strongly distorted shape in the continuum the transition density must be normalized to the total strength of the transitions in the considered section of the excitation spectrum.

The definition (75) of the transition density and the

normalization contain the external field and the effective field. For discrete states, of course, the transition density is an intrinsic characteristic of the excitation and should not depend on  $V_0$ . For narrow, well-localized resonances the dependence on  $V_0$  is only apparent and in fact cancels. In any case, in the calculations for the resonances we used external fields differing somewhat in form and verified that the transition density is independent of them. In practice, it is found that the  $\rho_{tr}$  concept can be used even for asymmetric resonances high in the continuum. They are always normalized to the integrated contribution of the corresponding section of the spectrum to the sum rule. Figures 4-6 give the radial components of  $\rho_{tr}$ , by means of which one can find the ordinary matrix elements of Fermi and Gamow-Teller transitions:

$$M_F^2 = 4\pi \left| \int \rho_{tr}^{00}(r) r^2 dr \right|^2; \quad (81)$$

$$M_{GT}^2 = 12\pi \left| \int \rho_{tr}^{01}(r) r^2 dr \right|^2. \quad (82)$$

For the three  $1^+$  excitations in  $^{48}\text{Sc}$  and  $^{90}\text{Nb}$  given in Table III the transition densities with  $L=0$  are shown in Figs. 4 and 5. A characteristic change in their shape with increasing excitation energy can be seen. It should be noted that for allowed particle-hole Gamow-Teller transitions between single-particle states with  $l>0$  the transition densities always have a bell shape with a maximum on the surface of the nucleus (see, for example, curve 1 in Fig. 6). For the lowest  $1^+$  states,  $\rho_{tr}^{01}$  has a volume nature, in contrast to the surface nature of a pure particle-hole configuration ( $pf_{7/2}, nf_{7/2}^{-1}$ ) and ( $pg_{9/2}, ng_{9/2}^{-1}$ ). The appearance of the volume component in the transition density is due to admixtures of particle-hole transitions to  $s$  states in the continuum, which are enhanced by one-pion exchange. With regard to the transition densities  $\rho_{tr}^{21}$  ( $L=2$ ) for these states, they have a surface nature, and at the maxima  $\rho_{tr}^{01}$  and  $\rho_{tr}^{21}$  are approximately equal (see curve 3 in Fig. 5). It is important to take into account these components of the transition densities in calculations of the angular distributions of  $(p, n)$ -type reactions at large angles.

The transition densities of the Gamow-Teller resonances in  $^{48}\text{Sc}$  and  $^{90}\text{Nb}$  have a clearly defined surface nature. In  $^{208}\text{Bi}$  (see Fig. 6, curves 2 and 3), the volume component is fairly large, i.e., here the contribu-

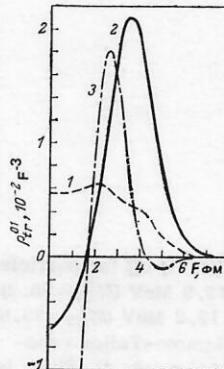


FIG. 4. Radial functions  $\rho_{tr}^{01}$  of transition densities of  $1^+$  excitations in  $^{48}\text{Sc}$  given in Table III ( $e_q=1$ ): 1)  $\omega=2.3$  MeV; 2)  $\omega=10.8$  MeV (Gamow-Teller resonance); 3)  $\omega=16.3$  MeV.

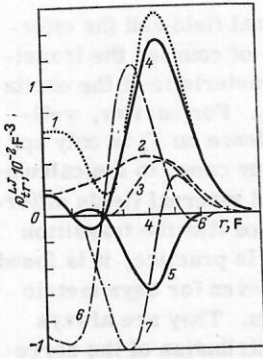


FIG. 5. Transition densities of excitations in  $^{90}\text{Nb}$ : 1)  $\rho_{tr}^{00}$  for the isobar analog state,  $\omega=12.5$  MeV ( $M_{GT}^2=9.6$ ); 2) and 3)  $\rho_{tr}^{01}$  and  $\rho_{tr}^{11}$ , respectively, for  $1^+$  excitations with  $\omega=9$  MeV ( $M_{GT}^2=3.5$ ); 4) and 5)  $\rho_{tr}^{01}$  and  $\rho_{tr}^{11}$ , respectively, for the Gamow-Teller resonance with  $\omega=16.4$  MeV ( $M_{GT}^2=23$ ); 6) and 7)  $\rho_{tr}^{01}$  and  $\rho_{tr}^{11}$ , respectively, for  $1^+$  excitations with  $\omega=21.3$  MeV ( $M_{GT}^2=1.4$ ).

tion of the particle-hole transitions to the continuum is appreciable. Comparison of curves 2 and 3 in Fig. 6 reveals a comparatively weak influence of one-pion exchange on  $\rho_{tr}^{01}$  for the Gamow-Teller resonance. Note that usually the shapes of the transition densities for the Gamow-Teller resonance and the isobar analog state are fairly similar in the surface region, as can be seen in Figs. 5 and 6. Figure 6 also shows the isovector density  $\rho^-$  calculated for  $^{208}\text{Pb}$ , normalized for convenience like the transition density  $\rho_{tr}^{00}$  for the isobar analog state. The difference between these quantities is due to the Coulomb isospin mixing (see, for example, Ref. 58). As a result,  $\rho_{tr}$  for the isobar analog state on the surface is systematically larger than  $\rho^-$  for all the nuclei we considered. This effect is important in connection with the question discussed in the literature of what transition densities must be used in reactions with excitation of an isobar analog state. For example, in Ref. 59 it is proposed to use as transition density for the isobar analog state, not  $\rho^-$ , but the excess density  $\rho_{exc}$  of neutrons, i.e., not to include the difference be-

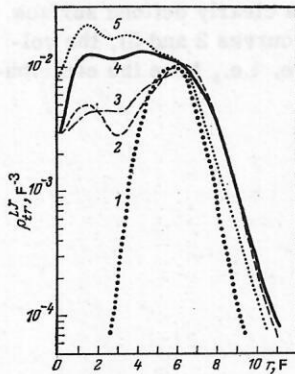


FIG. 6. The same as in Fig. 5, for  $^{208}\text{Bi}$ : 1)  $\rho_{tr}^{01}$  for particle-hole configurations ( $pl i_{11/2}, nl i_{13/2}$ ),  $\omega=12.9$  MeV ( $M_{GT}^2=25.2$ ); 2)  $\rho_{tr}^{01}$  for Gamow-Teller resonance,  $\omega=19.2$  MeV ( $M_{GT}^2=73.8$ ),  $g'=1.1$ ,  $g_r=-1.45$  ( $c_r=0.1$ ); 3)  $\rho_{tr}^{01}$  for Gamow-Teller resonance,  $\omega=19.2$  MeV ( $M_{GT}^2=72.6$ ),  $g'=0.95$ ,  $g_r=0$ ; 4)  $\rho_{tr}^{00}$  for isobar analog state,  $\omega=18.8$  MeV ( $M_{GT}^2=40$ ); 5) isovector density  $c\rho^-$ , where  $c$  is chosen such that  $|\int \rho_{tr}^{00} r^2 dr|^2 = c |\int \rho^- r^2 dr|^2 \equiv M_F^2/4\pi$ .

tween the densities of neutrons and protons in closed shells with the same quantum numbers. The calculations show that  $\rho_{exc}$  is larger on the surface than  $\rho^-$ . This leads to an appreciable difference between the cross sections for charge exchange of pions ( $\pi^+$ ,  $\pi^0$ ), which are strongly absorbed on the surface. We believe it is correct to use in calculations of the cross sections, not  $\rho^-$  or  $\rho_{exc}$ , but the microscopic transition density for the isobar analog state  $\rho_{tr}^{00}$  determined by Eq. (75). On the surface of the nucleus,  $\rho_{exc}$  and  $\rho_{tr}^{00}$  are not very different, but in the interior their difference may be appreciable. True, this difference between  $\rho_{exc}$  and  $\rho_{tr}^{00}$  is hardly important for the cross sections of the ( $\pi^+$ ,  $\pi^0$ ) reaction.

The transition densities  $\rho_{tr}$  for  $1^+$  resonances above the Gamow-Teller resonance have a quite different nature (see Figs. 4 and 5). They are characterized by a node on the surface and large volume components,  $\rho_{tr}^{01}$  and  $\rho_{tr}^{21}$  being comparable at the maxima (in contrast to the Gamow-Teller resonance, for which the  $\rho_{tr}^{21}$  are small). Therefore, particle-hole transitions to the continuum play a decisive role in the formation of these excitations. Note that if the third  $1^+$  excitations in  $^{48}\text{Sc}$  and  $^{90}\text{Nb}$  were analogs of an M1 resonance, their transition densities  $\rho_{tr}^{01}$  would have shapes similar to those obtained for the Gamow-Teller resonance. The difference between  $\rho_{tr}$  for these excitations and the Gamow-Teller resonance can be traced in the difference between the angular distributions of the cross sections of ( $p, n$ ) reactions at large angles (at momentum transfers  $q \approx 1 \text{ F}^{-1}$ ). However, for angles  $\theta < 15^\circ$  as well the cross section  $d\sigma/d\Omega$  for the Gamow-Teller resonance must decrease more rapidly than for the higher-lying  $1^+$  excitations. This effect was obtained in the calculations made in Ref. 60.

#### Effective charges and the problem of the suppression of Gamow-Teller transitions

We turn to the discussion of the matrix elements  $M_{GT}^2$  in the light of the currently known experimental data. A direct method of measurement is  $\beta$  decay to  $1^+$  levels, which is energetically forbidden for all the cases we consider. Indirect information could sometimes be given by the  $\beta$  decays of the neighboring nuclei (for example, the  $1^+$  level with  $\omega=9$  MeV in  $^{90}\text{Nb}$  is populated by the  $\beta$  decay of  $^{90}\text{Mo}$ ). However,  $M_{GT}^2$  may then vary strongly because of nucleon pairing effects in the unfilled shell and differences between the correlation effects in the ground states of  $^{90}\text{Zr}$  and  $^{90}\text{Mo}$ . Therefore, great interest attaches to attempts to extract the  $M_{GT}^2$  values directly from the cross sections  $d\sigma/d\Omega$  of the ( $p, n$ ) reactions at angle  $\theta \approx 0^\circ$  (see, for example, Ref. 61). It was noted that in the distorted-wave Born approximation the cross section of the ( $p, n$ ) reaction at this angle can be represented as a sum of components proportional to the matrix elements of the Fermi ( $M_F^2$ ) or Gamow-Teller ( $M_{GT}^2$ ) transition (for even-even targets):

$$\frac{d\sigma(0^\circ)}{d\Omega} \sim \left\{ \begin{array}{l} N_D^F |J_\pi|^2 M_F^2; \\ N_D^{GT} |J_{\sigma\pi}|^2 M_{GT}^2, \end{array} \right. \quad (83)$$

where  $N_D$  are distortion factors which depend on  $A$  and



the proton energy, and  $J_\tau$  and  $J_{\sigma\tau}$  are volume integrals of the central components (for  $q=0$ ) of the isospin and spin-isospin effective interactions of the incident nucleons with the nucleons of the nucleus.<sup>62</sup> Numerical calculations showed that the ratio  $|J_{\sigma\tau}/J_\tau|^2$  increases rather rapidly from 1 to 7 in the interval of proton energies  $E_p$  from 50 to 200 MeV. This, in particular, also explains well the experimentally observed preferred excitation of spin modes for  $E_p \gtrsim 120$  MeV. The simple relations (83) were used for calibration in the cases when the matrix elements were known from  $\beta$  decay, for example, for the nuclei  ${}^7\text{Li}$ ,  ${}^{13}\text{C}$ ,  ${}^{26}\text{Mg}$ ,  ${}^{27}\text{Al}$ , and others.<sup>61</sup> It was found that the ratio  $[d\sigma(0^\circ)/d\Omega]_{\text{exp}}/M_{\text{GT}}^2$  has a regular dependence proportional to  $A^{-1/3}$  for given proton energy. This makes it possible to extract the empirical values of  $J_{\sigma\tau}$  and  $J_\tau$  and to obtain estimates for  $M_{\text{GT}}^2$  in regions of the spectra not accessible to investigation in  $\beta$  decay, in particular in the region of the Gamow-Teller resonance. The values of  $M_{\text{GT}}^2$  obtained in  $(p, n)$  reactions are systematized in Ref. 50. Figure 7 shows part of the total strength of the Gamow-Teller transitions observed in  $(p, n)$  reactions for different nuclei.<sup>50</sup>

The main difficulty in determining  $M_{\text{GT}}^2$  is associated with the uncertainty in the separation of the background, particularly in the region of the Gamow-Teller resonance. For example, the calculations of Ref. 63 showed that for  ${}^{48}\text{Ca}$  most of the background separated by the experimentalists must in reality be included in the cross section for the resonance, which increases it by approximately 25%.

The experimental estimates of  $M_{\text{GT}}^2$  and of the total strength of the Gamow-Teller transitions for the considered nuclei in the region 0–30 MeV of excitation energies are given in Table III. The value of  $M_{\text{GT}}^2$  for the Gamow-Teller resonance in  ${}^{48}\text{Sc}$  given in Ref. 51 is increased by 25% in accordance with the calculations of the background in Ref. 63. For the Gamow-Teller resonances in  ${}^{90}\text{Nb}$  and  ${}^{208}\text{Bi}$  and in the integral sums the experimental data are taken from Ref. 50. The observed integrated strength of the Gamow-Teller transitions is systematically about 50–60% of the total possible strength  $3(N-Z)$ .

In the framework of the approximations that we have used in the theory of finite Fermi systems, the quenching of the strength of the Gamow-Teller transitions can be phenomenologically described by the introduction of a local charge  $e_q[\sigma\tau]$ ; this cannot yet be calculated, so that it must be found from experimental data. There-

fore, the theoretical results for  $M_{\text{GT}}^2$  in Table III are given for the two values  $e_q[\sigma\tau]=1$  and 0.8. It can be seen from the table that the observed transition strength agrees well with the calculations for  $e_q[\sigma\tau]=0.8$ . For individual  $1^+$  excitations, the situation is not entirely uniform. Thus, in  ${}^{48}\text{Sc}$  the value of  $M_{\text{GT}}^2$  for the Gamow-Teller resonance exceeds the experimental error, while for other  $1^+$  excitations the  $M_{\text{GT}}^2$  are somewhat smaller than the empirical values. We emphasize once more that  $M_{\text{GT}}^2$  for the Gamow-Teller resonance in  ${}^{208}\text{Bi}$  that we obtained with exact allowance for the single-particle continuum is the smallest of all the values obtained in the literature. From comparison with the experiment in this case we obtain the estimate  $0.8 \leq e_q[\sigma\tau] < 0.9$  for the local charge.

Of course, the introduction of an effective charge as a phenomenological quantity does not answer the question of where the remaining fraction of the integrated transition strength is to be sought. Physically, the local charge takes into account some of the effects associated with many-particle admixtures (for example,  $2p-2h$ ) and other degrees of freedom not included in the particle-hole picture. Among the latter, much attention is at present devoted to the contribution associated with the virtual  $\Delta$ -isobar-nucleon-hole excitation (see, for example, Refs. 50, 53, 54, 57, and 64). Estimates of the renormalization of the strength of the Gamow-Teller transitions due to this mechanism show that  $\approx 30\%$  of the total strength may be attributed to it. In Ref. 65, an estimate is made of the part played by  $(2p-2h)$  configurations in the redistribution of the strength of the Gamow-Teller transitions over the excitation spectrum for  ${}^{90}\text{Zr}$ . It is demonstrated that this mechanism could lead to transfer of about half the transition strength to the continuum above the Gamow-Teller resonance and to "spreading" of it over a wide energy region (up to  $\varepsilon_F$ ).

#### Dependence of the strength functions on the momentum transfer

Hitherto, we have discussed the results of calculations made for  $q=0$ , i.e., in fact the  $\beta$ -decay characteristics. However, in reactions with hadrons the momentum transfer is small only for measurements near  $\theta=0^\circ$ . With increasing angle of the measurements and energy of the incident particles  $q$  increases, and it is therefore of interest to follow the relative behavior of the cross sections for different  $1^+$  excitations with increasing  $q$ . In the Born approximation, qualitative information of this kind is given by the behavior of the strength functions  $S(\omega, q)$  calculated for the external fields (72). The strength functions of  $1^+$  excitations for the isobars  ${}^{208}\text{Pb} \rightarrow {}^{208}\text{Bi}$  calculated in Ref. 42 for  $g' = 1.1$  and  $g_r = -1.45$  for three values of  $q$  are given in Fig. 8. Comparison of the calculations for  $q=0$  and  $0.3 \text{ F}^{-1}$  reveals approximately the same rapid decrease of the maxima of  $S(\omega)$  for all  $1^+$  excitations. A strong difference commences at  $q \approx 1 \text{ F}^{-1}$ . Although in absolute magnitude  $S(\omega)$  are small for all states, it is important that there is a significant redistribution of the transition strength: The Gamow-Teller resonance almost disappears, but the part played by low-lying ex-

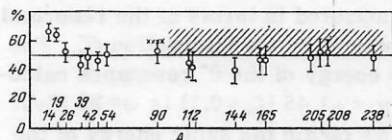


FIG. 7. Experimental data on the total strength of Gamow-Teller transitions (as a percentage of the  $3(N-Z)$  sum rule) observed in  $(p, n)$  reactions.<sup>50</sup> The region corresponding to uncertainty in the determination of the background is hatched (the upper limit includes the total background as due solely to Gamow-Teller transitions).

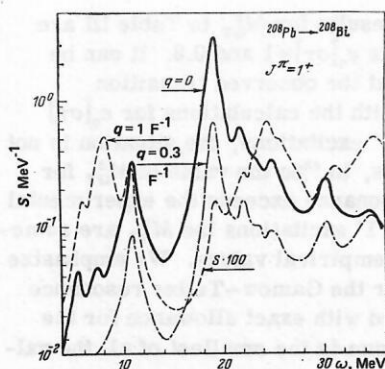


FIG. 8. Dependence of the strength functions of Gamow-Teller transitions on the momentum transfer  $q$  for the isobars  $^{208}\text{Pb} \rightarrow ^{208}\text{Bi}$ .

citations ( $\omega \approx 8$  MeV) increases strongly and a new broad maximum is formed above the resonance ( $\omega \approx 25$  MeV). Its width  $\Gamma_{\text{osc}}$  (several MeV) is appreciably greater than the widths of the analogous resonances in  $^{48}\text{Ca}$  and  $^{90}\text{Zr}$ . For this reason, and also because in the same energy region an  $L=1$  spin-flip resonance is formed, it has not yet been observed.

Note also that the relative enrichment of the low-lying  $1^+$  excitations with increasing  $q$  is largely due to the influence of one-pion exchange and is one of the possible precritical effects of pion condensation. Of course, allowance for distortion in the Born approximation may render all these effects less pronounced.

## 7. EXCITATIONS WITH $L=1$ ( $S=1, 0$ )

Besides the Gamow-Teller resonance, one can expect resonances due to transitions with  $L>0$  to be manifested in charge-exchange reactions. Indeed, in numerous experimental investigations, mainly in  $(p, n)$  reactions (see Refs. 45, 47, 48, and 66) a broad ( $\Gamma \approx 10$  MeV) maximum has been systematically observed in the excitation spectra above the Gamow-Teller resonance. The measured angular distributions for this maximum were characteristic of  $L=1$  transitions. The protons used in the reactions had energies  $\approx 120$  MeV, at which excitations with  $S=0$  are suppressed, and it was therefore concluded that the new resonance is basically associated with spin-dipole transitions. The resonance has by now been observed in numerous nuclei, including the nuclei  $^{90}\text{Zr}$  and  $^{208}\text{Pb}$  that we have been discussing, at an energy of about 25 MeV.

Resonances with  $L=1$  have also been observed in  $(p, n)$  reactions at  $E_p = 45$  MeV for a number of Zr, Mo, Sn isotopes and  $^{208}\text{Pb}$ .<sup>67</sup> At such proton energies, the effective isospin interactions are at least of the same order as (or are larger than) the spin-isospin interactions, and it can be expected that the dipole resonance with  $S=0$  makes an appreciable contribution to the cross section. If the energy of this resonance differs appreciably from the energies of spin-dipole resonances, the centroid of the observed excitation will be shifted when the energy of the incident protons is changed. Such a shift (by about 2–3 MeV) has indeed been observed, and its interpretation is given below.

From the point of view of theory,  $L=1$  transitions are particularly interesting in that they make it possible to test the correctness of the parametrization of the effective interactions, the isovector  $\mathcal{F}^-$  and the spin-isospin  $G^-$ , and also to study more fully the influence of one-meson exchange, since it can be expected on general grounds that  $L=1$  transitions are accompanied by a larger transfer  $q$  than  $L=0$  transitions. On the other hand, in contrast to Gamow-Teller transitions with  $\Delta T_z = 1$ , which are suppressed in the considered nuclei, such transitions with  $L=1$  can be compared with transitions to the daughter nuclei with  $\Delta T_z = -1$ , i.e., they are of independent interest for investigating them in reactions of the type  $(n, p)$ ,  $(^7\text{Li}, ^7\text{Be})$ , etc. This makes it possible to verify the dipole sum rules and, in particular, the universality of the phenomenon of quenching of spin-multipole transitions as observed for Gamow-Teller excitations.

## Strength functions and energies of $L=1$ resonances

Calculations of the strength functions for  $L=1$  were made with the parameters of the effective interactions given in the previous sections. The results of the calculations are given in Figs. 9–11 for the case  $q=0$  and  $\Gamma_D = 1$  MeV. For the dipole transitions with  $S=0$  and  $J=L$  the external fields

$$V_0(r, q) \tau_{\mp} = [(2L+1)!!/q^L] j_L(qr) Y_L(n) \tau_{\mp} \quad (84)$$

were used, and for the spin-dipole transitions ( $S=1, J=L, L\pm 1$ ), the fields (72).

As for the Gamow-Teller transitions, the effective interactions transfer to the continuum the main strength of the  $L=1$  transitions and form resonances. For  $J^\pi = 2^-$ , there is not a single giant resonance; the main strength of the transitions is concentrated in an interval of excitation energies with a width of about 10 MeV (see Figs. 9a, 10a, and 11a).

The interaction  $G_r^-$  makes a contribution only for  $0^-$  and  $2^-$  transitions, displacing the energies of the corresponding resonances downward. The shifts for the  $0^-$  resonances in the daughter nuclei with  $\Delta T_z = -1$  are particularly large (about four times larger than for the Gamow-Teller resonance), namely, about 4.7 MeV in  $^{48}\text{Sc}$ , almost 3.9 MeV in  $^{90}\text{Nb}$ , and about 3.2 MeV in  $^{208}\text{Bi}$ . As for the Gamow-Teller resonance, the magnitude of the shifts due to one-pion exchange decreases approximately as  $A^{-1/3}$ . The fact that for the  $0^-$  resonances the shifts increase strongly indicates that there are large transfers  $q$  in the process of spin-dipole transitions (see also Ref. 55). The same quality of  $L=1$  transitions can be illustrated in terms of the renormalization of the parameter  $g'$  by the interaction  $G_r^-$ . For example, in  $^{208}\text{Bi}$  the energy of the  $0^-$  resonance calculated for  $g'=1.1$  and  $g_r = -1.45$  ( $\xi_s = 0.1$ ) is  $\omega \approx 28$  MeV. If we set  $g_r = 0$ , then we obtain the same energy of the resonance at the value  $g' \approx 0.65$  (in the case of the Gamow-Teller resonance,  $g' \approx 0.95$  for  $g_r = 0$ ), i.e., the influence of one-meson exchange on the  $L=1$  transitions is appreciably greater than on the  $L=0$  transitions. Therefore, without allowance for one-meson exchange the theory will, if  $g'$  is chosen on the basis of the en-



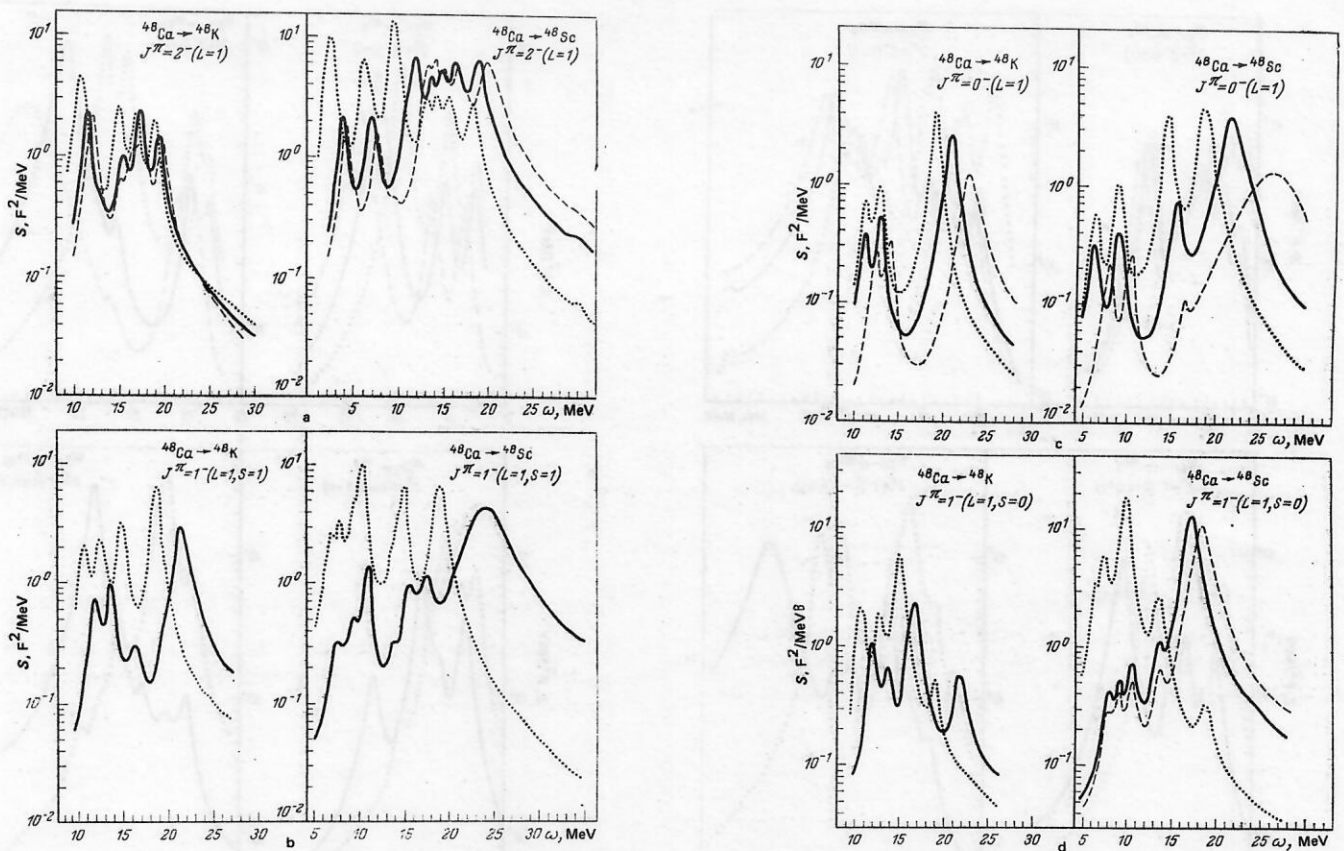


FIG. 9. Strength functions of transitions with  $L=1$  ( $q=0$ ) for the isobars  $^{48}\text{Ca} \rightarrow ^{48}\text{Sc}$  ( $\Delta T_z = -1$ ) and  $^{48}\text{Ca} \rightarrow ^{48}\text{K}$  ( $\Delta T_z = 1$ ): a), b), and c) spin-dipole ( $S=1$ ) excitations with  $J^\pi = 2^-, 1^-$ , and  $0^-$ , respectively; d) dipole ( $S=0$ ) excitations with  $J^\pi = 1^-$ . The remaining notation is as in Fig. 1. (For additional explanations, see the text.)

ergy of the Gamow-Teller resonance, always predict too large energies of the spin-dipole resonances with  $J = 0$  and  $2$ , as was noted in Refs. 50 and 52.

The dipole transitions with  $J^\pi = 1^-$  can be distinguished approximately by means of the spin quantum number  $S$  ( $0$  or  $1$ ), although the interactions  $\mathcal{F}^-$  and  $G^-$  occur simultaneously in the equations describing such transitions. Each  $1^-$  excitation is characterized by two components of the transition density (74), which are proportional to  $Y_1$  ( $S=0$ ) and  $[\sigma \otimes Y_1]^1$  ( $S=1$ ). A distinction based on the quantum number  $S$  has meaning only when one of the components of  $\rho_{tr}$  is significantly larger than the other. In other words, states with a good quantum number  $S$  must be strongly excited only in external fields of the corresponding symmetry, i.e., proportional to  $Y_L$  or  $[\sigma \otimes Y_L]^J$ .

Our calculations showed that the strength functions of excitations with  $J^\pi = 1^-$  ( $S=0$ ) vary weakly with variation of  $G^-$ . A similar weak dependence on  $\mathcal{F}^-$  is obtained for spin-dipole excitations. Comparing cases b and d in Figs. 9–11, we see that the dipole ( $S=0$ ) and spin-dipole ( $S=1$ ) resonances are everywhere well separated in energy, the former lying systematically lower than the latter by about 5–6 MeV. This shift is actually due to the difference between the distributions for the dipole and spin-dipole particle-hole transitions (i.e., when  $\mathcal{F}^- = G^- = 0$ ), which are shown by the dotted curves in Figs. 9–11. It is associated with the spin-orbit splitting. For example, in  $^{90}\text{Nb}$  (see Figs. 10b and 10d)

the lower maximum in the strength functions of the particle-hole transitions at  $\omega \approx 14.8$  MeV is due to  $n1f_{5/2} \rightarrow p1g_{7/2}$  and  $n1g_{9/2} \rightarrow p1h_{11/2}$  transitions with  $\Delta S = 0$ . In the spin-dipole strength function (see Fig. 10b) there are higher maxima with energies around 21 and 23 MeV associated with the  $n1f_{7/2} \rightarrow p1g_{7/2}$  and  $n1g_{9/2} \rightarrow p1h_{9/2}$  transitions ( $\Delta S=1$ ) respectively. These transitions are suppressed in the dipole strength function but play the main part in forming the spin-dipole resonance.

The effect of the spin-orbit splitting persists when the effective interactions are included. We note, however, a rather interesting feature for  $1^-$  ( $S=0$ ) resonances—the fairly strong shift of the energy centroid upward with increasing value of the parameter  $b$ , which characterizes the degree of interpolation of  $\mathcal{F}^-$ . This feature is illustrated in Fig. 9d for  $^{48}\text{Sc}$  (the continuous and broken curves correspond to the values  $b=0$  and  $2$ ) and in Fig. 11d for  $^{208}\text{Bi}$  (the broken and continuous curves correspond to the values  $b=0$  and  $4$ ). The parameter  $b$  was varied in accordance with the consistency condition (69), i.e., the value of  $a'_0$  was changed simultaneously (the dependence on  $a'_0$  is effectively unimportant).

Thus, interpolation of the interactions  $\mathcal{F}^-$  compensates to a certain degree the influence of the spin-orbit splitting. However, even for  $b=4$ , when  $f_{ex}^-/f_{in}^- \approx 5$ , the  $1^-$  ( $S=0$ ) resonance in  $^{208}\text{Bi}$  still lies appreciably below (by about 3 MeV) the spin-dipole resonance. In this

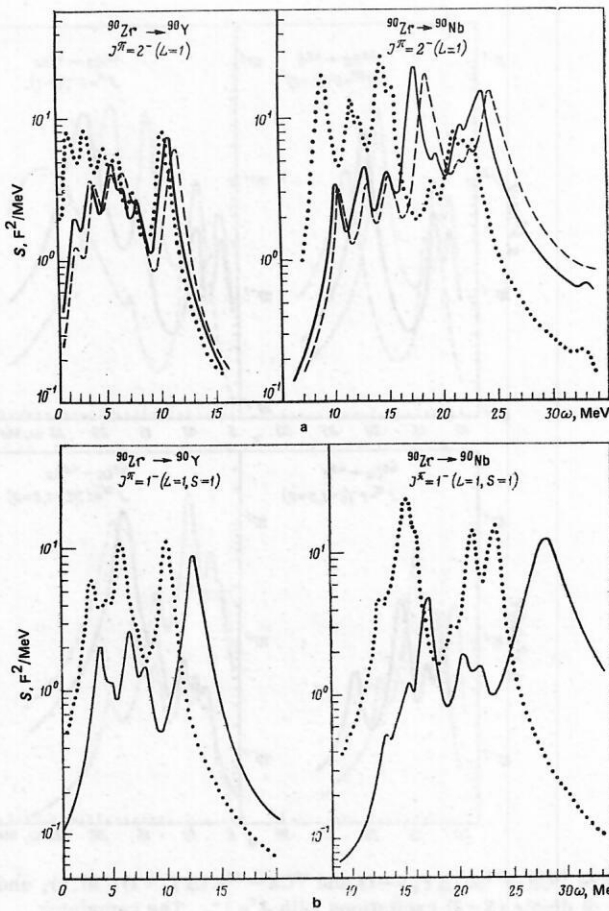


FIG. 10. The same as in Fig. 9, for the isobars  $^{90}\text{Zr} \rightarrow ^{90}\text{Nb}$  ( $\Delta T_z = -1$ ) and  $^{90}\text{Zr} \rightarrow ^{90}\text{Y}$  ( $\Delta T_z = 1$ ).

connection, we mention Ref. 68, in which dipole excitations in  $^{208}\text{Bi}$  were calculated using a Hartree-Fock single-particle spectrum (Skyrme forces with  $m^*/m = 0.76$ ), and also density-dependent interactions  $\mathcal{F}^-$  of zero range and spin-isospin interactions of one-meson ( $\pi$  and  $\rho$ ) exchange, augmented by a  $\delta$ -function repulsion. We have already noted that for Hartree-Fock potentials with  $m^* < m$  there is characteristically an appreciable excess of the energies of the particle-hole

differences compared with the phenomenological shell potentials (and compared with the experimental single-particle spectra) and a weaker spin-orbit splitting. The  $\mathcal{F}^-$  interactions used in Ref. 68 were not matched to the Hartree-Fock potential. Their parametrization makes it possible to reproduce the experimental energy of the giant dipole resonance in  $^{208}\text{Pb}$  (see Ref. 23).

We note that the repulsive spin-isospin interactions used in Ref. 68 were apparently weaker than those in our calculations. This is indicated by the fact that according to Ref. 23 the energy of the Gamow-Teller resonance in  $^{208}\text{Bi}$  calculated with the experimental spectrum and the same spin-isospin interactions as in Ref. 68 is 2.7 MeV below the experimental energy. These factors taken together were responsible for the  $1^-$  ( $S=0$ ) resonance in Ref. 68 being actually higher than the spin-dipole resonance and at least 5 MeV higher than in our calculations. For the  $0^-$  and  $1^-$  ( $S=1$ ) resonances the quenching of the spin-isospin forces is compensated by the large energies of the particle-hole differences, which exceed the ones we used by about 4–5 MeV. As a result, the energies of these resonances as obtained in our calculations and in Ref. 68 are about the same.

We also mention the calculations of the dipole excitations in  $^{208}\text{Bi}$  and  $^{208}\text{Tl}$  made in Ref. 69 on the basis of the theory of finite Fermi systems. These used the experimental single-particle spectrum, weakly interpo-

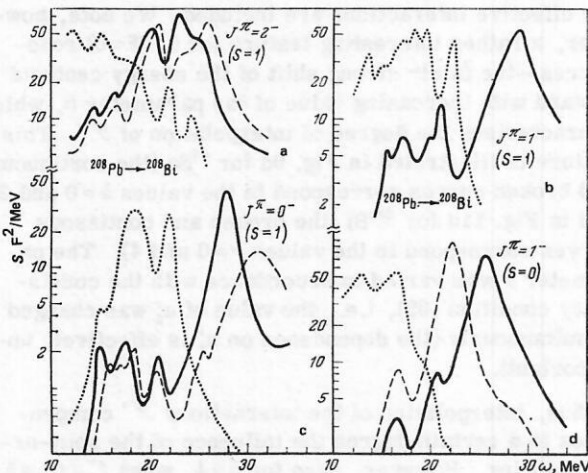


FIG. 11. The same as in Fig. 9, for the isobars  $^{208}\text{Pb} \rightarrow ^{208}\text{Bi}$  ( $\Delta T_z = -1$ ).



lated effective interactions  $\mathcal{F}^-$ , and zero-range spin-isospin forces  $G^-$  weaker than in our calculations. One-pion exchange was not included, and the calculation was made with a restricted single-particle basis. To a certain degree, this last circumstance compensates the weakness of the effective interactions, since with increasing completeness of the single-particle basis it is usually necessary to increase the force constants of the repulsive interactions (to obtain the same excitation energy). Therefore, the energy found in Ref. 69 for the  $1^-$  ( $S=0$ ) resonance ( $\approx 21$  MeV) is only about 1 MeV lower than in our calculations for  $b=0$  (see Fig. 11d). However, the energies of the  $0^-$  and  $1^-$  ( $S=1$ ) resonances in  $^{208}\text{Bi}$  are appreciably lower than ours and the ones obtained in Ref. 68.

We also mention the calculations of dipole  $1^-$  ( $S=0$ ) resonances in  $^{48}\text{Ca}$  and  $^{90}\text{Zr}$  made with Skyrme forces in Ref. 70. The energies of the centroids of the distributions for the dipole transitions were here calculated on the basis of sum rules with different energy weights. The predicted energies of the dipole resonances in  $^{48}\text{Sc}$  and  $^{90}\text{Nb}$  exceed those that we obtained by about 4–5 MeV, which is due to the more rarefied single-particle spectra, as for  $^{208}\text{Bi}$ .<sup>68</sup>

Finally, we mention the calculations of the spin-dipole excitations in  $^{90}\text{Nb}$  made in Ref. 52 without allowance for one-meson exchange. The estimates obtained there for the energies of the  $0^-$ ,  $1^-$  ( $S=1$ ), and  $2^-$  resonance states are close to our results for  $g_r=0$  shown in Figs. 10a–10c.

Summarizing this discussion, we can say that the results of the different theoretical calculations for the spin-dipole resonances with allowance for one-meson exchange, which is particularly important for a  $0^-$  resonance, agree qualitatively with one another. An appreciable concentration of the transition strength is predicted in the  $0^-$  and  $1^-$  ( $S=1$ ) resonances, together with a broad "smearing" of the transition strength for  $2^-$  excitations. At the same time, there is no quantitative agreement in the estimates of the energy of the dipole  $1^-$  ( $S=0$ ) resonance. In this case, as for the isobar analog  $0^+$  excitations, it seems to us very important to make an exact matching of the isovector potential and the effective interactions in order to see clearly the need to use potentials with  $m^* < m$  and interpolated interactions  $\mathcal{F}^-$ . As yet, this problem has not been fully investigated.

We turn to the discussion of the experimental data<sup>67</sup> on the  $L=1$  resonance obtained in  $(p, n)$  reactions at proton energy 45 MeV. This resonance was interpreted as the antianalog of an  $E1$  resonance in the parent nucleus, or as a  $1^-$  ( $S=0$ ) resonance in the classification used here. This interpretation is based essentially on the assumption that at proton energy 45 MeV the excitation of the spin-dipole modes is strongly suppressed. If this is the case, the dipole resonance ( $S=0$ ) must lie somewhat higher in energy than the spin-dipole resonance ( $S=1$ ). In connection with these experiments, the cross sections were calculated<sup>68</sup> and confirmed the dominant part played by the spin-dipole (especially with  $J^\pi = 2^-$ ) excitations at  $E_p = 45$  MeV, the excitations of the

spin-dipole and dipole modes are comparable. Quenching of the contributions of the spin-dipole excitations is possible only if in the considered region of excitation energies about 1/3 of the entire strength of the spin-dipole transitions is localized, i.e., if  $e_q[\sigma\tau] \approx 0.6$ . However, the calculated cross sections for the lowest  $2^-$  excitation in  $^{208}\text{Bi}$  ( $\omega = 6.5$  MeV) agree with the experimental data for  $e_q[\sigma\tau] \approx 1$ . It is concluded that there is a strong dependence of the effective charge on the angular momentum and degree of collectivization of the state. In Ref. 60, calculations were also made of the cross section of the  $(p, n)$  reaction for a low-lying  $2^-$  level in  $^{208}\text{Bi}$ , and good agreement with experiment (for  $E_p = 200$  MeV) was obtained with  $e_q[\sigma\tau] \approx 1$ . However, this estimate of  $e_q[\sigma\tau]$  may be incorrect, since near the  $2^-$  level in  $^{208}\text{Bi}$  there is an entire conglomeration of states of the type  $1^*, 2^*, 3^*$  (see Table II), whose contribution to the cross section may be comparable with the contribution of the  $2^-$  excitation (and, therefore,  $e_q[\sigma\tau]$  will decrease when they are taken into account). In addition, calculations were made in Ref. 60 of the cross sections for excitation of  $L=1$  resonances in  $^{90}\text{Nb}$ , in which the situation is similar to  $^{208}\text{Bi}$ . From comparison of the calculations with the experimental data at  $E_p = 200$  MeV one can conclude that  $e_q[\sigma\tau] \approx 0.8$ , i.e., we obtain a value appreciably larger than what follows from the calculations of Ref. 68.

Thus, the interpretation given here to the data of Ref. 67 cannot yet be regarded as sufficiently justified, though it is possible that the data indicate proximity of the energies of the dipole ( $S=0$ ) and spin-dipole ( $S=1$ ) resonances.

#### Sum rules and transition densities

The integrated characteristics of the dipole excitations with  $\Delta T_z = \pm 1$  (sum rules) and the centroid energies  $\omega_R^{(\pm)}$  of the main resonances are given in Table IV. According to Eq. (48), we obtain for dipole transitions ( $L=1$ ) the following sum rules (setting  $e_q=1$ ):

$$m_0^{(-)} - m_0^{(+)} = \frac{2J+1}{4\pi} (N \langle r_n^2 \rangle - Z \langle r_p^2 \rangle) = S^J, \quad (85)$$

TABLE IV. Sum rules and energies of charge-exchange spin-dipole ( $S=1$ ) and dipole ( $S=0$ ) resonances. The energies  $\omega_R^{(\pm)}$  correspond to the states in the daughter nuclei with  $\Delta T_z = \pm 1$ . The results of calculations for particle-hole transitions when  $\mathcal{F}^- = G^- = G_r = 0$  are given in the brackets.

| Nucleus          | $J^\pi(S)$ | $\Sigma^J$ ,<br>$F^2$ | $m_0^{(-)}$ ,<br>$F^2$ | $m_0^{(+)}$ ,<br>$F^2$ | $\Delta m_0^{(\mp)}$ ,<br>$F^2$ | $\omega_R^{(-)}$ ,<br>MeV | $\omega_R^{(+)}$ ,<br>MeV |
|------------------|------------|-----------------------|------------------------|------------------------|---------------------------------|---------------------------|---------------------------|
| $^{48}\text{Ca}$ | $0^-(1)$   | 9.95                  | (18.2)<br>16           | (8.4)<br>6.4           | (9.8)<br>9.6                    | 6.3; 9.2; 15.6; 21.8      | 11; 13; 21.7              |
|                  | $1^-(4)$   | 29.8                  | (49.7)<br>37.8         | (20)<br>10.3           | (29.7)<br>27.5                  | 10.7; 17; 23.5            | 13.8; 21.5                |
|                  | $2^-(4)$   | 49.7                  | (65)<br>58.5           | (17)<br>11.2           | (48)<br>47.3                    | 4.2; 7.5; 12–20           | 11.6; 17.4                |
|                  | $1^-(0)$   | 29.8                  | (43.7)<br>36.1         | (14.8)<br>8.1          | (28.9)<br>28.0                  | 10.5; 17.4                | 12; 16.8; 21.7            |
|                  |            |                       |                        |                        |                                 |                           |                           |
| $^{90}\text{Zr}$ | $0^-(1)$   | 18.6                  | (38)<br>32             | (19.5)<br>14.5         | (18.5)<br>17.5                  | 15; 26.6                  | 3; 5.6; 12                |
|                  | $1^-(4)$   | 55.8                  | (104)<br>78            | (50)<br>28             | (54)<br>50                      | 17; 27.6                  | 3; 6; 6.3; 12             |
|                  | $2^-(1)$   | 93                    | (138)<br>116           | (47)<br>27             | (91)<br>89                      | 17.5; 23.8                | 5; 10.5                   |
|                  | $1^-(0)$   | 55.8                  | (94)<br>75.5           | (40)<br>23             | (54)<br>52.5                    | 21.5                      | 3.6; 7.8; 12              |
|                  |            |                       |                        |                        |                                 |                           |                           |

where

$$m_0^{(\mp)} = \int S(\omega, \Delta T_z = \mp 1) d\omega. \quad (86)$$

We mention here the equality of the sum rules for dipole ( $S=0$ ) and spin-dipole ( $S=1$ ) transitions with  $L=1$ . The integrals  $m_0^{(\pm)}$  were calculated both for particle-hole transitions, when  $\mathcal{F}^- = G^- = G_\pi = 0$ , and with the inclusion of effective interactions. The calculations showed that in  $^{48}\text{Ca}$  and  $^{90}\text{Zr}$  dipole transitions with  $\Delta T_z = +1$  systematically give 20–40% of the strength of the transitions with  $\Delta T_z = -1$ . For  $^{208}\text{Pb}$ , the dipole transitions with  $\Delta T_z = +1$ , like the Gamow-Teller transitions, are rather weak. Here, the calculated integrals  $m_0^{(\pm)}$  are rather close to the values ( $F^2$ ) of  $\Sigma^J = 115(2J+1) F^2$  (see also Ref. 69). It is important to take into account this circumstance when planning  $(n, p)$ ,  $(^7\text{Li}, ^7\text{Be})$ , etc., experiments.

It can be seen from the data of Table IV that the effective interactions decrease the sums  $m_0^{(\mp)}$  but in such a way that their difference, as follows from (85), does not change (cf. the values of  $\Sigma^J$  and  $\Delta m_0^{(\mp)}$ ). A certain difference between  $\Sigma^J$  and  $\Delta m_0^{(\mp)}$  is due to the fact that the integration is performed over a finite energy interval ( $\approx 35$  MeV), and some of the transition strength is situated higher in the continuum. In the literature, one sometimes finds the assertion that the effective interactions only redistribute the transition strength over the excitation spectrum but do not change the complete sum of the strengths. This is valid only when the transitions with  $\Delta T_z = 1$  are negligibly small (for example, for Gamow-Teller transitions in the considered nuclei). In the general case, the effective interactions not only redistribute but also change the total strength of the particle-hole transitions for each branch of charge excitations.

The distribution of the transition strength over the excitation spectrum when effective interactions are included depends on  $J$ , as can be seen from Figs. 9–11. As a rule, the  $0^-$  and  $1^-$  ( $S=1$ ) resonances in nuclei with  $\Delta T_z = -1$  gather 80–95% of the sum  $m_0^{(\pm)}$ . For the  $2^-$  states, a more uniform distribution over the excitation spectrum is characteristic. With regard to the  $1^-$  ( $S=0$ ) states, for them transitions with  $\Delta T_z = -1$  are concentrated mainly in one resonance, while the transitions with  $\Delta T_z = +1$  are distributed in wider intervals of the excitation spectra.

Of particular interest are the dipole transitions with  $\Delta T_z = 1$  for the isobars  $^{90}\text{Zr} \rightarrow ^{90}\text{Y}$ . Here, the theory predicts a concentration of almost the entire transition strength in a rather small interval of excitation energies (see Fig. 10 and Table IV,  $\omega_R^{(\pm)}$ ). A local concentration of the strength of the spin-dipole transitions is expected in the regions of energies 3–6 and 10–12 MeV [we recall that these energies correspond to the  $Q$  values in reactions of  $(n, p)$  type]. In the first interval,  $2^-$  excitations play the dominant role; in the second, the strength of all the spin-dipole excitations is about the same. With regard to the dipole ( $S=0$ ) transitions, for them the main maximum is at an energy of about 8 MeV. The first experimental data confirming these predictions of the theory are now available. They were obtained in the  $(n, p)$  reaction with neutron energy of

about 20 MeV (Ref. 71) and in the  $(^7\text{Li}, ^7\text{Be})$  reaction.<sup>49</sup> In the first, dipole ( $S=0$ ) states are mainly excited; in the second, mainly spin-dipole states.

The transition densities of dipole resonances are interesting from the point of view of their similarity to the known transition densities of  $E1$  giant resonances, which have a surface nature. In Fig. 12, we show the  $\rho_{tr}$  of the dipole and spin-dipole resonances in  $^{90}\text{Nb}$ . We recall that for a  $0^-$  resonance there exists one radial component  $\rho_{tr}^{10}(r)$ , while a  $2^-$  resonance is characterized by two radial components—the spin-dipole  $\rho_{tr}^{12}(r)$  and the spin-octupole  $\rho_{tr}^{32}(r)$ . The dipole  $1^-$  ( $S=0$ ) and spin-dipole  $1^-$  ( $S=1$ ) resonances each have two radial components  $\rho_{tr}^{11}(r)$  with  $S=0$  and 1. The  $\rho_{tr}$  shown in Fig. 11 are normalized to the matrix elements of the transitions for external fields  $r\tau_-$  and  $[r \times \sigma] \tau_-$ :

$$M_{0 \rightarrow J}^2 = (2J+1) \left| \sum_{S(J=1)} \int \rho_{tr}^{1J}(r) r^3 dr \right|^2, \quad (87)$$

with the values

$$\left. \begin{aligned} M_{0 \rightarrow 0}^2 &= 31.3 F^2; & M_{0 \rightarrow 1}^2 (S=0) &= 72.5 F^2; \\ M_{0 \rightarrow 1}^2 (S=1) &= 57.8 F^2; & M_{0 \rightarrow 2}^2 &= 54.3 F^2. \end{aligned} \right\} \quad (88)$$

Comparison of the values of these matrix elements with the integrals in Table IV shows that the  $0^-$  and  $1^-$  ( $S=0$ ) resonances exhaust almost the entire possible transition strength. The spin-dipole resonance ( $S=1$ ) has about 75% of the total strengths, and the  $2^-$  excitation about 50%, which corresponds to the integrated contribution to  $m_0^{(\pm)}$  in the interval of energies 20–30 MeV (see Fig. 10a). The other half of the strength of the  $2^-$  excitations is in a lower resonance with energy around 17.8 MeV.

All the transition densities are characterized by a surface peak and relatively small volume components. We note also that the spin quantum number  $S$  distinguishes well between the spin and spin-dipole resonances, for which the spin-dipole (see Fig. 12, curve 7) and the dipole (curve 3) components of  $\rho_{tr}$ , respectively, are small. This fact, and also the difference between the energies, offers hope of the possibility of se-

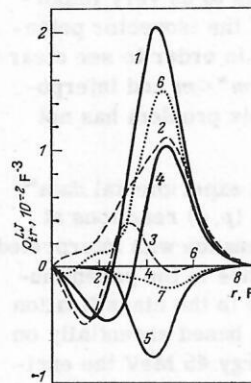


FIG. 12. Transition densities of spin-dipole resonances in  $^{90}\text{Nb}$ : 1)  $0^-$  resonance with energy 26.6 MeV; 2) and 3) the spin-dipole and dipole components, respectively, for the  $1^-$  ( $S=1$ ) resonance with energy 27.7 MeV; 4) and 5) the  $L=1$  and 3 components, respectively, for the  $2^-$  excitation with energy 23.8 MeV; 6) and 7) the dipole and spin-dipole components, respectively, for the  $1^-$  ( $S=0$ ) resonance with energy 21.5 MeV.



lective excitation of these resonances in different nuclear reactions. Attempts of this kind in the  $(p, n)$  reaction with different proton energies have already been discussed. With regard to the  $2^-$  resonance, its transition density  $\rho_{tr}^{12}$  (curve 4 in Fig. 12) is characterized by an appreciably larger volume component than the  $\rho_{tr}$  of the  $0^-$  resonance. The spin-octupole transition density  $\rho_{tr}^{32}$  (curve 5) for it is also fairly large. All this indicates the presence of fairly large components with large  $q$  in the Fourier expansion of the transition density for the  $2^-$  resonance. For this reason, the repulsive properties of the total interaction  $G^- + G_+$  are weakened for  $2^-$  excitations. As a result, the shift of the resonance relative to the particle-hole energy differences is, as can be seen in Fig. 10a, relatively small. For the same reason there is no complete concentration of the transition strength in one  $2^-$  resonance, as there is for  $0^-$  and  $1^-$  resonances. Such features are also characteristic of  $2^-$  excitations in  $^{48}\text{Sc}$  and  $^{208}\text{Bi}$ .

## 8. EXCITATIONS WITH $L = 2$ AND 3

At the present time, there are experimental indications of the existence of a broad ( $\Gamma \approx 14$  MeV) resonance with centroid energy 31–32 MeV in  $^{90}\text{Nb}$  and  $^{208}\text{Bi}$ .<sup>48</sup> The angular distributions for the resonances are characteristic of quadrupole ( $L = 2$ ) transitions.

Theoretical calculations of the strength functions for  $L > 1$  excitations have hitherto been made only in Ref. 42. In Figs. 13 and 14 we show the strength functions for quadrupole ( $L = 2$ ) and octupole ( $L = 3$ ) excitations in  $^{208}\text{Bi}$ , calculated with the same values of the parameters of the effective interactions as the results for  $L = 0$  and 1 discussed above. For  $L = 2$ , admittedly broad but nevertheless well-formed resonances with  $J^\pi = 1^+$  and  $2^+$  ( $S = 0$  and 1) with energy 30–35 MeV exist. The spin-quadrupole transitions with  $J^\pi = 3^+$  are distributed in a broad interval of excitation energies above 20 MeV. Thus, in the region of the observed  $L = 2$  resonance all spin-quadrupole excitations make an important contribution [one might think that, as for an  $L = 1$  resonance, the contribution of excitations with  $J^\pi = 2^+$  ( $S = 0$ ) is suppressed at proton energies  $> 100$  MeV].

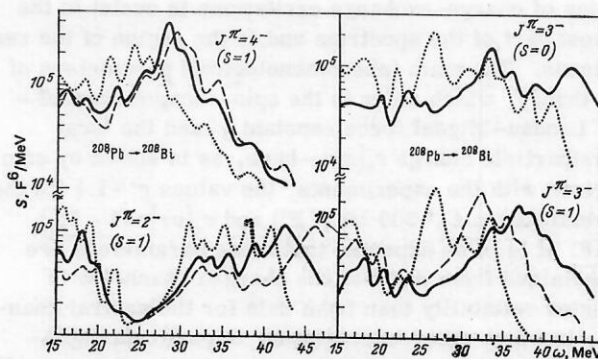


FIG. 14. The same as in Fig. 13, for excitation with  $L = 3$ . For  $J^\pi = 4^-$  and  $2^-$  ( $S = 1$ ) the broken curve shows the results of calculations with  $g_r = 0$  and  $g' = 0.95$ .

Octupole transitions (see Fig. 14) form a definite resonance at an energy around 29 MeV only for  $J^\pi = 4^-$ . The remaining transitions are distributed in broad intervals of the excitation energies. Thus, with increasing  $L$  the resonance structure of the strength functions is smoothed and the main strength of the transitions is shifted ever higher in energy into the continuum.

The energy shifts of the resonances associated with the one-pion exchange interaction are particularly large for  $J^\pi = 1^+$  ( $L = 2$ ) and  $2^-$  ( $L = 3$ ). With increasing  $L$ , the effective renormalization of  $g'$  by this interaction also increases. To illustrate this effect, Fig. 14 shows calculations for  $4^-$  and  $2^-$  excitations with  $g' = 1.1$ ,  $g_r = -1.45$  (continuous curves) and  $g' = 0.95$ ,  $g_r = 0$  (broken curves). For  $1^+$  ( $L = 0$ ) excitations, the two sets of parameters give the same experimental energy of the Gamow-Teller resonance. In the case of  $L = 3$  the uncompensated shifts of the resonances still remain large for such renormalization of  $g'$  (especially for  $J^\pi = 2^-$ ). Therefore, with increasing  $L$  the part played by transitions with large  $q$  also increases. We note also the increasing importance of the dependence of the effective forces  $\mathcal{F}^{\pi}$  on the density with increasing  $L$ . For  $2^+$  ( $S = 0$ ) and  $3^+$  ( $S = 0$ ) transitions the shifts of the main maxima as the parameter  $b$  is increased from 0 to 4 reach 4–5 MeV.

Our calculations showed that in the region of localization of the spin-dipole resonance (20–30 MeV) an appreciable strength of spin-quadrupole transitions with  $J^\pi = 3^+$  is contained, and it is important to take this into account when identifying the background for this resonance and estimating cross sections and, therefore, the effective charge  $e_q[\sigma\tau]$  for spin-dipole transitions. Similarly, in the region of localization of the  $L = 2$  (25–40 MeV) resonance there is an appreciable strength of spin-octupole transitions with  $J^\pi = 3^-$  and  $4^-$ . Therefore, in an estimate of the excitation cross sections of the resonances it is important to make a direct calculation of the background, as is done in Ref. 63 for  $^{48}\text{Ca}$ .

## CONCLUSIONS

As follows from this review, the microscopic approach based on the theory of finite Fermi systems gives an entirely satisfactory description of the prop-

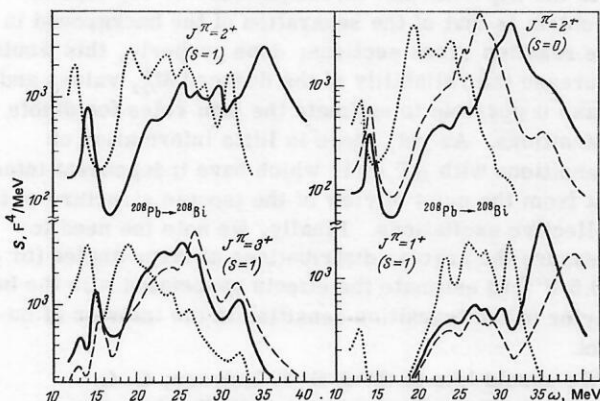


FIG. 13. Strength functions of excitations with  $L = 2$  for the isobars  $^{208}\text{Pb} \rightarrow ^{208}\text{Bi}$ . The notation is the same as in Figs. 1 and 9–11.

erties of charge-exchange excitations in nuclei in the lowest part of the spectrum and in the region of the resonances. The main (phenomenological) parameters of the theory, which refer to the spin-isospin channel—the Landau-Migdal force constant  $g'$  and the local quasiparticle charge  $e_q[\sigma\tau]$ —have, as is shown by comparison with the experiments, the values  $g' \approx 1.1$  (in the normalization  $C_0 = 300 \text{ MeV} \cdot \text{F}^3$ ) and  $e_q[\sigma\tau] = (1 - 2\zeta_s) \approx 0.8$ . It is to be expected that these parameters are determined from data for the charged channel with greater reliability than from data for the neutral channel, in which other interactions, in particular spin-spin interactions, play an important part. To no small degree the possibility of discovering precritical effects in nuclei, the so-called *precursors of pion condensation*, depends on what are the actual values of  $g'$  and  $e_q[\sigma\tau]$ . If  $\zeta_s = 0.1$ , the one-pion exchange amplitude is suppressed on account of the factor  $e_q^2$  by 36%, and the critical value of  $g'$  corresponding to onset of instability of the pion mode is  $g'_{cr} = 0.5-0.6$  (for  $0^-$  and  $1^+$  excitations in  $^{48}\text{Ca}$ ,  $^{90}\text{Zr}$ , and  $^{208}\text{Pb}$ ). Thus, the actual value  $g'$  found in our analysis is greater than  $g'_{cr}$  by at least 0.5. As is shown by the calculations of Ref. 31, appreciable precritical effects associated with softening of the pion mode can be manifested in  $(p, p')$  reactions with excitation of low-lying anomalous-parity states if  $g' - g'_{cr} \leq 0.2$ . But if in reality  $g' - g'_{cr} \geq 0.5$ , then in these reactions these effects become “invisible,” and the possibility of discovering them in other processes becomes problematic.

Also of great interest is the experimentally observed quenching of the strength of the charge-exchange transitions (at small  $q$ ). In the theory of finite Fermi systems, this corresponds to  $e_q[\sigma\tau] = 1 - 2\zeta_s \approx 0.8$ , and one can speak of a universality of this value for different nuclei and excitations in different sections of the spectrum. Effectively, this is the first time that  $e_q[\sigma\tau]$  has been determined so reliably and physical effects associated with the effective charge have been demonstrated so clearly. We note that the value found for  $e[\sigma\tau]$  “returns” the axial-vector constant  $g_A = -1.25$  known from neutron  $\beta$  decay to the “bare” lepton-quark value  $g_A = -1$  in nuclear matter, i.e., the medium appears to restore the symmetry  $[SU(4)]$ ; Ref. 10] between the vector and axial-vector vertices that is broken in the lepton-nucleon sector in vacuum. Clearly, this fact is not trivial and important consequences may flow from it (see, in particular, Ref. 72). It would be interesting to establish the extent to which the parameter  $\zeta_s$  is universal in the description of other reactions in which anomalous-parity states are excited, including the neutral channel [in particular, in the description of the  $(p, p')$  reaction].

One of the most important tasks of theory is to establish the contributions made by the various mechanisms which suppress the transition strengths and to identify possible energy regions in which the missing transition strength is localized. It is also important in the experiments to advance into the region of excitation energies  $\omega \approx \varepsilon_F$  and establish what is the “multipair” contribution to the probability of spin-flip transitions (at small  $q$ ). In reactions with hadrons, the situation

is complicated by the problem of the subtraction of the background. From this point of view, “lepton charge-exchange” reactions (inverse  $\beta$  decay) are the “cleanest”; there are some prospects associated with neutrinos of meson factories, which in principle make it possible to investigate the integrated probability of excitation of a nucleus in both charged channels up to energies  $\approx \varepsilon_F$ . The experiments are complicated but do not appear to be without hope.

Our comparison of different theoretical approaches has shown that it is frequently difficult to judge their advantages, since in the studies of even the same authors the computational schemes (the single-particle potentials and the interaction parameters) are changed from nucleus to nucleus in order to achieve agreement with the experimental data. In this connection, it is very important to make completely self-consistent calculations, especially for excitations with  $S=0$  ( $0^+, 1^-, \dots$ ), in order to draw real conclusions about the necessity of using self-consistent potentials with  $m^* < m$  (of Hartree-Fock type) and interpolated effective interactions  $\mathcal{F}^-$ .

It is also necessary to make additional investigations of the anomalous-parity states ( $1^+, 2^-, \dots$ ), in particular, the low-lying ones, in order to establish whether it is necessary to introduce nonlocality of the spin-isospin forces and also to determine more precisely the part played by one-meson exchange (in particular,  $\rho$ -meson exchange).

The isospin structure of the considered excitations has not been discussed in the present paper, since isospin is not conserved in the formalism of the microscopic approaches. Accurate separation of the effects of Coulomb isospin mixing requires exact matching of  $\mathcal{F}^-$  and  $U^-$ , and also similar matching between the isovector spin-orbit effective interactions and the component corresponding to them in the spin-orbit potential  $U_{ss}^n - U_{ss}^p$  if such is contained in the self-consistent field. Such matching has not hitherto been made in any study, and this, particular, may lead to distortion of the characteristics of the  $1^+$  excitations lying above the Gamow-Teller resonance (for example, of the  $M1$  analog). It is also important to carry out such matching to obtain a correct estimate of the energies of the isospin splitting of the resonance states.

In the experimental investigations, a very topical problem is that of the separation of the background in the reaction cross sections; done properly, this would increase the reliability of the deduced  $M_{GT}^2$  values and make it possible to estimate the sum rules for dipole transitions. As yet, there is little information on transitions with  $\Delta T_\pi = +1$ , which have independent interest from the point of view of the isospin structure of the collective excitations. Finally, we note the need to measure the angular distributions at large angles (or  $q > 0.5 \text{ F}^{-1}$ ) to estimate the effects associated with the behavior of the transition densities in the interior of nuclei.

We should like to thank S. T. Belyaev, G. G. Bunatyan, F. A. Gareev, and S. V. Tolokonnikov for helpful discussions and V. V. Pal'chik for assistance in the calculations.



- <sup>1</sup>Isospin in Nuclear Physics (ed. D. H. Wilkinson), North-Holland, Amsterdam (1969).
- <sup>2</sup>P. G. Hansen, *Adv. Nucl. Phys.* **7**, 159 (1973).
- <sup>3</sup>W. J. Courtney and J. D. Fox, *At. Data Nucl. Data Tables* **15**, 141 (1975).
- <sup>4</sup>In: Proc. of the Intern. Symposium on Highly Excited States in Nuclear Reactions (eds. H. Ikegami and M. Muraoka), Osaka University, Osaka (1980); in: Proc. of the Fourth Intern. Conf. on Nuclei Far from Stability, Helsingør (1981); CERN 81-09, Geneva (1981).
- <sup>5</sup>P. Franzini and L. A. Radicati, *Phys. Lett.* **6**, 322 (1963).
- <sup>6</sup>K. Ikeda *et al.*, *Phys. Lett.* **3**, 271 (1963); J. Fujita and K. Ikeda, *Nucl. Phys.* **67**, 145 (1965); *Prog. Theor. Phys.* **36**, 288 (1966).
- <sup>7</sup>S. I. Gabrakov *et al.*, *Phys. Lett.* **B36**, 275 (1971); S. P. Ivanova, A. A. Kuliev, and D. I. Salamov, *Yad. Fiz.* **24**, 278 (1976) [*Sov. J. Nucl. Phys.* **24**, 145 (1976)]; *Izv. Akad. Nauk SSSR, Ser. Fiz.* **41**, 131 (1977).
- <sup>8</sup>Yu. V. Gaponov and Yu. S. Lyutostanskii, *Yad. Fiz.* **19**, 62 (1974) [*Sov. J. Nucl. Phys.* **19**, 33 (1974)].
- <sup>9</sup>S. I. Gabrakov and N. I. Pyatov, in: Proc. of the Symposium on Nucleons and Weak Interactions (eds. B. Eman and D. Tadić), Zagreb (1971).
- <sup>10</sup>Yu. V. Gaponov and Yu. S. Lyutostanskii, *Fiz. Elem. Chastits At. Yadra* **12**, 1324 (1981) [*Sov. J. Part. Nucl.* **12**, 528 (1981)].
- <sup>11</sup>A. B. Migdal, *Teoriya Konechnykh fermi-sistem i svoystva atomnykh yader*, Nauka, Moscow (1965); English translation: *Theory of Finite Fermi Systems*, Interscience, New York (1967).
- <sup>12</sup>N. Auerbach *et al.*, *Rev. Mod. Phys.* **44**, 481 (1972); A. M. Lane and A. Z. Mekjian, *Adv. Nucl. Phys.* **7**, 97 (1973); S. Shlomo, *Rep. Prog. Phys.* **41**, 957 (1978); M. G. Urin, *Fiz. Elem. Chastits At. Yadra* **11**, 991 (1980) [*Sov. J. Part. Nucl.* **11**, 395 (1980)].
- <sup>13</sup>V. A. Khodel' and S. A. Fayans, *Yad. Fiz.* **12**, 717 (1970) [*Sov. J. Nucl. Phys.* **12**, 388 (1971)].
- <sup>14</sup>S. A. Fayans and V. A. Khodel', *Pis'ma Zh. Eksp. Teor. Fiz.* **17**, 633 (1973) [*JETP Lett.* **17**, 444 (1973)].
- <sup>15</sup>E. E. Sapershtein *et al.*, *Fiz. Elem. Chastits At. Yadra* **9**, 221 (1978) [*Sov. J. Part. Nucl.* **9**, 91 (1978)]; S. A. Fayans *et al.*, *Nucl. Phys.* **A317**, 424 (1979); V. A. Khodel and E. E. Saperstein, *Nucl. Phys.* **A348**, 261 (1980).
- <sup>16</sup>G. G. Bunatyan and M. A. Mikulinskiĭ, *Yad. Fiz.* **1**, 38 (1965) [*Sov. J. Nucl. Phys.* **1**, 26 (1965)]; G. G. Buntyan, *Yad. Fiz.* **4**, 707 (1966) [*Sov. J. Nucl. Phys.* **4**, 502 (1967)].
- <sup>17</sup>Z. Bochnacki, I. M. Holban, and I. N. Mikhaĭlov, *Nucl. Phys.* **A97**, 33 (1967); V. B. Belyaev and I. N. Mikhaĭlov, "Ot del'nye voprosy teorii yadra" ("Some questions of nuclear theory"), Supplement to the Russian translation published by Atomizdat, Moscow (1967) of: A. M. Lane, *Nuclear Theory*, Benjamin, New York (1964).
- <sup>18</sup>S.-O. Bäckman *et al.*, *Nucl. Phys.* **A321**, 10 (1979).
- <sup>19</sup>T. H. R. Skyrme, *Nucl. Phys.* **9**, 615 (1959); D. Vautherin and D. Brink, *Phys. Rev. C* **5**, 626 (1972).
- <sup>20</sup>B. A. Fomin and V. D. Efros, *Yad. Fiz.* **34**, 587 (1981) [*Sov. J. Nucl. Phys.* **34**, 327 (1981)].
- <sup>21</sup>J. P. Blaizot, *Phys. Lett.* **B60**, 435 (1976); S.-O. Bäckman *et al.*, *Phys. Lett.* **B56**, 209 (1975); S. Krewald *et al.*, *Nucl. Phys.* **A281**, 166 (1977).
- <sup>22</sup>I. Hamamoto and P. Siemens, *Nucl. Phys.* **A269**, 199 (1976).
- <sup>23</sup>S. Krewald *et al.*, *Phys. Rev. Lett.* **46**, 103 (1981).
- <sup>24</sup>G. Brown *et al.*, *Nucl. Phys.* **A330**, 290 (1979).
- <sup>25</sup>A. P. Platonov, *Yad. Fiz.* **34**, 612 (1981) [*Sov. J. Nucl. Phys.* **34**, 342 (1981)].
- <sup>26</sup>E. E. Sapershtein and V. A. Kordel', *Zh. Eksp. Teor. Fiz.* **81**, 22 (1981) [*Sov. Phys. JETP* **54**, 12 (1981)]; V. A. Khodel and E. E. Saperstein, *Phys. Rep.* **92**, 183 (1982).
- <sup>27</sup>V. A. Khodel', *Yad. Fiz.* **19**, 792 (1974) [*Sov. J. Nucl. Phys.* **19**, 404 (1974)].
- <sup>28</sup>E. E. Sapershtein and V. A. Kordel', *Yad. Fiz.* **6**, 256 (1967) [*Sov. J. Nucl. Phys.* **6**, 186 (1967)].
- <sup>29</sup>A. B. Migdal, *Zh. Eksp. Teor. Fiz.* **61**, 2209 (1971); **63**, 1993 (1972) [*Sov. Phys. JETP* **34**, 1184 (1972); **36**, 1052 (1973)]; *Nucl. Phys.* **210A**, 421 (1973).
- <sup>30</sup>A. B. Migdal, *Fermiony i bozony v sil'nykh pol'yakh* (Fermions and Bosons in Strong Fields), Nauka, Moscow (1978); A. B. Migdal, *Rev. Mod. Phys.* **50**, 107 (1978).
- <sup>31</sup>I. N. Borzov *et al.*, *Fiz. Elem. Chastits At. Yadra* **12**, 848 (1981) [*Sov. J. Part. Nucl.* **12**, 338 (1981)].
- <sup>32</sup>E. E. Sapershtein and M. A. Troitskii, *Yad. Fiz.* **22**, 257 (1975) [*Sov. J. Nucl. Phys.* **22**, 132 (1975)]; *Izv. Akad. Nauk SSSR, Ser. Fiz.* **40**, 95 (1976).
- <sup>33</sup>J. Speth *et al.*, *Nucl. Phys.* **A343**, 382 (1980).
- <sup>34</sup>J. Meyer-ter-Vehn, *Phys. Rep.* **74**, 323 (1981); E. Oset *et al.*, *Phys. Rep.* **83**, 281 (1982).
- <sup>35</sup>A. Bohr and B. R. Mottelson, *Nuclear Structure*, Vols. 1 and 2, Benjamin, New York (1969, 1975); O. Bohigas *et al.*, *Phys. Rep.* **51**, 267 (1979); T. Suzuki, *Phys. Lett.* **B104**, 92 (1981); *Nucl. Phys.* **A379**, 110 (1982); G. Bertsch *et al.*, *Phys. Rev. C* **24**, 533 (1981); K. Nakayama *et al.*, *Phys. Lett.* **B114**, 217 (1982); D. Y. Horen *et al.*, *Phys. Lett.* **B99**, 383 (1981); N. Auerbach *et al.*, *Phys. Lett.* **B106**, 347 (1981).
- <sup>36</sup>S. V. Tolokonnikov and S. A. Fayans, in: *Tezisy dokladov XXXII Soveshchaniya po yadernoi spektroskopii i strukture atomnogo yadra* (Abstracts of Papers at the 32nd Symposium on Nuclear Spectroscopy and Nuclear Structure), Nauka, Moscow-Leningrad, p. 155; N. I. Pyatov and S. A. Fayans, in: *Elektromagnitnye vzaimodeystviya yader pri mal'nykh i srednikh energiyakh*. V. Seminar, M., 15-17 iyunya 1981 (Electromagnetic Interactions of Nuclei at Low and Medium Energies. Fifth Seminar, Moscow, June 15-17, 1981), Nauka, Moscow (1981), p. 253.
- <sup>37</sup>B. L. Birbrair *et al.*, *Yad. Fiz.* **28**, 625 (1978) [*Sov. J. Nucl. Phys.* **28**, 321 (1978)]; V. V. Pal'chik *et al.*, *Yad. Fiz.* **34**, 903 (1981); **35**, 1374 (1982) [*Sov. J. Nucl. Phys.* **34**, 504 (1981); **35**, 801 (1981)].
- <sup>38</sup>I. N. Borzov and S. A. Fayans, Preprint FÉI-1129 [in Russian], Obninsk (1981).
- <sup>39</sup>V. I. Isakov *et al.*, Preprint No. 627 [in Russian], Leningrad Institute of Nuclear Physics (1980).
- <sup>40</sup>I. Angeli and M. Csatlos, *ATOMKI Kozl.* **20**, 1 (1978).
- <sup>41</sup>G. D. Alkhazov, *Izv. Akad. Nauk SSSR, Ser. Fiz.* **42**, 2218 (1978); J. W. Negele *et al.*, *Commun. Nucl. Part. Phys.* **8**, 135 (1979); G. W. Hoffman *et al.*, *Phys. Rev. C* **21**, 1488 (1980); P. Gretillat *et al.*, *Nucl. Phys.* **A364**, 270 (1981).
- <sup>42</sup>S. A. Fayans and N. I. Pyatov, in: Proc. of the Fourth Intern. Conf. on Nuclei Far from Stability Helsingør (1981); CERN 81-09, p. 287.
- <sup>43</sup>J. R. Beene, *Nucl. Data Sheets* **23**, 1 (1978); J. W. Watson *et al.*, *Phys. Rev.* **23**, 2373 (1981).
- <sup>44</sup>J. P. Schiffer and W. W. True, *Rev. Mod. Phys.* **48**, 191 (1976).
- <sup>45</sup>D. E. Bainum *et al.*, *Phys. Rev. Lett.* **44**, 1751 (1980).
- <sup>46</sup>B. D. Anderson *et al.*, *Phys. Rev. Lett.* **45**, 699 (1980).
- <sup>47</sup>D. J. Horen *et al.*, *Phys. Lett.* **B95**, 27 (1980).
- <sup>48</sup>C. Gaarde *et al.*, *Nucl. Phys.* **A369**, 258 (1981).
- <sup>49</sup>A. A. Vinogradov *et al.*, *Pis'ma Zh. Eksp. Teor. Fiz.* **33**, 233 (1981) [*JETP Lett.* **33**, 222 (1981)].
- <sup>50</sup>C. Gaarde *et al.*, in: Proc. of the Intern. Conf. on Spin Excitations in Nuclei, Telluride, Colo., USA (1982); in: Proc. of the Intern. Conf. on Nuclear Structure, Amsterdam (1982); Preprints NBI, Copenhagen (1982).
- <sup>51</sup>C. Gaarde *et al.*, Preprint NBI, Copenhagen (1982).
- <sup>52</sup>G. Bertsch *et al.*, *Phys. Rev. C* **24**, 533 (1981).
- <sup>53</sup>H. Sagawa *et al.*, *Phys. Lett.* **B113**, 119 (1982).
- <sup>54</sup>T. Suzuki *et al.*, *Phys. Lett.* **B107**, 9 (1981).
- <sup>55</sup>J. Speth *et al.*, in: Proc. of the Intern. Conf. on Spin Excitations in Nuclei, Telluride, Colo., USA (1982).
- <sup>56</sup>C. Gaarde *et al.*, *Nucl. Phys.* **A334**, 248 (1980).
- <sup>57</sup>F. Osterfeld *et al.*, *Phys. Rev. Lett.* **49**, 11 (1982).

- <sup>58</sup>N. I. Pyatov *et al.*, *Yad. Fiz.* 29, 22 (1979); 34, 600 (1981) [*Sov. J. Nucl. Phys.* 29, 10 (1979); 34, 335 (1981)].
- <sup>59</sup>N. Auerbach and Nguen van Giai, *Phys. Rev. C* 24, 782 (1981); N. Auerbach and A. Yeverechyahu, *Phys. Rev. C* 25, 2841 (1982).
- <sup>60</sup>F. A. Gareev *et al.*, Preprint R4-82-437 [in Russian], JINR, Dubna (1982).
- <sup>61</sup>C. D. Coodman *et al.*, *Phys. Rev. Lett* 44, 1755 (1980).
- <sup>62</sup>F. Petrovich *et al.*, *Phys. Rev. C* 21, 1718 (1980).
- <sup>63</sup>F. Osterfeld, *Phys. Rev. C* 26, 762 (1982).
- <sup>64</sup>M. Ericson *et al.*, *Phys. Lett.* B45, 19 (1973); E. Oset and M. Rho, *Phys. Rev. Lett.* 42, 47 (1979); A. Bohr and B. R. Mottelson, *Phys. Lett.* B100, 10 (1981); G. E. Brown and M. Rho, *Nucl. Phys.* A372, 397 (1981).
- <sup>65</sup>G. F. Bertsch and I. Hamamoto, *Phys. Rev. C* 26, 1323 (1982).
- <sup>66</sup>D. J. Horen *et al.*, *Phys. Lett.* B99, 383 (1981).
- <sup>67</sup>W. A. Sterrenburg *et al.*, *Phys. Rev. Lett.* 45, 1839 (1980).
- <sup>68</sup>F. Osterfeld *et al.*, *Phys. Lett.* B105, 257 (1981).
- <sup>69</sup>F. Krmpotic *et al.*, *Nucl. Phys.* A342, 497 (1980).
- <sup>70</sup>N. Auerbach *et al.*, *Phys. Lett.* B106, 347 (1981).
- <sup>71</sup>W. R. McMurray *et al.*, in: *Proc. of the Intern. Conf. on Nuclear Structure* (eds. A. Van der Woude and B. J. Verhaar), Vol. 1, Amsterdam (1982), p. 75.
- <sup>72</sup>J. Delorme *et al.*, *Phys. Lett.* B115, 86 (1982).

Translated by Julian B. Barbour